Molecular Mechanisms Controlling Synaptic Vesicle Fusion

Daniel Radoff

Submitted in partial fulfillment of the
Requirements for the degree of
Doctor of Philsophy
In the Graduate School of Arts and Sciences

COLUMBIA UNIVERSITY

2011

ABSTRACT

Molecular Mechanisms Controlling Synaptic Vesicle Fusion

Daniel Radoff

SNARE proteins are the engines that drive membrane fusion throughout the cell. They provide this energy by zippering up into a parallel four helix bundle in a thermodynamically favored process. Because the zippering of SNAREs is spontaneous, fusion events occur immediately upon a vesicle interacting with its target membrane. But, in certain circumstances, such as in synaptic vesicles, spontaneous fusion is not desired, so a clamp protein is necessary to prevent this fusion until signaled to do otherwise. In synapses, this protein is called Complexin and a second protein, called Synaptotagmin, releases the clamp upon a rapid influx of calcium, the hallmark of an action potential. How Complexin clamps is a subject of great interest in the field, and an area of active research.

What is known is that a so-called Accessory helix (residues 28-47) is responsible for clamping, while another, Central Helix (reisudes 48-70) is responsible for physically binding to the helix. A recently solved crystal structure revealed how CPX might behave before the SNAREs fully zipper, namely that the accessory helix extends away from the SNAREs at a 45° angle. But, because of the packing of the crystal, it is entirely possible that the crystal is an artifact of packing, and/or truncation.

In this thesis, my work first validates the crystal structure, using a FRET pair I developed for this purpose. I establish that the angled-out positioning of the accessory helix does, in fact, occur in solution, and is not due to crystal packing or the truncation of the VAMP2 (the neuronal vesicle-associated SNARE), but rather is due to the fact that its C-terminus is not present. I describe a mechanism by which Complexin can clamp. Further, I demonstrate that the residues in VAMP2 which are responsible for the switch from the "open" to the "closed" conformation are a patch of asparatates in VAMP2 (residues 64, 65, an 68). I also establish that these three aspartates are responsible for the release of the clamp and that without them, Complexin cannot be brought into the angled-in configuration. I propose a model for how the clamp might be released by Synaptotagmin.

TABLE OF CONTENTS

LIST OF FIGURES

LIST OF TABLES

ACKNOWLEDGEMENTS

I could not have done this work without the help of all of the members of the Rothman lab. Specifically, I want to thank Shyam Krishnakumar for helping me design experiments, teaching me about FRET, protein purification, and being a great mentor and friend. I want to thank Daniel Kümmel from Karin Reinisch's lab for assistance in protein purification, for extremely fruitful discussions, and for assistance in making figures. Jeff Coleman is always willing to help with molecular biology and to brighten my spirits. I also want to thank all of the lab's support staff both at Columbia (Martine LeCorps) and at Yale (Willa Bellamy and Pat Sullivan) for their never-ending work for all of us. Without our lab managers, we would be helpless, so I want to thank Will Eng, Jaya Ahuja, and Iris Douglas.

I dedicate this thesis to my friends and family who have helped me through this long process. Specifically, I dedicate this to my parents Fred and Ava, my brother David, and my wonderful boyfriend Hillel, without whom I could not have done any of this.

CHAPTER ONE

INTRODUCTION

Neurons are responsible for transmitting sensory information in all animals from worms to humans. Dendrites receive a stimulus from a preceding cell, in the form of a neurotransmitter, which opens transmitter-gated ion channels, allowing sodium to flow into the cell resulting in an electric potential difference [1]. This electrical signal, called an action potential, then proceeds down the length of the neuron by opening potential-gated ion channels present along the plasma membrane, although the cell body and along the axon to the terminal branches, where it finally reaches the presynaptic bulb, a small reservoir before the synapse, the space between two neighboring neurons. At the presynaptic bulb, when the electrical impulse depolarizes the plasma membrane, voltage-gated Ca^{2+} channels open, resulting in a large increase in the local cytosolic calcium concentration. This triggers the release of neurotransmitters from the presynaptic cell, where they are stored in vesicles, which are docked in the presynaptic bulb and ready to be released across the synapse to the postsynaptic cell's dendrites, where they bind to transmitter-gated ion channels, and allow the electrical signal to further propagate to its ultimate destination, Figure 1 [1].

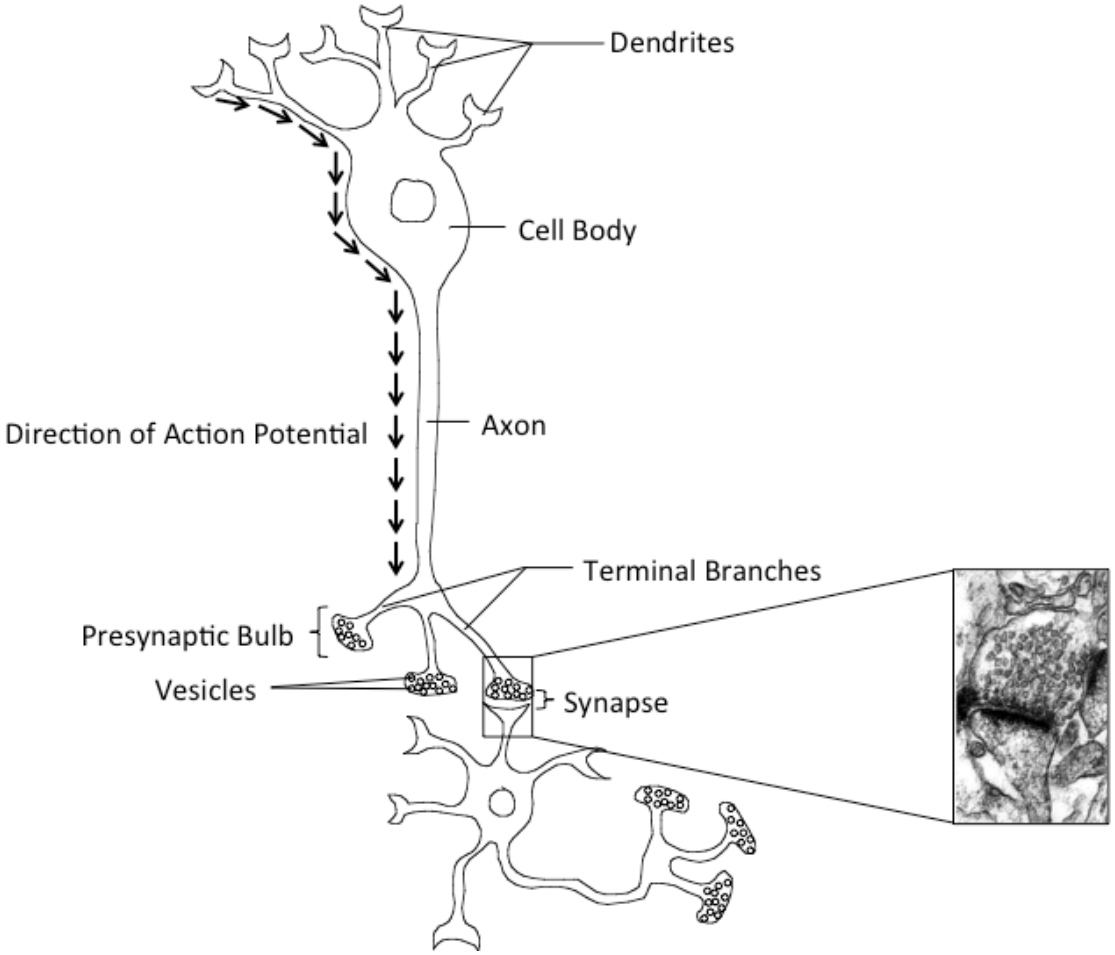

Figure 1: A diagram of two nerve cells with selected regions of the cell labeled to accentuate the regions involved in nervous signal transmission from one cell to a neighbor. The action potential proceeds from the dendrites, through the cell body, and along the axon before ultimately reading the terminal branches of the presynaptic bulb. Upon arrival of this electrical signal, calcium enters the presynaptic bulb and the vesicles, which had previously been building up in concentration, are rapidly and synchronously released. INSET: an EM micrograph from [7] showing the synapse. In the presynaptic bulb, vesicles have accumulated, awaiting an action potential, which will trigger their fusion to the neighboring cell's dendrite.

The mechanisms of these processes are starting to be more fully understood via both *in vivo* and *in vitro* experiments, but significant controversy still remains in some of the details, especially in the later stages of signal transduction. Specifically, questions remain as to how the action potential is able to cause synchronous release of vesicles on the order of less than one millisecond [2]. To understand the problem more completely, there is value in understanding the molecular mechanisms of cellular trafficking.

Cellular trafficking follows a relatively straightforward pathway [3-5]. Various molecules (like glutamate, hormones, and neuropeptides, [1]) are created in the endoplasmic reticulum or other parts of the cell and shuttled through the Golgi where they are enclosed in secretory vesicles which then bud from the *trans*-Golgi network and are transported along microtubules to their target membranes (Reviewed in [6], Figure 2). For neurotransmitters, this target is a region near the plasma membrane of the presynaptic cell called the presynaptic bulb, where they are observed to remain, primed and ready for fusion until the action potential signals their release, Figure 1, inset [7]. The action potential is an electrical signal which initiates fast fusion of the vesicles and allows the release of the vesicles' contents. This is in stark contrast with vesicle-target membrane in other parts of the cell [8]. In those cases, fusion is not arrested, awaiting an external signal, but rather rather the fusion process occurs asynchronously, whenever the vesicle arrives at the target membrane [9]. Understanding the mechanism of how vesicles fuse to target membranes is of extreme interest, as is understanding how synaptic vesicles specifically are able to achieve such precise temporal control over the fusion process unlike their counterparts in the other parts of the cell.

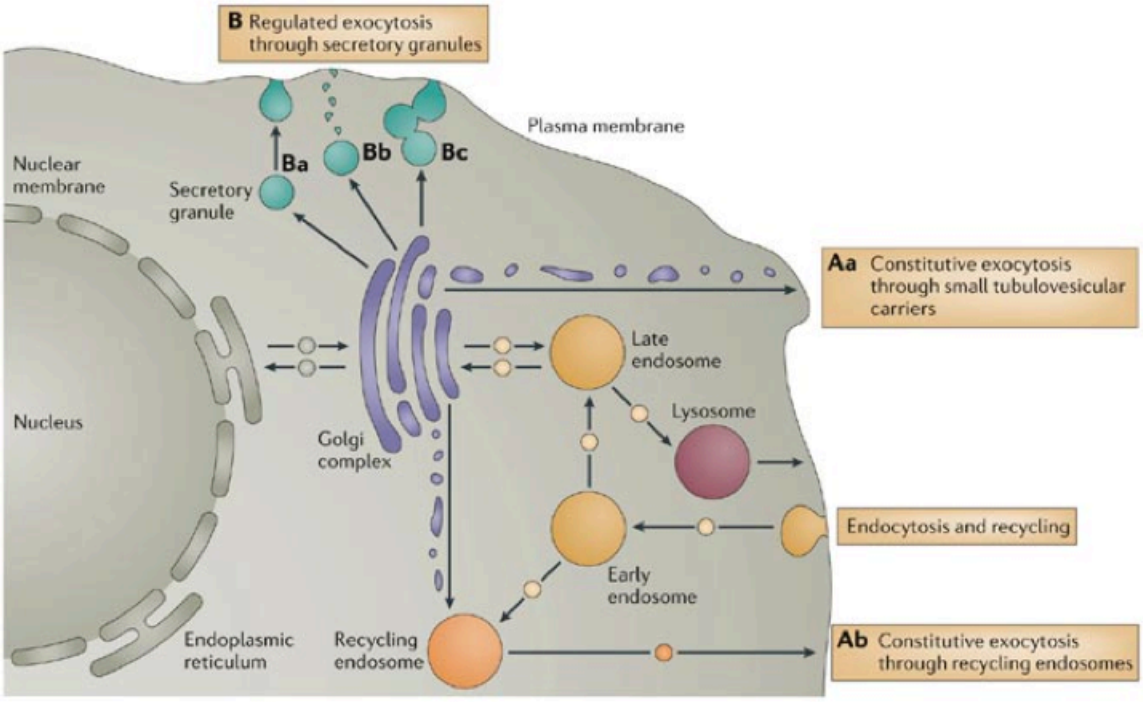

Figure 2: A diagram of cellular trafficking from [4]. Proteins and peptides are created in the ER, where they are enclosed in vesicles and shuttled to the Golgi, where these proteins are post-translationally modified and sorted. From the Golgi, the proteins can be sent to various cellular compartments like the endosome or the lysosome, or they can be exocytosed. It is the regulated exocytosis process that this thesis focuses on.

VESICLE FUSION TO TARGET MEMBRANES

The question of phospholipid bilayer fusion has been the subject of numerous biophysical and biochemical studies (for reviews, see [9-12], in which many aspects have been examined from the energetics [10, 13-19] and the mechanics [11, 18, 20] of fusion to the proteins responsible for providing the forces necessary to achieve such a technically difficult task so rapidly.

To fully appreciate the scope of this problem, it is useful to briefly consider the energy-intensive steps that have to be overcome to enable two membranes to fuse [10]. Before two membranes can fuse, the vesicle must be brought into close proximity with the target membrane, interstitial water molecules and proteins must be removed, from the interface between the two membranes and the repulsive forces between the charged headgroups on the lipid molecules must be overcome [9]. Further, most models of fusion have the two membranes locally puckering just before fusion occurs, as this state is more fusogenic due to the membrane deformation. The energy for such curvature deformations during fusion-pore formation and the ones that follow in the subsequent expansion of the fusion pore must also be overcome. Finally, and perhaps most importantly, the physical rupture of the outer leaflets and the inner leaflets of the membrane requires a significant amount of energy to occur. This process is depicted in Figure 3. The role of fusion proteins is to provide the energy that these processes require to allow fusion to occur. The energetics will be discussed more in depth later, after I fully introduce the proteins involved in fusion.

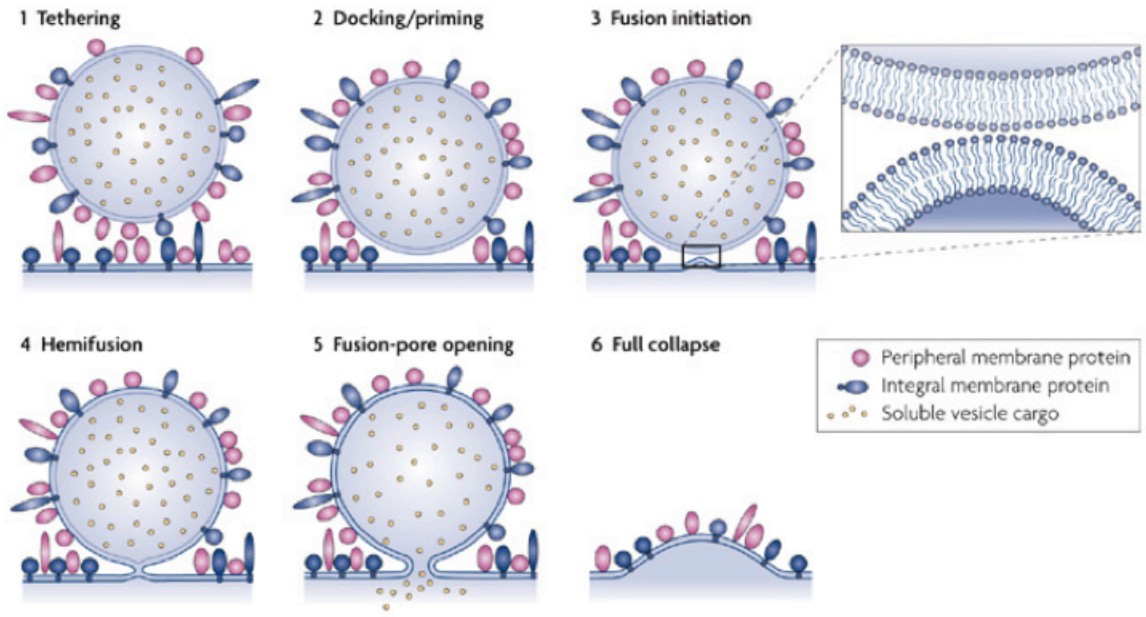

Figure 3: The steps involved in membrane fusion, from [95]. First, a vesicle is brought into close proximity to its target membrane by tethering factors. Then, as the interstitial proteins and water molecules are removed, SNAREs bring the membranes even closer together and provide the energy required for fusion. Fusion can be paused at this stage in exocytosis by certain regulatory factors like the Complexin family, which are discussed later. The two membranes then pucker towards each other, lowering the energy barrier to fusion. First, hemifusion, in which only the outer leaflets fuse, and then full fusion, in which both the outer and inner leaflets fuse, occurs. This is then either followed by quick resealing of the nascent fusion pore (called kiss-and-run) or rapid opening of the pore, and ultimately collapse of the vesicle into the target membrane.

STEPS OF MEMBRANE FUSION

Through biochemical evidence [9, 21], the following picture has emerged of how membrane fusion must occur, Figure 3. Briefly, the vesicle is first captured by so-called tethering factors like the exocyst, COG, GARP, or Dsl1 complexes (reviewed in [22]) located on the target membrane which are thought to bring the vesicle in close proximity with the membrane and position the membranes for optimal fusion. Then, resident proteins called SNAREs on both the target membrane (called t-SNAREs) and the vesicle membrane (called v-SNAREs) begin to interact with each other via their N-termini. These interactions lead to partial structuring of the SNAREs' N-termini into α helices. In the majority of fusion events in the cell, the SNAREs proceed to interact very quickly to form an extremely stable four helix bundle [23], and this interaction is thought to provide the energy for fusion [24, 25]. It certainly brings the vesicle even closer to the target membrane. Through some process, which may just be thermal fluctuations, but which might be protein-mediated, there is a local puckering of the membranes, which serves to ease fusion and allow for a stage called hemifusion in which only the outer leaflets of the membrane fuse to occur. This is followed by full fusion, where the inner leaflets of the membrane fuse too. The nascent fusion pore can then either reclose, in a phenomenon called kiss-and-run [26], or it can enlarge resulting in full release of the vesicles' contents.

Afterwards, the SNARE protein four-helix bundle is recycled to its individual proteins via an ATPase called NSF and its binding partner αSNAP to be ready for subsequent rounds of transport [26, 27]. Interaction of a hexamer of NSF and three

αSNAPs with the *cis*-SNARE complex leads to the formation of a transient 20S complex[28, 29]. ATP hydrolysis by NSF leads to the disassembly of this 20S complex as well as of the *cis*-SNARE complex. The freed v-SNAREs can then be recycled back to the donor compartment by retrograde vesicle transport, while the t-SNAREs can be reorganized into functional t-SNAREs, ready for the next round of vesicle docking and fusion [30].

HOW DO VESICLES FIND THE CORRECT MEMBRANE?

Fusion can occur at various membranes throughout the cell. To answer the question of how vesicles fuse in a specific manner, a more in depth understanding of the responsible SNARE proteins must be undertaken. SNARE proteins belong to a class of small (100-300 amino acids), and mostly unstructured [31] proteins, which, upon contact with relevant cognate partners, progressively gain alpha helical structure from their N- to C-termini to make parallel four helix bundles in a process referred to as "zippering" [32]. According to the SNARE hypothesis [33], only certain pairings of v- and t-SNAREs form productive four helix bundles, helping to provide the specificity for the fusion process. The examples in a mammalian cell of known cognate partners and where they occur are shown in Figure 4 [34]. Because the zippering process is thermodynamically favored [18], it can provide some or all of the energy to overcome the barrier to fusion. In theory, each helix in the four helix bundle can be provided by a different protein forming a quaternary complex; however, although in several cases, like in the synaptic SNAREs and SNAP25, one protein contributes two helices instead of one, making a ternary complex [34].

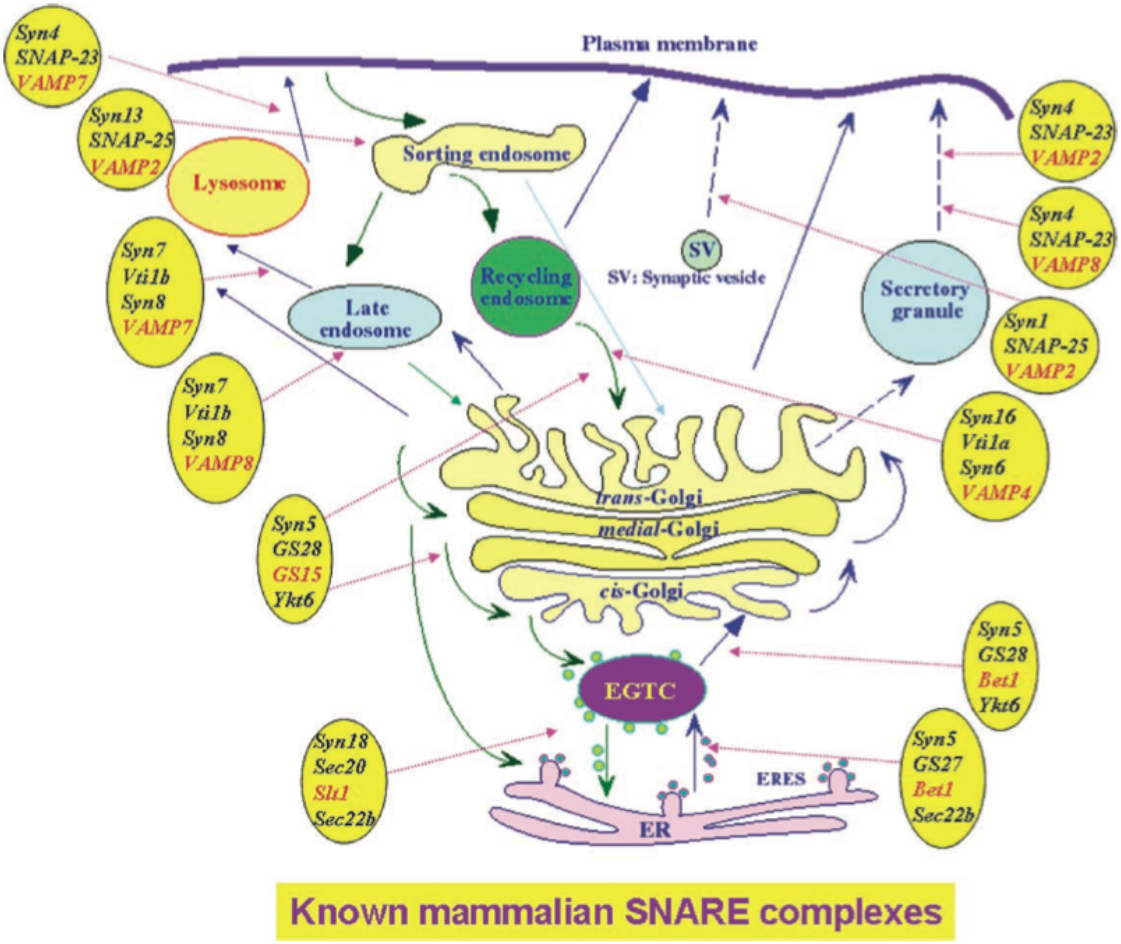

Figure 4: A diagram of the known SNARE complexes for many of the cellular trafficking events in a cell from [34]. The vesicle-associated SNARE is labeled in red. The main focus of this thesis, the synaptic vesicle is depicted in the top middle of the diagram as SV, and utilizes the SNAREs Syntaxin1 (Syn1), SNAP25, and VAMP2. Other abbreviations used in this figure are EGTC (ER Golgi Transport Container) and ERES (ER Exit Site).

STRUCTURE AND FUNCTION OF SNARES

Humans have 36 members of the SNARE protein family [34-36], and all members of this family either have transmembrane domains or palmitoylation or farnesylation motifs to tether them to the membranes [34]. The phylogenetic tree of the 36 SNAREs is shown in Figure 5 [34]. The majority of any individual SNARE protein, be it a v- or a t-SNARE, is expressed on the cytoplasmic side of the membrane [34]. For those examples which have transmembrane domains, there is often a short extracellular or intralumenal tail for t- or v-SNAREs, respectively.

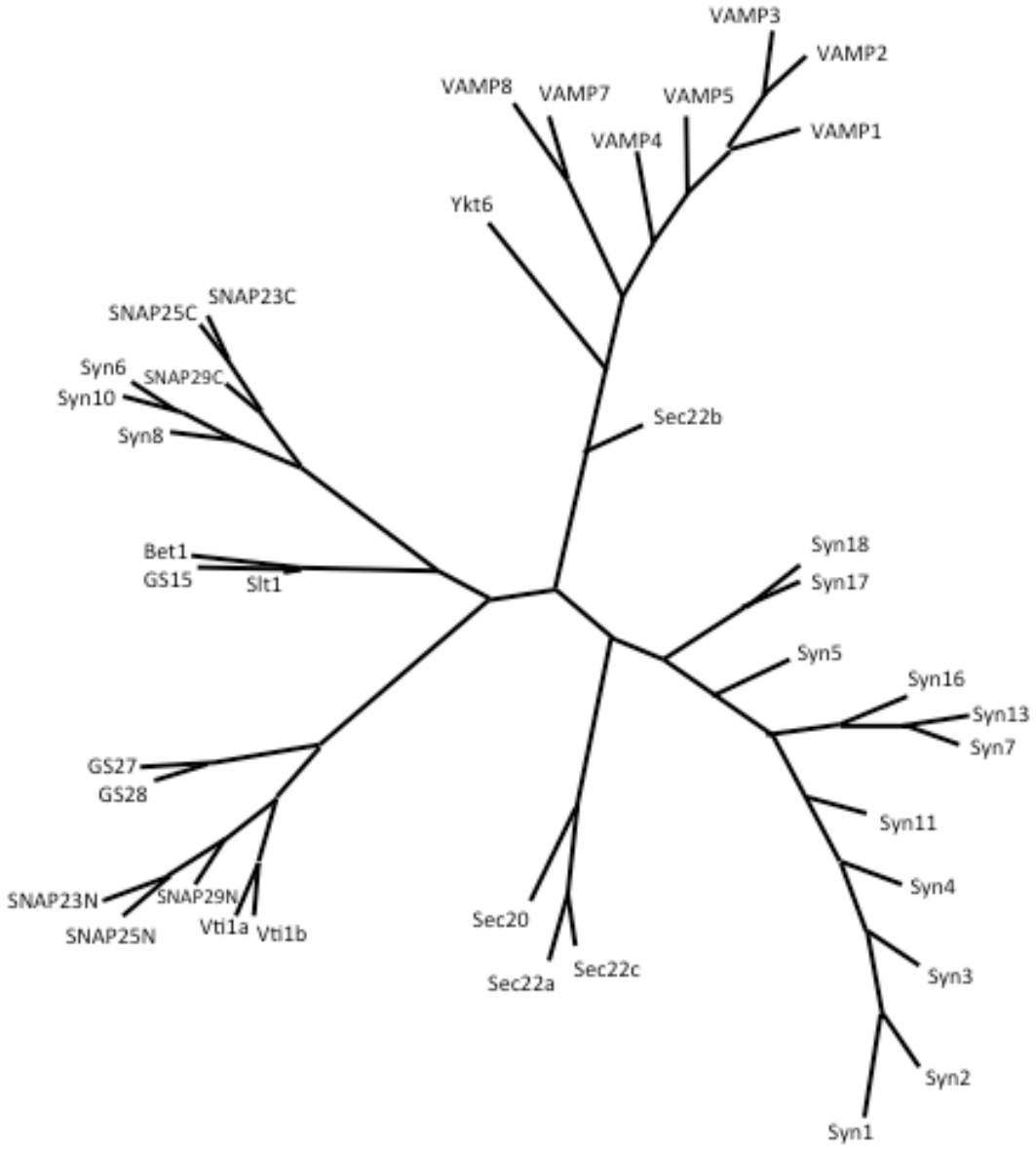

Figure 5: A phylogenetic tree of the SNAREs, adapted from [34]. SNARE four helix bundles form by using one helix from each of the four main brances of SNAREs. All but three SNAREs only possess one helix; those three occur twice on this diagram, once for each helix.

All SNARE proteins consist of a simple domain structure, Figure 6. The most characteristic domain of SNARE proteins is the evolutionarily conserved "SNARE motif," a stretch of between 60 and 70 amino acids arranged in heptad repeats, which form the basis for the alpha helical interaction domains of the SNARE four helix bundle. [27, 37-40] These are the domains that are responsible for the "zippering" from the N- to the C-terminus. This motif is characterized by 16 layers of interacting hydrophobic side chains which form the binding interface that keep the coiled-coil together [41]; all hydrophobic that is, except for a central "0" layer which contains three highly conserved glutamine residues and one highly conserved arginine residue[42]. The seven hydrophobic layers located N-terminal to the "0" layer are denoted as "-7" to "-1," while the eight layers C-terminal to the "0" layer are called "+1" through "+8." Most SNAREs (33/36 in humans) contain only one SNARE motif; the other three, like the neuronal SNAP25, contain two SNARE motifs, and are the proteins mentioned above which are capable of contributing two alpha helices to the four helix bundle. In 1998, Sutton *et al.* solved a crystal structure of the neuronal synaptic SNAREs' SNARE motifs[37]. In the crystal structure, Figure 7, the SNARE domains form a complex which is 12 nm long and between 1.3 and 1.5 nm in diameter[37].

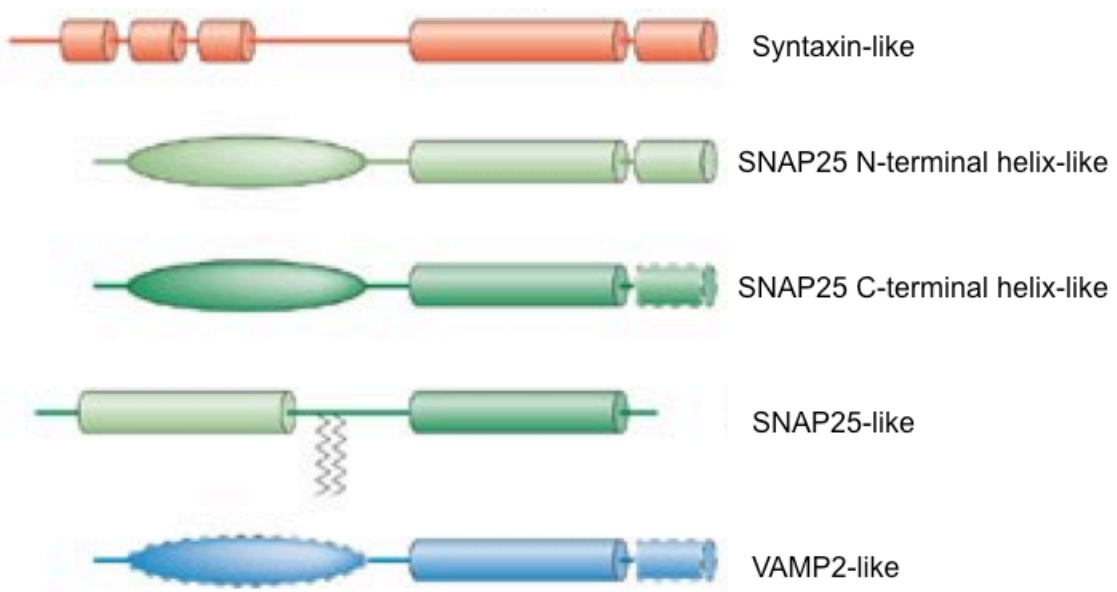

Figure 6: The generic domain structure of the SNAREs. The cylindrical domains represent alpha helices, while the zig-zag structures represent the SNAREs which are tethered to the membrane not by transmembrane domains, but rather by palmitoylation or farnesylation. The domains surrounded by dashed lines are not present in all members of each class of SNARE.

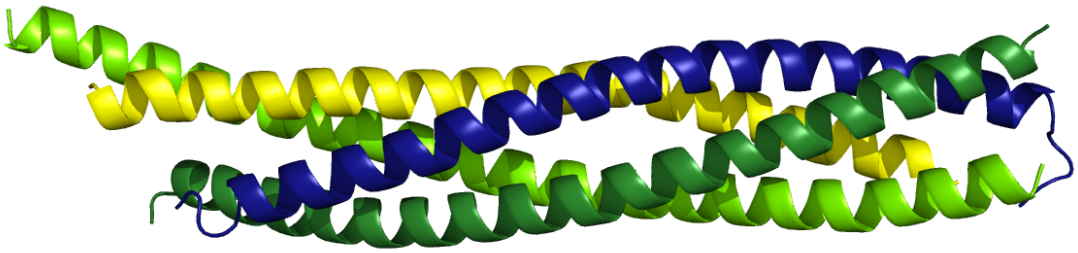

Figure 7: The SNARE domains of the neuronal synaptic four helix bundle [37]. The t-SNAREs are in yellow (Syntaxin1) and green (SNAP25; N-terminal helix is in lime; C-terminal helix is in forest). The v-SNARE (VAMP2) is in blue. The SNAREs are fully zippered into a parallel four helix bundle.

At the C-terminus, the majority (31/36 in humans) of SNAREs has a transmembrane domain which adjoins the SNARE motif via a short linker peptide [34].This transmembrane domain is required for fusion[39], and if it is disrupted, no fusion can occur. In fact, even if the linker between the four helix bundle and the transmembrane domain is disrupted, fusion is inhibited [43, 44]. The energy of zippering is transmitted through these domains and they are at least partially responsible for ensuring membrane fusion occurs. In addition, *in vivo*, for membrane fusion to occur, the zippering of the four helix bundle must be coupled energetically to the transmembrane region of the SNAREs. The insertion of flexible linkers between the SNARE motif and the transmembrane region either reduces or abolishes fusion both *in vitro* and *in vivo* [45]. Also, replacement of the transmembrane domain by lipid anchors allows vesicle docking, but it prevents fusion to a large degree[46].

Recently, a crystal structure was published of the neuronal SNAREs including their transmembrane domains[47], Figure 8, which showed that even in the membranes, in the *cis*-SNARE complex, the helicity is maintained throughout. This gives further credence to the necessity for helicity of the SNAREs in the fusion process. Because the transmembrane domains physically interact with both the inner and the outer leaflets [47] of the membrane, it is throught the interaction between the transmembrane regions of both v- and t-SNAREs may contribute to the transition from hemifusion to full fusion.

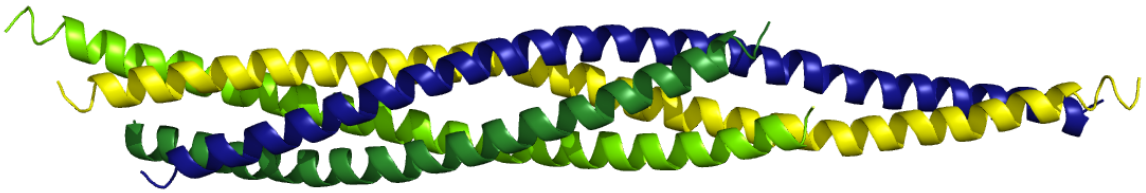

Figure 8: The SNARE domains of the neuronal synaptic four helix bundle, extended to include their transmembrane domains from [47]. Note that SNAP25 does not extend into the membranes. The t-SNAREs are in yellow (Syntaxin1) and green (SNAP25; N-terminal helix is in lime; C-terminal helix is in forest). The v-SNARE (VAMP2) is in blue. This crystal structure suggests that the transmembrane domains are helical throughout the membrane.

A smaller majority (26/36 in humans) also has some sort of N-terminal domain [34]. The proteins without N-terminal domains are called "brevins," and included in this category is the neuronal protein VAMP2, also called synaptobrevin [48], as well as VAMP3 [49], called cellubrevin, a protein which can substitute for VAMP2 *in vivo* [49, 50]. There are a few subclasses of proteins with N-terminal domains, most of which are inhibitory towards four helix bundle formation. One subclass consists of an antiparallel three-helix bundle, called an Habc domain. (An example of this class is the neuronal protein Syntaxin1 (SYN).) [51-53]. The Habc domain is connected to the SNARE motif by a flexible linker, and it can reversibly associate with the SNARE motif to form a four-helix bundle known as a "closed" complex, which effectively prevents interaction of the protein in question with other SNAREs, rendering it incapable of forming a productive four-helix bundle. Another class of N-terminal domains in the SNAREs are the longin domains, which form a beta-sheet surrounded by three alpha helices[54]. It appears these longin domains have a similar inhibitory function to Habc domains. This "closed" conformation must be opened by a regulatory protein (like a member of the SM class of proteins including Munc18 which works on the neuronal t-SNARE syntaxin) before and/or during the assembly of the SNAREs [51, 55, 56]. This provides a mechanism by which membrane fusion pathways can be regulated at an early state in the fusion pathway, before the SNAREs even associate, if fusion is for some reason undesirable.

NEURONAL SNARES

Because this thesis focuses specifically on synaptic vesicle fusion, there is

further benefit to discuss the history of the SNAREs involved in this complex, the t-SNAREs, SNAP25 and Syntaxin1, and the v-SNARE, VAMP2 [34, 39].These proteins were among the first SNAREs to be discovered because of their prevelance in the synapse[48, 57, 58] as well as though their interactions with other prevalent synaptic proteins like NSF [34, 59]. NSF (N-ethylmaleimide Sensitive Fusion protein) was discovered in 1988 by Rothman and colleagues[60] as a protein which rescues Golgi transport upon blocking by N-ethylmaleimide (NEM). In 1990, Rothman and colleagues[61] discovered a class of proteins which physically interact with NSF called Soluble NSF Attachment Proteins (SNAPs), as a set of proteins thought to be involved somehow in membrane fusion. Recall, these are the proteins responsible for disassembly of the SNARE complex[30].

VAMP2 and SNAP25 were both discovered in 1989. VAMP2, the neuronal v-SNARE by Elferink *et al.* [48] and SNAP25, one of the neuronal t-SNAREs by [57], both as widely expressed neuronal proteins. VAMP2 has a transmembrane domain[48], while SNAP25 has a CAAX box which is post-translationally palmitoylated, tethering it to the membrane without a transmembrane domain [36]. Syntaxin1, the other synaptic t-SNARE, was discovered in 1992 by Bennett *et al.* [58] as a 35 kDa protein that interacts with another prevalent synaptic vesicle-associated protein called Synaptotagmin, which is an important SNARE regulatory protein, and will be discussed more in depth later. Rothman and colleagues [59] recognized that all of these proteins were binding partners of SNAPs and named them SNAP Receptors (SNAREs) in 1993 [59].

THE SNARE FUSION PATHWAY

To understand the temporal control synapses have over fusion, it is vitally important to understand the steps involved in SNARE-mediated fusion. The general consensus is that SNAREpin assembly itself occurs in a stepwise manner, starting at the amino-terminal, membrane-distal end of the SNARE motif and proceeding toward the carboxy-terminal, membrane-proximal end[35, 62-65]. Initially, the membrane-proximal regions are largely unstructured and are targets for regulatory components that either accelerate or delay SNAREpin assembly [24, 42, 65-68]. Once the N-terminal portions of the SNARE domains of the v- and t-SNAREs are zippered, the remainder of the t-SNARE domains begin to form α helices, forming so-called "acceptor" complexes[24, 39, 69, 70], ready for the v-SNARE to continue to zipper up and provide the energy needed for fusion. Figure 9 shows a schematic of the steps of SNARE association.

Another question debated in the field is how many four helix bundles, also known as SNAREpins, are required for fusion to occur. In PC12 cells, at least three SNARE complexes seem to be required to fuse secretory granules with the plasma membrane [71]. And in another study, between 5 and 8 were suggested based on sterics of interaction.[72] Karatekin *et al.* showed that the number of SNAREpins required for fusion is between five to ten[73]. A much higher number (10-15) was predicted by titrating in neurotoxins into cultured neurons.[74] Though, somewhat contradictorily, it has been observed that only one SNARE complex is sufficient for fusion [75] via single molecule studies. Furthermore, the minimal number of required SNAREpins is likely influenced significantly by membrane curvature, the lipid/protein composition of a compartment, and the presence of lipid bilayer perturbing regulators [55]. That said, it is

generally assumed that between five and ten SNARE complexes are required for exocytic vesicle fusion within neuronal cells.

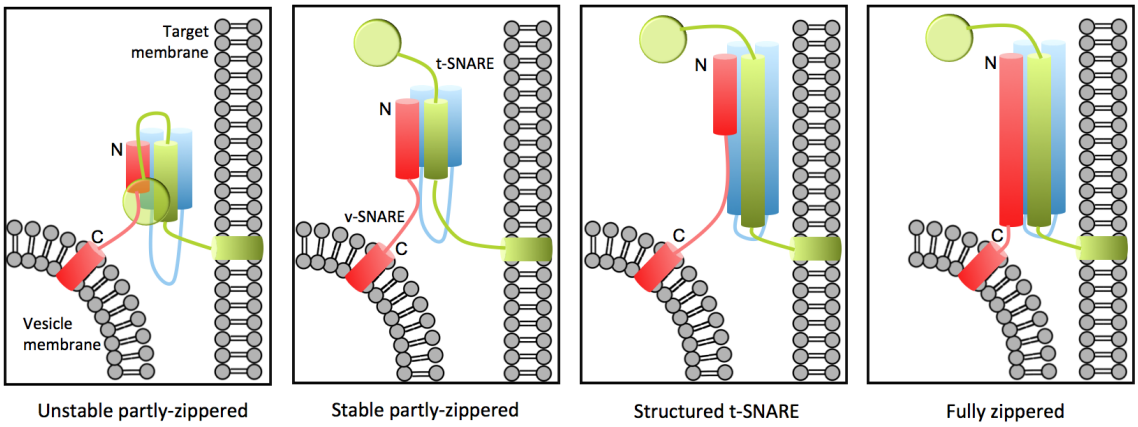

Figure 9: The steps of SNARE-mediated fusion, adapted from [65]. First, when the SNAREs associate, they do so via their N-termini. The SNAREs then structure and zipper form their N- to C-termini. The t-SNAREs may associate with each other first, forming what is called an "acceptor" complex, to which a v-SNARE can then associate via its N-terminus, forming a *trans*-SNARE intermediate. This state proceeds rapidly to a fully zippered SNARE complex unless acted upon by a regulatory protein like Complexin.

It has, however, been shown that different t- and v-SNARE-containing complexes can form *in vitro*. Such different t- and v-SNARE states can exist on a timescale of seconds, as shown by single-molecule FRET measurements. For example, Weninger *et al.* [76] showed that *in vitro*, as many as 88% of SNAREs do not form parallel four-helix bundles at any given time. And that although parallel four-helix bundles presumably correspond to the lowest energy state [76], suggesting there must be folding and refolding that can occur, at least *in vitro*, suggesting the possibility of similar occurrences *in vivo*.

Other *in vitro* single molecule experiments on both exocytic *S. cerevisiae* and synaptic SNARE complexes [24, 69, 70] have shown that SNARE complex assembly proceeds through a defined and partially helical t-SNARE intermediate, the formation of which is rate limiting. This suggests, not surprisingly, that assembly is an ordered, sequential reaction rather than a random collision of four SNARE motifs[39]. Only when an "acceptor" t-SNARE complex, possibly lacking a v-SNARE in which the N-terminal ends of the t-SNARE SNARE motifs are structured is the v-SNARE able to bind with biologically relevant kinetics and initiate the zippering reaction. It is important to note that this "acceptor" complex is theoretical and has never been experimentally observed.

Acceptor SNARE complexes lacking the v-SNARE and containing only t-SNAREs are expected to be highly reactive, extremely transient species, explaining why they are notoriously difficult to characterize[39]. For example, *in vitro*, the neuronal acceptor complex quickly recruits a second syntaxin, leading to the formation of a "dead-

end" complex, consisting of a four-helix bundle, two helices from one SNAP25, and one each from two different Syntaxin molecules [69]. This interaction prevents the binding of the v-SNARE altogether and may be responsible for the observed *in vitro* slow kinetics of core complexes.

There has been until now, very little information regarding the existence of acceptor t-SNARE complexes *in vivo* or in intact cells[77-79]. Furthermore, upon recognition of the v-SNARE by the t-SNARE-acceptor complex, a *trans*-SNARE complex, in which the t-SNAREs are fully zippered while only the N-terminal SNARE domain of the v-SNARE is α-helical and zippered, is formed[39]. *Trans*-SNARE complexes are also extremely short-lived structures and attempts to isolate them have included the detergent solubilization of membranes [39], which ultimately resulted in their immediate conversion from partially-zippered *trans*- to fully-zippered *cis*- forms.

The best *in vivo* evidence for the existence of *trans*-SNARE intermediates comes from the study of regulated neuronal exocytosis. Because neuronal exocytosis is regulated at a late step just before membrane fusion, it is unlike other intracellular fusion events[80]. Recall that vesicles sit, docked at the plasma membrane, primed, and ready for fusion, but unable to fuse until the action potential signal arrives [1, 2]. In this circumstance, it is probable that metastable *trans*-SNARE complexes exist [80] and are responsible for this docked state. Evidence for this is provided by the observation that, in chromaffin cells, kinetically distinct pools of vesicles, potentially representing sequential steps along the exocytosis pathway, can be distinguished by electrophysiological methods like patch clamp [39]. SNARE assembly has been perturbed in these cells by various

means, including the use of SNARE-cleaving toxins, anti-SNARE antibodies, and the expression of SNAP25 and VAMP variants in knockout cells[80, 81], and exocytosis is reduced when using manipulations that are expected to impair the zippering of SNAREs. The data are best explained by a model in which there is an equilibrium between free SNAREs and partially zippered *trans*-SNARE complexes before exocytosis [39, 80]. To date, it has been impossible to characterize the *trans*-SNARE complexes better than this *in vitro* because of the *trans*-SNARE complex's inherent instability and propensity to zipper into a four helix bundle. This charicterization was overarching goal of my graduate research.

Several assays have been developed to examine SNAREpin formation *in vitro*. In one assay, diagrammed in Figure 10, SNARE proteins are incorporated into liposomes containing either both of the fluorophores NBD and rhodamine (the v-SNARE liposomes) or neither fluorophore (the t-SNARE liposomes). The presence of rhodamine in the v-SNARE vesicles quenches the fluorescence of NBD (7-nitro-2-1,3-benzoxadiazol-4-yl) via FRET, but when fusion occurs, so does lipid exchange, meaning the dye-labeled lipids move further apart and the energy transfer between the two fluorophores decreases, causing an increase in NBD signal. Thus, fusion can be measured as an increase in fluorescence. This method has been used in many papers [45, 82-86] but suffers from the limitations that (1) it's been strictly an in vitro assay, (2) it's involving the fusion of two vesicles, not a vesicle and a flat membrane, and (3) the observed kinetics are signifcantly slower than that what occurs in live cells [87, 88].

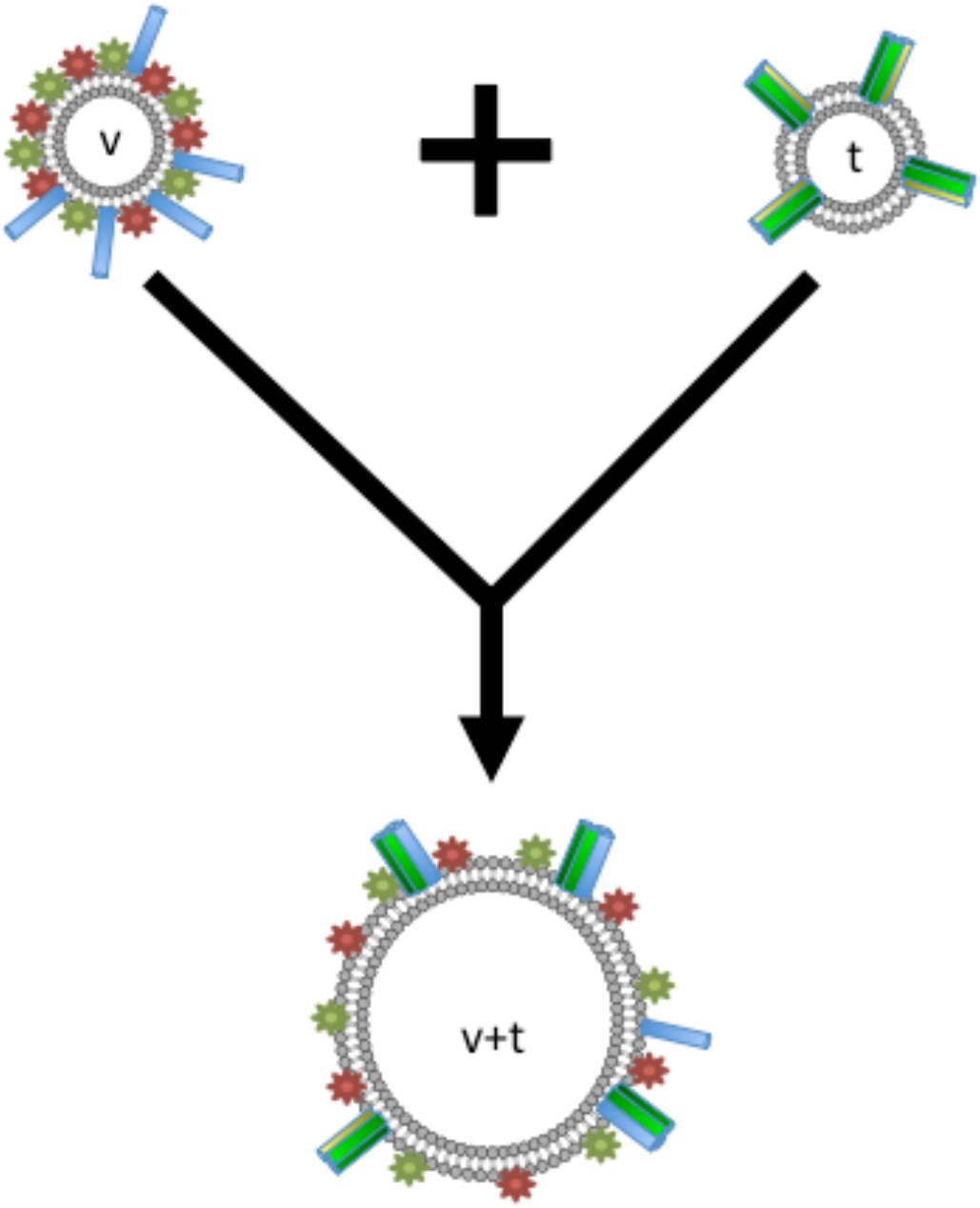

Figure 10: A schematic of the Liposome Fusion Assay. A liposome containing both v-SNARE (blue cylinders) and the fluorophores NBD (green stars) and Rhodamine (red stars) is allowed to interact with a liposome containing t-SNAREs (yellow and green cylinders) and no fluorophore. Before fusion NBD fluorescence is quenched by the rhodamine's proximity. Once fusion occurs, though, the liposome increases in size, allowing the NBD and rhodamine to separate in space, which in turn allows NBD to fluoresce, as it is no longer quenched by rhodamine. Fusion is thus measured as an increase in NBD signal.

In a more biologically relevant assay, the formation of a SNARE complex can facilitate fusion between cells when expressed with complementary SNARE motifs exposed outside the cells, depicted in Figure 11. That is, if the v-SNARE is expressed on the cell surface of HeLa cells expressing a red cytosolic marker, and if the t-SNAREs Syntaxin1 and SNAP25 are coexpressed on the cell surface of HeLa cells expressing a blue nuclear marker, after an overnight incubation, fusion can be observed by looking for red cells with blue nuclei. This powerful assay is called a cell-cell fusion assay or a flipped-SNARE assay, and it is useful to determine the fusogenic capability of individual SNAREs, both wild type and mutant, in a more *in vivo* manner. This assay too has been used in several assays[89-92] and despite its extreme power, it suffers from a fuew limitations too. For example, the membranes which fuse here are not the same dimensions as what occurs in vivo. Also, the time resolution on this assay is one day, so kinetics are impossible to discern.

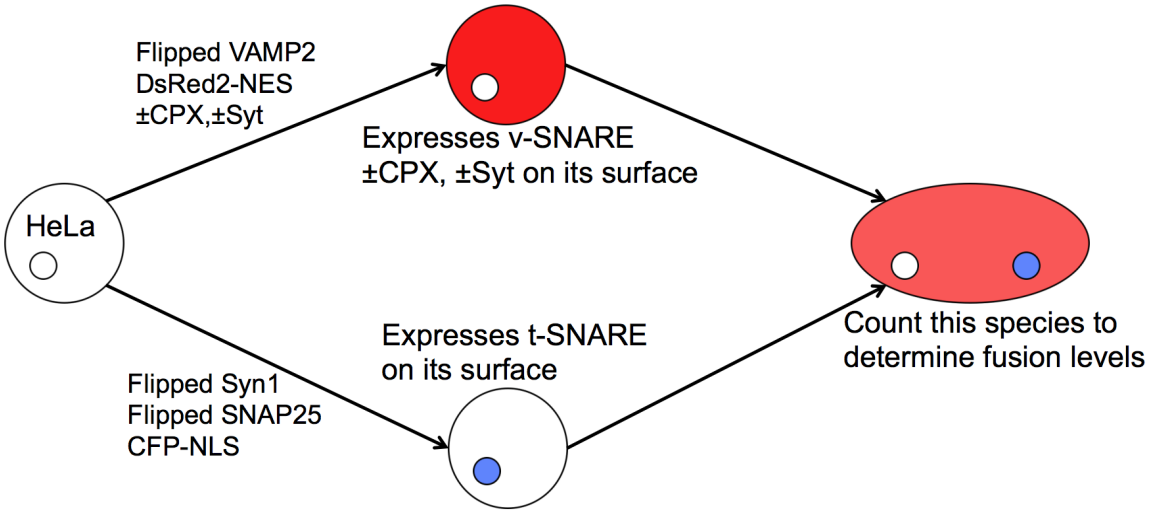

Figure 11: A schematic of the Cell-Cell Fusion Assay. A subpopulation of HeLa cells containing t-SNARE on its surface is created so that it has a blue marker targeted to its nucleus. Another subpopulation of HeLa cells containing v-SNARE on its surface has a red marker targeted to its cytoplasm. These two subpopulations are allowed to interact and fuse over night at 37°. The next day, fusion is measured by examining how many cells have both red cytoplasms and blue nuclei.

ENERGETICS OF SNARE FUSION

Since cognate v- and t-SNAREs fuse membranes without an additional input of energy or other proteins as demonstrated by both the cell-cell and liposome fusion assays [82, 92], it is assumed SNARE zippering provides enough energy to overcome the repulsive forces that keep membranes apart. The energy results from the formation of an extremely tight-binding four-helix bundle. In fact, fully assembled SNARE complexes are so stable, they can even resist both SDS and thermal denaturation up to 90°C [37]. It is worthwhile to examine the rare stability of this protein complex

Indeed, as the SNARE complex assembly zippers up from the N-terminal side and progresses toward the C-terminal end, 35±7 k_BT (around 20 kcal/mol) of energy is provided as calculated from Surface Force Apparatus (SFA) experiments, [18] and this may be enough energy to overcome the energy barrier due to membrane opposition resulting from the immense dehydration forces which has been calculated to be around 40-50 k_BT [18, 93]**.** At the minimum, SFA measurements establish SNARE fusion provides enough energy to hemifuse opposing membranes [19]. The transition of several membrane-bound, pre-fusion *trans*-SNARE complexes to *cis*-SNARE complexes is thus likely to enable fusion of the two membranes. The activation energy for lipid bilayer fusion has been calculated to be in the range of 50-100 k_BT, so it is likely that more than one SNARE complex is required to provide enough energy to drive fusion. And while it is possible that the driving force for membrane fusion might arise from other sources, for example, from the energy of protein-lipid interactions or from other, non-SNARE

protein-protein interactions, it is extremely unlikely. This suggests that membrane fusion occurs spontaneously upon zippering of the SNAREs. While this may be desirable for many biological instances, it is certainly not desirable in all biological circumstances.

Because *trans*-SNARE complexes are so unstable and have a high propensity toward zippering, at a synapse there must be a layer of control over the spontaneity of fusion to ensure synchronous and specific release of vesicle contents upon the arrival of the action potential. Without it, nerve cells would constitutively fire at low levels, causing a lack of specificity with regard to nerve cell function. In order to provide that layer of control, neurons contain two proteins which help regulate this process, Complexin and Synaptotagmin. These proteins can either raise or lower the energy required for fusion, and either inhibit or facilitate the fusion. Complexin and Synaptotagmin are thought to be involved in the late stages of SNARE-mediated fusion[94], when the t-SNARE is mostly zippered but only the N-terminus of the v-SNARE is in the four helix bundle. Because this thesis mostly focuses on Complexin, Synaptotagmin will only be discussed briefly, and the reader is referred to a number of excellent reviews on the subject[64, 85, 95-97].

COMPLEXIN

In order to prevent asynchronous release in synaptic fusion, nature has devised a clamp/release system which can prevent fusion until the appropriate signal given, while still allowing vesicles to build up at the synaptic terminal, and securing a large burst of neurontransmitter once an action potential does arrive. This clamp protein is likely a member of the Complexin (CPX) family. Complexins were first identified in 1995 by

Ishizuka *et al.* and McMahon *et al.*, nearly simultaneously. Ishizuka *et al.* described CPX as a 19kDa protein which copurifies with the SNARE complex, irrespective of the detergent used for the solubilization of the complex, suggesting Complexin binds so tightly that it does not dissociate from the complex. In fact, even in the presence of 0.5 M NaCl, CPX remains associated with the SNARE complex. They identified Complexin as a 134 amino acid protein with a prediction of significant alpha helicity throughout[98]. McMahon, *et al.*, on the other hand, isolated Complexin based on a search for proteins which regulate the SNARE complex, as a family capable of competing with αSNAP for binding to the SNARE[99]. Both laboratories discovered that Complexin is a soluble, highly charged protein[99, 100].

Since its initial discovery, the Complexin family has been found to have four isoforms in mammals[101]. CPX1 and CPX2 are widely found in to be expressed in the central nervous system[102], but CPX2 is also found relatively ubiquitously, and functions in other secretory cell systems [2, 103]. CPX3 appears at very low levels in the brain but primarily in the retinal rod cells[101], while CPX4 appears solely in the retinal rod and cone cells[101]. CPX1 and 2 share ~80% amino acid identity[104] while CPX3 and 4 share ~60% amino acid identity to each other, but not to CPX1 and 2 (to which they only share about 25% identity) [2, 105]. CPX3 and 4 also possess CAAX boxes at their C-termini which tether them to the membranes via prenylation.[101] Some say CPX2 is in excitatory neurons, whereas CPX1 is in inhibitory neurons[104, 106-110], but that's since been discounted.[102] Also, the kinetics of fusion of CPX3 and CPX4 make them suited for the retina.[111] This protein familiy is highly conserved throughout

species with CPX being more than 39% amino acid from *C elegans* to mice. Disruptions in CPX function have been associated with many disorders including, but not limited to Schizophrenia[112] , Huntington's disease[113-117], depression[118-121], bipolar disorder[119, 122, 123], Parkinson's disease[124, 125], Alzheimer's disease[126],ataxia [127, 128], traumatic brain injury[129], social behavior defects[121, 130], cognitive function defects [131],Wernicke's encephalopathy[132], and fetal alcohol syndrome[133, 134]. Of these, the link between CPX2 and schizophrenia has been the subject of great interest of late, as disruption of CPX2 has been shown to be a marker for Schizophrenia[106, 107, 112, 119, 120, 122, 135-140]. On the other hand Fung *et al.* recently have suggested that CPX1 or CPX2 expression does not correlate with Schizophrenia at all [141].

HOW DOES COMPLEXIN REGULATE SYNAPTIC VESICLE FUSION?

Initial biochemical studies showed that both Complexin-1 and Complexin-2 interact with assembled SNARE complexes through a central α-helical domain, located at residues 48 to 70 in mammals, termed, appropriately, the Central Helix [142]. Complexin does not bind individual SNARE components[99] or influence NSF/αSNAP-mediated disassembly of SNARE complexes[143]. It can, however, weakly bind a t-SNARE complex[144]. The binding of CPX to SNARE complexes depends on the Syntaxin isoform present[145], and CPX1binds most tightly to, the neuronal syntaxin isoform, Syntaxin-1[143, 146]. CPX binds to soluble, assembled, neuronal SNAREpins in a 1:1 stoichiometry with k_{on} and k_{off} rates of $3.1 \bullet 10^{7}$ $M^{-1}s^{-1}$ and 0.31/s respectively[147]. That is, Complexin binds SNARE complexes rapidly and with high

affinity, given its k_D value, 10 nM[147]. How does the function of CPX result from this tight binding, which is restricted to the fully formed SNARE complex?

The X-ray crystal structure of the neuronal SNARE-complexin complex, solved in 2002[142, 148], helps to answer this question. It is depicted in Figure 12 and shows that a single CPX molecule binds in an antiparallel fashion, directly in the groove formed between the VAMP2 and the Syntaxin-1 helices in the four helix bundle. This binding occurs via Complexin's Central Helix, in agreement with the *in vivo* requirements for the Central Helix to function properly [145, 149-152]. Also shown in the crystal structure is a more N-terminal, Accessory Helix, residues 27-47, demonstrated to be responsible for Complexin's actual clamping activity [151, 152]. In the crystal structure, this Accessory Helix is running alongside the four-helix bundle without making any physical interactions with the SNAREs themselves. From this structure, it is difficult to predict a mechanism of clamping via the Accessory Helix.

Sadly, the currently available structural data on the Complexin-SNARE complex do not provide information on Complexin's protein domains outside of its Central and Accessory Helices, the aptly named N-terminal and C-terminal domains as they are likely to be unstructured[143]. However based on deletion and mutation studies, the N-terminal domain is thought to be faciliatory to fusion by somehow interacting with the C-terminal domains of the SNAREs[151, 153], or potentially interacting with lipid membranes [151, 154] perhaps by helping them to form α helices, so a structure of this domain would be especially interesting. To this end, Met5 and Lys6 appear to be the most important residues in this region [153]. Interestingly, in *C. elegans*, the N-terminal

domain does not seem to have any effect whatsoever on fusion [152].

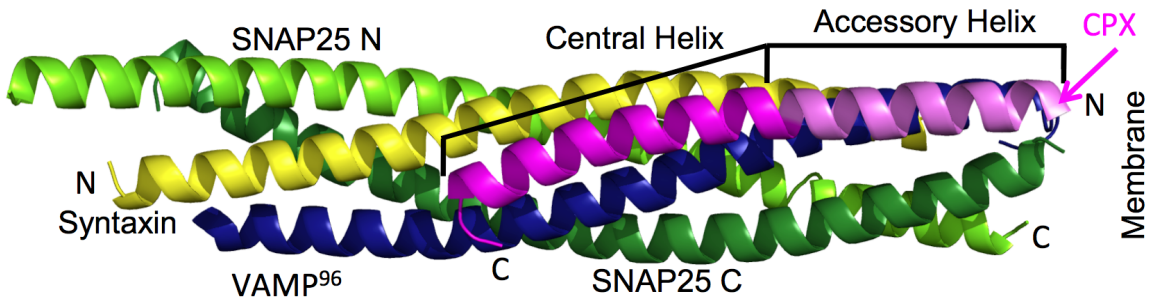

Figure 12: The crystal structure of the SNARE four helix bundle with Complexin's Central and Accessory Helices from [142]. The four helix bundle is the same as that without Complexin; namely, it is parallel and fully zippered. Again, the t-SNAREs are yellow (Syntaxin1) and green (SNAP25). The VAMP2 is blue. The Complexin molecule is represented in magenta. It runs alongside the four helix bundle in the groove between VAMP2 and Syntaxin in an antiparallel fashion. The Central Helix (dark magenta) is responsible for interacting with the four helix bundle, and the Accessory Helix (light magenta) is responsible for the clamping, but the mechanism of clamping is not clear from this structure. The N- and C-terminal domains of Complexin are not present in this X-ray structure.

Further, structural knowledge of the C-terminal domain would be of use given its somewhat mysterious role in the fusion process. Both Xue *et al.* and Martin *et al.* suggest this domain is inhibitory [150, 152], while Malsam *et al.* demonstrate this domain is facilitatory to fusion [83], perhaps through a predicted amphipathic helix which likely targets the C-terminal domain to the membrane [84], and may help deform the membrane, priming it for fusion. In fact, S115 in the C-terminal domain has been shown to have a putative phosphorylation site [83, 151, 153, 155], and this prevents binding to the membrane, suggesting a potential regulatory role for the C-terminal domain of Complexin. Mutation of this serine to an alanine, aspartate, or glutamate resulted in a decrease in facilitatory function of the C-terminal domain [83], while mutation of a nearby residue to a tryptophan (L117W) increased the Complexin's facilitatory function [84], likely by anchoring the amphipathic helix into the membrane. This further confirms membrane binding is somehow relevant for the facilitatory function of CPX's C-terminal domain. Because of these distinct functions for individual domains of CPX [151, 152], much debate has occurred about the true nature of Complexin's function.

IS COMPLEXIN A CLAMP?

In synaptic vesicles, after the vesicles have docked, the *trans*-SNARE structure forms and keeps vesicles at the target membrane, ready to fuse [39]. Under the majority of circumstances, SNAREs proceed through the *trans*-SNARE state very quickly, and fusion occurs on the order of less than 1 ms [2]. But at the synapse, a clamp protein is required to prevent this rapid fusion; nerve cells require strict temporal control over neurotransmitter release for obvious reasons. As a result of various *in vitro* and *in vivo*

experiments, it has been postulated that Complexin may, in fact, be this clamp. However, there is significant controversy regarding this hypothesis because depending on cell type, organism, experimental approach, or domains of Complexin used, directly opposite results are obtained. In the next few paragraphs, I intend to describe the arguments for and against Complexin as a clamp.

In the earliest studies of Complexin function, injection of antibodies against mouse CPX2 into the sea slug *Aplysia* ganglia was found to increase transmitter release, while injection of rat CPX2 decreased it [156], suggesting an Complexin has an inhibitory effect on fusion. Further, overexpression of Complexin 1 or 2 in various cell lines decreased exocytosis [157]. In PC12 cells, release of acetylcholine and dopamine, was decreased [158, 159]; in insulin-secreting β cells, insulin exocytosis was decreased [160]; in *X. laevis* oocytes and renal cell lines [161], exocytosis-mediated surface expression of epithelial sodium channels was decreased, and in chromaffin cells [162], release was slowed. Furthermore, overexpression of a CPX1-VAMP2 fusion protein in wild-type GABAergic cortical rat or mouse neurons decreased spontaneous fusion events as well as evoked calcium-triggered release [157]. Into *Drosophila melanogaster* KO mutants, when all four mammalian Complexins were individually added back, all functioned as fusion clamps [163]. On the other hand, overexpression of Complexin had no effect on release in mouse hippocampal neurons (CPX1) [151] or glutamatergic hippocampal neurons (CPX3 & 4)[164]. In porcine oocytes, CPX is responsible for the docking process of cortical granules [165]. Furthermore, *in vitro* studies of Complexin have demonstrated it does, in fact, act as a clamp in both the cell-cell fusion [91] and

liposome fusion assays [166]. Based on these lines of evidence, having extra Complexin in a cell is conducive to clamping fusion.

On the other hand, antibody attempts to perturb CPX function as well as Complexin knockouts often lead to the conclusion that CPX has a faciliatory role in fusion. For example, injection of a Complexin "blocking peptide," meant to disrupt Complexin's interaction with Syntaxin in squid giant presynaptic terminals reduced neurotransmitter release [167]. The introduction of anti CPX1/2 antibodies into permeabilized human sperm cells decreased acrosome exocytosis [168]. Antisense knockdown of Complexin in renal cells decreases exocytosis[169], as does RNAi knockdown of CPX1 in insulin-secreting β cell lines [160], and antisense DNA-mediated knockdown of CPX2 in mast cells [169]. Knockouts of CPX in mouse hippocampal neurons [102], sperm [170], *D. melanogaster* neuromuscular junctions [171], and vertebrate autapses [102, 151] have all decreased exocytosis. Thus, the removal of Complexin appears to decrease fusion as well, suggesting a facilitatory role for the protein in membrane fusion. On the other hand knockout of *D. melanogaster* CPX actually stimulates calcium-independent fusion in neuromuscular junctions [171], suggesting an inhibitory role. And KO of CPX1 in mouse auditory synapses impaired synchronization of release [172]. Furthermore, deleting Complexin in *C elegans* decreases calcium-evoked release, but increases non-calcium-specific "tonic" release [152, 173]. Other *in vitro* experiments suggest Complexin stimulates fusion [83, 144]. Clearly the understanding of Complexin's function *in vivo* is lacking.

Because of this debate, many labs have settled on the conclusion that

Complexin has a dual function [144, 151, 152, 154, 163, 173-175]. And while this is an attractive model, the mechanism remains unexplained. Perhaps, as Xue *et al.* suggest, various domains of CPX in various species interact differently and are inhibitory or facilitatory to various extents [150]. Another option is that the protein operates differently at different times; it may facilitate fusion by interacting with the SNAREs to help their N-terminal regions to come together but then arrest fusion by blocking the association of the v-SNARE's C-terminal domain with the remainder of the four helix bundle. The differences among species may be due to slight variations in the sequences of the N-terminal domain, the Accessory Helix, or the C-terminal domain. Surely the interplay among all four domains of Complexin warrants further study.

Assuming CPX is a clamp, or at the very least that its Accessory Helix does clamp SNARE fusion, an unanswered question in the field has been just how it clamps the SNARE assembly in the *trans*- state, and with which domains of the synaptic proteins it interacts at this state. In the Complexin-SNARE complex crystal structure [142], the Accessory Helix is localized near the SNARE domains' C-termini which link the SNARE motifs of VAMP2 and Syntaxin with their respective transmembrane domains. Thus, one possibility proposed by both Tang *et al.* and Brose [2, 157] is that the Accessory Helix simply has a sterical effect; that is, it might interfere with the full zippering of the SNARE complex, and thereby prevent full fusion. A similar proposal is that the Accessory Helix blocks the zippering not only by sterics, but by actually binding to the pre-structured C-terminal SNARE domains of the t-SNAREs [89, 175]. In this model, first proposed by Giraudo *et al.* in 2009 [89] and depicted in Figure 13, the Accessory

Helix prevents VAMP2 from forming the four helix bundle by forming an intramolecular "alternate four-helix bundle," and specific residues in the CPX Accessory Helix help form the hydrophobic layers while other hydrophilic residues prevent the extra-tight binding VAMP2 natively possesses and allow the clamp to be released [89, 175]. This model was further supported by mutagenesis in the Accessory Helix region in which changes were made to make the Accessory Helix have even more hydrophobic layer contacts, and they caused CPX to be a better clamp, as evidenced in the cell-cell fusion assay [89]. On the other hand, when the corresponding hydrophilic mutations were made, no clamping function was observed whatsoever [175].

Another recently proposed model [175] suggests that Complexin clamps fusion by blocking a secondary calcium sensor, working in tandem with Synaptotagmin to clamp release. While I cannot rule out this mechanism, the identity of this secondary calcium sensor remains a mystery. A suggest of an as-yet-unidentified protein is proposed [176]. In light of what will be presented in the following chapters, however, I find this model unlikely.

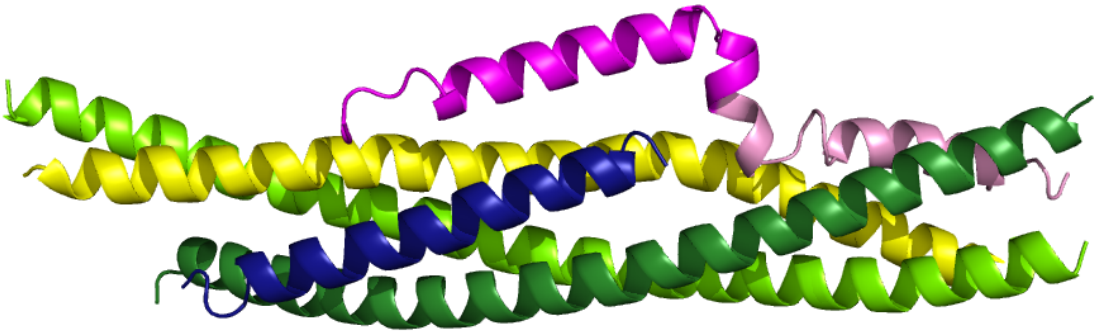

Figure 13: The Intramolecular Alternate Four Helix Bundle Model. This structure was proposed in [89] as a model for the clamped, *trans*-SNARE structure. The t-SNAREs are represented in yellow and green (Syntaxin and SNAP25, respectively), as previously, and VAMP2 is represented in blue again as well. VAMP2 is truncated to represent the lack of zippering of its C-terminus Complexin is magenta, and its Central Helix binds as before [142], but its Accessory Helix comes in and binds in the region where the VAMP2 would have bound were it zippered, which would block the full zippering of VAMP2, according to this model.

Even in light of the observation that distinct domains of Complexin can regulate neurotransmitter release differently [151], the fact that Complexin affects SNARE-mediated vesicle fusion in a predominantly facilitatory manner in certain settings and an inhibitory manner in others remains confusing. It is possible that the *in vitro* fusion assays do not recapitulate all aspects of Complexin *in vivo* due to the lack of certain binding partners as yet unidentified. The inhibitory effect of the Complexin Accessory Helix might also be exaggerated in the *in vitro* assays, causing a net reduction in fusion activity. It is also possible, as Xue *et al.* suggest [151], that certain organisms' Complexins are more designed for clamping, while others are designed for a faciliatory role helping to explain the difference between organisms. On the other hand, it is possible that *in vivo*, there is another undiscovered protein, or an unknown function of a known protein that can act on this system which can confound *in vivo* results. An answer to the question of how CPX can be both an activator and an inhibitor of fusion has been suggested by Li. *et al.*, 2011 (under submission). In this paper, the authors suggest that while the Accessory Helix is responsible for the clamping activity observed in CPX, the Central Helix (and potentially both the N-terminal and C-terminal domains) serve to aid the CPX in helping the *trans*-SNARE complex to form. Thus up to three domains help the SNARE domain to form into a meta-stable *trans*-SNARE, while the other domain prevents the full fusion of the SNAREs until acted upon by an external signal. To be specific, in the absence of Complexin, v- and t-SNAREs assemble and yield ~35 k_BT per SNAREpin at a distance of 9nm. In the presence of CPX, the SNAREs begin to assemble at a greater distance (15 nm) and form a SNAREpin of lower energy (~15 k_BT) which has

its membrane-proximal zippering inhibited. This is the first time the energetics of a fusion intermediate structure have been described. While this is an appealing model, for now, some aspects of CPX's activity must remain a mystery.

HOW IS THE COMPLEXIN CLAMP RELEASED?

It is known that fusion is induced by an increase in the local calcium concentrations in the presynaptic bulb. Katz *et al.* established that synaptic vesicle exocytosis is triggered by calcium in 1969 [8]. So, identification of the calcium sensor that regulates the fusion reaction would help with understanding this pathway. A protein called Synaptotagmin (SYT) is likely just this protein. Identified first in 1981 by Matthew *et al.* as a 65 kDa protein exposed on the outer surface of neuronal synaptic vesicles alongside VAMP2 [177], it wasn't until a decade later that this protein was named "Synaptotagmin" [178]. It was discovered that Synaptotagmin can bind both calcium and acidic phospholipids like phosphotidylserine [179, 180]. It has since been shown that Synaptotagmins form a large family of proteins with seven members in *Drosophila* and 17 members in mammals [181]. Since SYT1 is the most abundant calcium binding protein present on synaptic vesicles, accounting for seven percent of the total vesicle protein, it was an obvious target of investigation for the calcium sensor [182, 183].

Synaptotagmin is thought to be the protein responsible for release of the CPX clamp not only because it has calcium binding sites, but also various lines of *in vivo* evidence [157]. For example, in flies, Synaptotagmin functions to synchronize exocytosis during calcium-evoked stimulation[179]. Synaptotagmin KO synapses exhibit a ~10 fold increase in spontaneous release. In addition, knockout mice have greatly

reduced synchronous transmitter release following nerve stimulation [184]. Xue *et al* found evidence for a genetic interaction between Complexin and Synaptotagmin [153]. It has even been suggested that Synaptotagmin and Complexin compete for a binding site[157]. On the other hand, Yang *et al.* suggest that Syaptotagmin acts at a stage later than that of Complexin [175]. Because a lack of Synaptotagmin is tied to a lack of synchronicity in fusion, SYT is likely responsible for tying fusion to calcium influx. On the other hand, in nerve cell cultures from Synaptotagmin knockouts, fusion still occurs as normal [182, 185], suggesting a deletion of Synaptotagmin has no effect on fusion in these cells. And in still other studies in Synaptotagmin-deficient mutants reported increases in the rate of spontaneous vesicle fusion events [186-188], suggesting Synaptotagmin may not be responsible for releasing the Complexin clamp. *In vitro*, however, in the same cell-cell fusion and liposome fusion assays that demonstrated CPX is a clamp, Synaptotagmin is able to release the clamp imposed by Complexin upon influx of calcium in keeping with the model in which Synaptotagmin senses calcium and causes the release of Complexin. Clearly more research is warranted into the true roles of and interplay between Synaptotagmin and Complexin, an interplay which is present in organisms as primitive as Trichoplax [175] which has both CPX and SYT analogs but no known nervous system. This suggests this interplay is of such importance, evolution sought to maintain it through millions of years. Because Synaptotagmin is thought to bind an inherently unstable partially-zippered *trans*-SNARE structure, structural information on these interactions is extremely difficult to obtain.

What is known structurally is that Synaptotagmin has a short intraluminal

domain, a single membrane-spanning domain, and a large cytoplasmic domain consisting of two C2, calcium-binding domains, called C2A and C2B, connected by a linker [178, 184, 189, 190], which is presented in figure 14. The crystal and NMR structures of Synaptotagmin showed the C2 domains exist as compact eight stranded beta barrels, each with two protruding loops which can bind three calcium ions or phospholipids through five conserved aspartate residues from the top loop [191-194]. Other findings suggested that SYT's ability to bind calcium and phospholipids involves electrostatic interactions between basic lysine patches on the C2A domains and the charges on phospholipid headgroups, insertion of hydrophobic residues into the lipid bilayer, and coordination of the calcium ions by these headgroups [195].

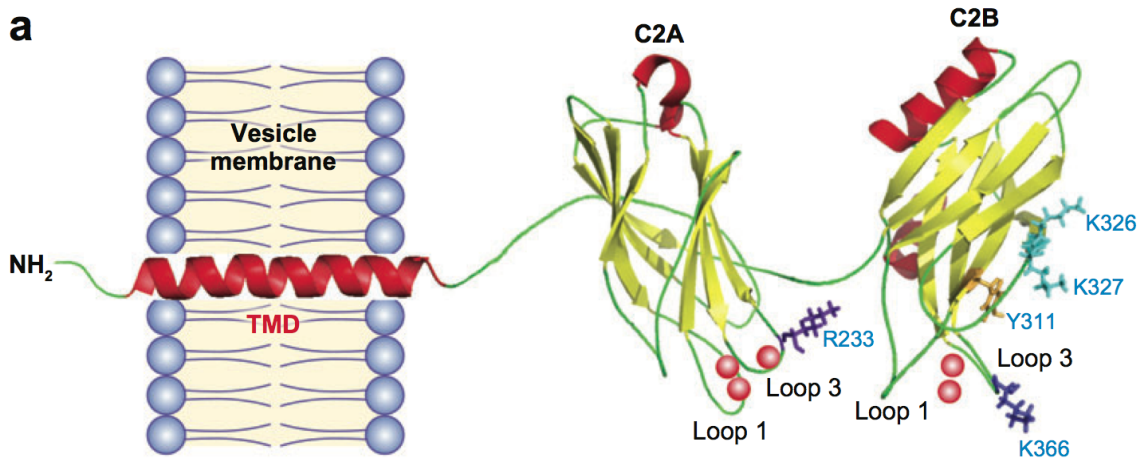

Figure 14: The Synaptotagmin Crystal Structure. This is the crystal structure of Synaptotagmin, showing the two calcium-binding domains, C2A and C2B. The calcium they bind is shown in red, and the basic residues on the surface are shown in blue and purple. The positioning of the C2A and C2B with respect to each other is not fully known, and their relative orientations with respect to the SNAREs is also unknown. From (Chapman 2008)

Interestingly, mutations in the calcium binding sites that severely impair calcium and phospholipid binding to the C2A domains have only small effects on vesicle fusion [189, 196, 197]. This was explained by examining the other C2 domain in synaptotagmin, the C2B domain. Structurally, the C2B domain resembles the C2A domain, as it also contains conserved aspartate residues [185]. Further, C2B also binds the membranes via lipids like PIP_2 and PS, suggesting that the two C2 domains may cooperate with each other in both calcium and phospholipid membrane binding [194, 198]. In fact, when the aspartates of the Ca^{2+}-binding loops of either the C2A and C2B domains (or both) were replaced by tryptophan residues (thereby increasing the hydrophobic surface area, effectively inserting them into membranes more efficiently), there are increases in the apparent calcium affinity of the Synaptotagmin and the calcium sensitivity of vesicle fusion [196, 199]. This suggests there is a link between the calcium-binding and thus membrane-binding ability of Synaptotagmin *in vitro* and the calcium sensitivity of neurotransmitter release *in vivo*. Further, this provides evidence that membrane binding is required for Synaptotagmin's calcium-dependent release of the Complexin clamp.

Both the C2A and the C2B domains bind phospholipids in a Ca^{2+}-dependent manner, and it has been shown that calcium induces simultaneous binding of Synaptotagmin to both the vesicle and target membranes, bringing the two membranes into close proximity (about 4 nm) [200]. The C2B domain appears to be the most responsible for this property, owing to the abundance of basic lysine residues which interact with the negatively charged phospholipids around its surface [193].

Taken all together, this leads to a model wherein, Complexin somehow prevents full zippering of the SNARE complex via its Accessory Helix. As a result of an action potential, calcium enters, and Synaptotagmin binds the membranes and cooperates with Complexin and the SNAREs in releasing the CPX clamp and bringing the synaptic vesicle and plasma membranes together allowing fusion to occur. In one model, the C2A domain of Synaptotagmin would have an accessory role, helping to bind phospholipids and contributing to the overall Ca^{2+} sensitivity of release while the C2B domain takes the dominant role in membrane binding and thus calcium-dependence on fusion [85]. Another possible mechanism is that both C2A and C2B bind membranes, and upon the calcium stimulus, a large rearrangement of Synaptotagmin occurs, severely disrupting the membranes and disrupting the CPX clamp somehow [201]. The goal of this thesis is to understand both how Complexin clamps, and also to gain some idea of how this clamp is released.

A NOVEL MODEL FOR CLAMPING AND RELEASE

In order to address the question of how the Accessory Helix of Complexin actually clamps SNARE-mediated fusion, and to assay the nature of the *trans*-SNARE complex, our collaborators solved a crystal structure of the four helix bundle, lacking the C-terminus of VAMP2, but in the presence of the Accessory and Central Helices of Complexin. This structure might serve as a mimetic of the *trans*-SNARE, wherein the C-terminus of the v-SNARE is not zippered. Interestingly, the solved structure is somewhat unexpected, and required external validation. My first goal was to develop a FRET assay that would validate their crystal structure (Chapter 2). From there, I extended the FRET

assay to further examine the nature of the *trans*-SNARE complex. From these experiments, we were able to develop a novel intermolecular clamping model which may even help explain how CPX can both stabilize the formation of the *trans*-SNARE complex, priming vesicle fusion, while also preventing fusion from occurring (Chapter 3). After that, I used the same FRET-based assay to examine the mechanism by which the CPX clamp is released. I identified three residues on VAMP2 which are required to permit CPX to unclamp (Chapter 4). In Chapter 5, I elaborate on the proposed model, discuss some of its limitations, and make some testable predictions that can further extend this work both *in vivo* and *in vitro*.

REFERENCES

1. Alberts, B., *Molecular biology of the cell*. 4th ed. 2002, New York: Garland Science. xxxiv, 1548 p.
2. Brose, N., *For better or for worse: complexins regulate SNARE function and vesicle fusion.* Traffic, 2008. **9**(9): p. 1403-13.
3. Rothman, J.E. and F.T. Wieland, *Protein sorting by transport vesicles.* Science, 1996. **272**(5259): p. 227-34.
4. Stow, J.L., A.P. Manderson, and R.Z. Murray, *SNAREing immunity: the role of SNAREs in the immune system.* Nat Rev Immunol, 2006. **6**(12): p. 919-29.
5. Glick, B.S. and A. Nakano, *Membrane traffic within the Golgi apparatus.* Annu Rev Cell Dev Biol, 2009. **25**: p. 113-32.
6. Park, J.J. and Y.P. Loh, *How peptide hormone vesicles are transported to the secretion site for exocytosis.* Mol Endocrinol, 2008. **22**(12): p. 2583-95.
7. Newell-Litwa, K., et al., *Hermansky-Pudlak protein complexes, AP-3 and BLOC-1, differentially regulate presynaptic composition in the striatum and hippocampus.* J Neurosci, 2010. **30**(3): p. 820-31.
8. Katz, B., *The release of neural transmitter substances*. The Sherrington lectures, 10. 1969, Springfield, Ill.,: Thomas. ix, 60 p.
9. Jahn, R. and T.C. Sudhof, *Membrane fusion and exocytosis.* Annu Rev Biochem, 1999. **68**: p. 863-911.

10. Liu, W. and V. Parpura, *SNAREs: could they be the answer to an energy landscape riddle in exocytosis?* ScientificWorldJournal, 2010. **10**: p. 1258-68.

11. Chernomordik, L.V. and M.M. Kozlov, *Mechanics of membrane fusion.* Nat Struct Mol Biol, 2008. **15**(7): p. 675-83.

12. Wickner, W., *Membrane fusion: five lipids, four SNAREs, three chaperones, two nucleotides, and a Rab, all dancing in a ring on yeast vacuoles.* Annu Rev Cell Dev Biol, 2010. **26**: p. 115-36.

13. Markin, V.S. and J.P. Albanesi, *Membrane fusion: stalk model revisited.* Biophys J, 2002. **82**(2): p. 693-712.

14. Marrink, S.J. and A.E. Mark, *The mechanism of vesicle fusion as revealed by molecular dynamics simulations.* J Am Chem Soc, 2003. **125**(37): p. 11144-5.

15. Cohen, F.S. and G.B. Melikyan, *The energetics of membrane fusion from binding, through hemifusion, pore formation, and pore enlargement.* J Membr Biol, 2004. **199**(1): p. 1-14.

16. Kasson, P.M., et al., *Ensemble molecular dynamics yields submillisecond kinetics and intermediates of membrane fusion.* Proc Natl Acad Sci U S A, 2006. **103**(32): p. 11916-21.

17. Katsov, K., M. Muller, and M. Schick, *Field theoretic study of bilayer membrane fusion: II. Mechanism of a stalk-hole complex.* Biophys J, 2006. **90**(3): p. 915-26.

18. Li, F., et al., *Energetics and dynamics of SNAREpin folding across lipid bilayers.* Nat Struct Mol Biol, 2007. **14**(10): p. 890-6.

19. Wiederhold, K. and D. Fasshauer, *Is assembly of the SNARE complex enough to fuel membrane fusion?* J Biol Chem, 2009. **284**(19): p. 13143-52.

20. Risselada, H.J., C. Kutzner, and H. Grubmuller, *Caught in the Act: Visualization of SNARE-Mediated Fusion Events in Molecular Detail.* Chembiochem, 2011.

21. Wickner, W., *Membrane Fusion: Five Lipids, Four SNAREs, Three Chaperones, Two Nucleotides, and a Rab, All Dancing in a Ring on Yeast Vacuoles.* Annu Rev Cell Dev Biol, 2010.

22. Yu, I.M. and F.M. Hughson, *Tethering factors as organizers of intracellular vesicular traffic.* Annu Rev Cell Dev Biol, 2010. **26**: p. 137-56.

23. Fasshauer, D., et al., *SNARE assembly and disassembly exhibit a pronounced hysteresis.* Nat Struct Biol, 2002. **9**(2): p. 144-51.

24. Fiebig, K.M., et al., *Folding intermediates of SNARE complex assembly.* Nat Struct Biol, 1999. **6**(2): p. 117-23.

25. Parlati, F., et al., *Rapid and efficient fusion of phospholipid vesicles by the alpha-helical core of a SNARE complex in the absence of an N-terminal regulatory domain.* Proc Natl Acad Sci U S A, 1999. **96**(22): p. 12565-70.

26. Smith, S.M., R. Renden, and H. von Gersdorff, *Synaptic vesicle endocytosis: fast and slow modes of membrane retrieval.* Trends Neurosci, 2008. **31**(11): p. 559-68.

27. Brunger, A.T., *Structure and function of SNARE and SNARE-interacting proteins.* Q Rev Biophys, 2005. **38**(1): p. 1-47.

28. Hohl, T.M., et al., *Arrangement of subunits in 20 S particles consisting of NSF, SNAPs, and SNARE complexes.* Mol Cell, 1998. **2**(5): p. 539-48.

29. Wimmer, C., et al., *Molecular mass, stoichiometry, and assembly of 20 S particles.* J Biol Chem, 2001. **276**(31): p. 29091-7.

30. Fasshauer, D., et al., *Mixed and non-cognate SNARE complexes. Characterization of assembly and biophysical properties.* J Biol Chem, 1999. **274**(22): p. 15440-6.

31. Margittai, M., et al., *Homo- and heterooligomeric SNARE complexes studied by site-directed spin labeling.* J Biol Chem, 2001. **276**(16): p. 13169-77.

32. Sorensen, J.B., et al., *Sequential N- to C-terminal SNARE complex assembly drives priming and fusion of secretory vesicles.* EMBO J, 2006. **25**(5): p. 955-66.

33. Scales, S.J., J.B. Bock, and R.H. Scheller, *The specifics of membrane fusion.* Nature, 2000. **407**(6801): p. 144-6.

34. Hong, W., *SNAREs and traffic.* Biochim Biophys Acta, 2005. **1744**(2): p. 120-44.

35. Chen, Y.A. and R.H. Scheller, *SNARE-mediated membrane fusion.* Nat Rev Mol Cell Biol, 2001. **2**(2): p. 98-106.

36. Lang, T. and R. Jahn, *Core proteins of the secretory machinery.* Handb Exp Pharmacol, 2008(184): p. 107-27.

37. Sutton, R.B., et al., *Crystal structure of a SNARE complex involved in synaptic exocytosis at 2.4 A resolution.* Nature, 1998. **395**(6700): p. 347-53.

38. Bassham, D.C. and M.R. Blatt, *SNAREs: cogs and coordinators in signaling and development.* Plant Physiol, 2008. **147**(4): p. 1504-15.

39. Jahn, R. and R.H. Scheller, *SNAREs--engines for membrane fusion.* Nat Rev Mol Cell Biol, 2006. **7**(9): p. 631-43.

40. Misura, K.M., et al., *Three-dimensional structure of the amino-terminal domain of syntaxin 6, a SNAP-25 C homolog.* Proc Natl Acad Sci U S A, 2002. **99**(14): p. 9184-9.

41. Bock, J.B., et al., *A genomic perspective on membrane compartment organization.* Nature, 2001. **409**(6822): p. 839-41.

42. Fasshauer, D., et al., *Conserved structural features of the synaptic fusion complex: SNARE proteins reclassified as Q- and R-SNAREs.* Proc Natl Acad Sci U S A, 1998. **95**(26): p. 15781-6.

43. Wang, Y., et al., *Functional analysis of conserved structural elements in yeast syntaxin Vam3p.* J Biol Chem, 2001. **276**(30): p. 28598-605.

44. Grote, E., et al., *Geranylgeranylated SNAREs are dominant inhibitors of membrane fusion.* J Cell Biol, 2000. **151**(2): p. 453-66.

45. McNew, J.A., et al., *The length of the flexible SNAREpin juxtamembrane region is a critical determinant of SNARE-dependent fusion.* Mol Cell, 1999. **4**(3): p. 415-21.

46. McNew, J.A., et al., *Close is not enough: SNARE-dependent membrane fusion requires an active mechanism that transduces force to membrane anchors.* J Cell Biol, 2000. **150**(1): p. 105-17.

47. Stein, A., et al., *Helical extension of the neuronal SNARE complex into the membrane.* Nature, 2009. **460**(7254): p. 525-8.

48. Elferink, L.A., W.S. Trimble, and R.H. Scheller, *Two vesicle-associated membrane protein genes are differentially expressed in the rat central nervous system.* J Biol Chem, 1989. **264**(19): p. 11061-4.

49. McMahon, H.T., et al., *Cellubrevin is a ubiquitous tetanus-toxin substrate homologous to a putative synaptic vesicle fusion protein.* Nature, 1993. **364**(6435): p. 346-9.

50. Hu, C., D. Hardee, and F. Minnear, *Membrane fusion by VAMP3 and plasma membrane t-SNAREs.* Exp Cell Res, 2007. **313**(15): p. 3198-209.

51. Misura, K.M., R.H. Scheller, and W.I. Weis, *Three-dimensional structure of the neuronal-Sec1-syntaxin 1a complex.* Nature, 2000. **404**(6776): p. 355-62.

52. Fasshauer, D., *Structural insights into the SNARE mechanism.* Biochim Biophys Acta, 2003. **1641**(2-3): p. 87-97.

53. Dietrich, L.E., et al., *Control of eukaryotic membrane fusion by N-terminal domains of SNARE proteins.* Biochim Biophys Acta, 2003. **1641**(2-3): p. 111-9.

54. Rossi, V., et al., *Longins and their longin domains: regulated SNAREs and multifunctional SNARE regulators.* Trends Biochem Sci, 2004. **29**(12): p. 682-8.

55. Malsam, J., S. Kreye, and T.H. Sollner, *Membrane fusion: SNAREs and regulation.* Cell Mol Life Sci, 2008. **65**(18): p. 2814-32.

56. Pevsner, J., S.C. Hsu, and R.H. Scheller, *n-Sec1: a neural-specific syntaxin-binding protein.* Proc Natl Acad Sci U S A, 1994. **91**(4): p. 1445-9.

57. Oyler, G.A., et al., *The identification of a novel synaptosomal-associated protein, SNAP-25, differentially expressed by neuronal subpopulations.* J Cell Biol, 1989. **109**(6 Pt 1): p. 3039-52.

58. Bennett, M.K., N. Calakos, and R.H. Scheller, *Syntaxin: a synaptic protein implicated in docking of synaptic vesicles at presynaptic active zones.* Science, 1992. **257**(5067): p. 255-9.

59. Sollner, T., et al., *SNAP receptors implicated in vesicle targeting and fusion.* Nature, 1993. **362**(6418): p. 318-24.

60. Block, M.R., et al., *Purification of an N-ethylmaleimide-sensitive protein catalyzing vesicular transport.* Proc Natl Acad Sci U S A, 1988. **85**(21): p. 7852-6.

61. Clary, D.O., I.C. Griff, and J.E. Rothman, *SNAPs, a family of NSF attachment proteins involved in intracellular membrane fusion in animals and yeast.* Cell, 1990. **61**(4): p. 709-21.

62. Pobbati, A.V., A. Stein, and D. Fasshauer, *N- to C-terminal SNARE complex assembly promotes rapid membrane fusion.* Science, 2006. **313**(5787): p. 673-6.

63. Jahn, R., T. Lang, and T.C. Sudhof, *Membrane fusion.* Cell, 2003. **112**(4): p. 519-33.

64. Sudhof, T.C., *The synaptic vesicle cycle.* Annu Rev Neurosci, 2004. **27**: p. 509-47.

65. Melia, T.J., et al., *Regulation of membrane fusion by the membrane-proximal coil of the t-SNARE during zippering of SNAREpins.* J Cell Biol, 2002. **158**(5): p. 929-40.

66. Lin, R.C. and R.H. Scheller, *Mechanisms of synaptic vesicle exocytosis.* Annu Rev Cell Dev Biol, 2000. **16**: p. 19-49.

67. Hua, S.Y. and M.P. Charlton, *Activity-dependent changes in partial VAMP complexes during neurotransmitter release.* Nat Neurosci, 1999. **2**(12): p. 1078-83.

68. Xu, T., et al., *Inhibition of SNARE complex assembly differentially affects kinetic components of exocytosis.* Cell, 1999. **99**(7): p. 713-22.

69. Fasshauer, D. and M. Margittai, *A transient N-terminal interaction of SNAP-25 and syntaxin nucleates SNARE assembly.* J Biol Chem, 2004. **279**(9): p. 7613-21.

70. Nicholson, K.L., et al., *Regulation of SNARE complex assembly by an N-terminal domain of the t-SNARE Sso1p.* Nat Struct Biol, 1998. **5**(9): p. 793-802.

71. Hua, Y. and R.H. Scheller, *Three SNARE complexes cooperate to mediate membrane fusion.* Proc Natl Acad Sci U S A, 2001. **98**(14): p. 8065-70.

72. Han, X., et al., *Transmembrane segments of syntaxin line the fusion pore of Ca2+-triggered exocytosis.* Science, 2004. **304**(5668): p. 289-92.

73. Karatekin, E., et al., *A fast, single-vesicle fusion assay mimics physiological SNARE requirements.* Proc Natl Acad Sci U S A, 2010. **107**(8): p. 3517-21.

74. Keller, J.E., F. Cai, and E.A. Neale, *Uptake of botulinum neurotoxin into cultured neurons.* Biochemistry, 2004. **43**(2): p. 526-32.

75. van den Bogaart, G., et al., *One SNARE complex is sufficient for membrane fusion.* Nat Struct Mol Biol, 2010. **17**(3): p. 358-64.

76. Weninger, K., et al., *Single-molecule studies of SNARE complex assembly reveal parallel and antiparallel configurations.* Proc Natl Acad Sci U S A, 2003. **100**(25): p. 14800-5.

77. Lang, T., et al., *SNAREs in native plasma membranes are active and readily form core complexes with endogenous and exogenous SNAREs.* J Cell Biol, 2002. **158**(4): p. 751-60.

78. An, S.J. and W. Almers, *Tracking SNARE complex formation in live endocrine cells.* Science, 2004. **306**(5698): p. 1042-6.

79. Kraynack, B.A., et al., *Dsl1p, Tip20p, and the novel Dsl3(Sec39) protein are required for the stability of the Q/t-SNARE complex at the endoplasmic reticulum in yeast.* Mol Biol Cell, 2005. **16**(9): p. 3963-77.

80. Sorensen, J.B., *Formation, stabilisation and fusion of the readily releasable pool of secretory vesicles.* Pflugers Arch, 2004. **448**(4): p. 347-62.

81. Borisovska, M., et al., *v-SNAREs control exocytosis of vesicles from priming to fusion.* EMBO J, 2005. **24**(12): p. 2114-26.

82. Weber, T., et al., *SNAREpins: minimal machinery for membrane fusion.* Cell, 1998. **92**(6): p. 759-72.

83. Malsam, J., et al., *The carboxy-terminal domain of complexin I stimulates liposome fusion.* Proc Natl Acad Sci U S A, 2009. **106**(6): p. 2001-6.

84. Seiler, F., et al., *A role of complexin-lipid interactions in membrane fusion.* FEBS Lett, 2009. **583**(14): p. 2343-8.

85. Rizo, J., X. Chen, and D. Arac, *Unraveling the mechanisms of synaptotagmin and SNARE function in neurotransmitter release.* Trends Cell Biol, 2006. **16**(7): p. 339-50.

86. Bhalla, A., et al., *Ca(2+)-synaptotagmin directly regulates t-SNARE function during reconstituted membrane fusion.* Nat Struct Mol Biol, 2006. **13**(4): p. 323-30.

87. Scott, B.L., et al., *Liposome fusion assay to monitor intracellular membrane fusion machines.* Methods Enzymol, 2003. **372**: p. 274-300.

88. Kreye, S., J. Malsam, and T.H. Sollner, *In vitro assays to measure SNARE-mediated vesicle fusion.* Methods Mol Biol, 2008. **440**: p. 37-50.

89. Giraudo, C.G., et al., *Alternative zippering as an on-off switch for SNARE-mediated fusion.* Science, 2009. **323**(5913): p. 512-6.

90. Giraudo, C.G., et al., *Distinct domains of complexins bind SNARE complexes and clamp fusion in vitro.* J Biol Chem, 2008. **283**(30): p. 21211-9.

91. Giraudo, C.G., et al., *A clamping mechanism involved in SNARE-dependent exocytosis.* Science, 2006. **313**(5787): p. 676-80.

92. Hu, C., et al., *Fusion of cells by flipped SNAREs.* Science, 2003. **300**(5626): p. 1745-9.

93. Zhang, Z. and M.B. Jackson, *Membrane bending energy and fusion pore kinetics in Ca(2+)-triggered exocytosis.* Biophys J, 2010. **98**(11): p. 2524-34.

94. An, S.J., C.P. Grabner, and D. Zenisek, *Real-time visualization of complexin during single exocytic events.* Nat Neurosci, 2010. **13**(5): p. 577-83.

95. Martens, S. and H.T. McMahon, *Mechanisms of membrane fusion: disparate players and common principles.* Nat Rev Mol Cell Biol, 2008. **9**(7): p. 543-56.

96. Rizo, J. and C. Rosenmund, *Synaptic vesicle fusion.* Nat Struct Mol Biol, 2008. **15**(7): p. 665-74.

97. Chapman, E.R., *How does synaptotagmin trigger neurotransmitter release?* Annu Rev Biochem, 2008. **77**: p. 615-41.

98. Ishizuka, T., et al., *Synaphin - a Protein Associated with the Docking/Fusion Complex in Presynaptic Terminals.* Biochemical and Biophysical Research Communications, 1995. **213**(3): p. 1107-1114.

99. McMahon, H.T., et al., *Complexins: cytosolic proteins that regulate SNAP receptor function.* Cell, 1995. **83**(1): p. 111-9.

100. Ishizuka, T., et al., *Synaphin: a protein associated with the docking/fusion complex in presynaptic terminals.* Biochem Biophys Res Commun, 1995. **213**(3): p. 1107-14.

101. Reim, K., et al., *Structurally and functionally unique complexins at retinal ribbon synapses.* J Cell Biol, 2005. **169**(4): p. 669-80.

102. Reim, K., et al., *Complexins regulate a late step in Ca2+-dependent neurotransmitter release.* Cell, 2001. **104**(1): p. 71-81.

103. Falkowski, M.A., D.D. Thomas, and G.E. Groblewski, *Complexin 2 modulates vesicle associated membrane protein (VAMP) 2 regulated zymogen granule exocytosis in pancreatic acini.* J Biol Chem, 2010.

104. Takahashi, S., et al., *Identification of two highly homologous presynaptic proteins distinctly localized at the dendritic and somatic synapses.* FEBS Lett, 1995. **368**(3): p. 455-60.

105. Zanazzi, G. and G. Matthews, *Enrichment and differential targeting of complexins 3 and 4 in ribbon-containing sensory neurons during zebrafish development.* Neural Dev, 2010. **5**: p. 24.

106. Eastwood, S.L., P.W. Burnet, and P.J. Harrison, *Expression of complexin I and II mRNAs and their regulation by antipsychotic drugs in the rat forebrain.* Synapse, 2000. **36**(3): p. 167-77.

107. Harrison, P.J. and S.L. Eastwood, *Preferential involvement of excitatory neurons in medial temporal lobe in schizophrenia.* Lancet, 1998. **352**(9141): p. 1669-73.

108. Webster, M.J., M. Elashoff, and C.S. Weickert, *Molecular evidence that cortical synaptic growth predominates during the first decade of life in humans.* Int J Dev Neurosci, 2011. **29**(3): p. 225-36.

109. Yamada, M., et al., *Immunohistochemical distribution of the two isoforms of synaphin/complexin involved in neurotransmitter release: localization at the*

distinct central nervous system regions and synaptic types. Neuroscience, 1999. **93**(1): p. 7-18.

110. Hazell, A.S. and D. Wang, *Identification of complexin II in astrocytes: a possible regulator of glutamate release in these cells.* Biochem Biophys Res Commun, 2011. **404**(1): p. 228-32.

111. Reim, K., et al., *Aberrant function and structure of retinal ribbon synapses in the absence of complexin 3 and complexin 4.* J Cell Sci, 2009. **122**(Pt 9): p. 1352-61.

112. Eastwood, S.L., D. Cotter, and P.J. Harrison, *Cerebellar synaptic protein expression in schizophrenia.* Neuroscience, 2001. **105**(1): p. 219-29.

113. Edwardson, J.M., et al., *Expression of mutant huntingtin blocks exocytosis in PC12 cells by depletion of complexin II.* J Biol Chem, 2003. **278**(33): p. 30849-53.

114. Freeman, W. and A.J. Morton, *Regional and progressive changes in brain expression of complexin II in a mouse transgenic for the Huntington's disease mutation.* Brain Res Bull, 2004. **63**(1): p. 45-55.

115. Morton, A.J., R.L. Faull, and J.M. Edwardson, *Abnormalities in the synaptic vesicle fusion machinery in Huntington's disease.* Brain Res Bull, 2001. **56**(2): p. 111-7.

116. Morton, A.J. and J.M. Edwardson, *Progressive depletion of complexin II in a transgenic mouse model of Huntington's disease.* J Neurochem, 2001. **76**(1): p. 166-72.

117. DiProspero, N.A., et al., *Early changes in Huntington's disease patient brains involve alterations in cytoskeletal and synaptic elements.* J Neurocytol, 2004. **33**(5): p. 517-33.

118. Zink, M., et al., *Reduced expression of complexins I and II in rats bred for learned helplessness.* Brain Res, 2007. **1144**: p. 202-8.

119. Eastwood, S.L. and P.J. Harrison, *Synaptic pathology in the anterior cingulate cortex in schizophrenia and mood disorders. A review and a Western blot study of synaptophysin, GAP-43 and the complexins.* Brain Res Bull, 2001. **55**(5): p. 569-78.

120. Sawada, K., et al., *Altered immunoreactivity of complexin protein in prefrontal cortex in severe mental illness.* Mol Psychiatry, 2002. **7**(5): p. 484-92.

121. Glynn, D., et al., *Clorgyline-mediated reversal of neurological deficits in a Complexin 2 knockout mouse.* Hum Mol Genet, 2010. **19**(17): p. 3402-12.

122. Eastwood, S.L. and P.J. Harrison, *Hippocampal synaptic pathology in schizophrenia, bipolar disorder and major depression: a study of complexin mRNAs.* Mol Psychiatry, 2000. **5**(4): p. 425-32.

123. Knable, M.B., et al., *Molecular abnormalities of the hippocampus in severe psychiatric illness: postmortem findings from the Stanley Neuropathology Consortium.* Mol Psychiatry, 2004. **9**(6): p. 609-20, 544.

124. Basso, M., et al., *Proteome analysis of human substantia nigra in Parkinson's disease.* Proteomics, 2004. **4**(12): p. 3943-52.

125. Patel, S., A. Sinha, and M.P. Singh, *Identification of differentially expressed proteins in striatum of maneb-and paraquat-induced Parkinson's disease phenotype in mouse.* Neurotoxicol Teratol, 2007. **29**(5): p. 578-85.

126. Tannenberg, R.K., et al., *Selective loss of synaptic proteins in Alzheimer's disease: evidence for an increased severity with APOE varepsilon4.* Neurochem Int, 2006. **49**(7): p. 631-9.

127. Glynn, D., et al., *Profound ataxia in complexin I knockout mice masks a complex phenotype that includes exploratory and habituation deficits.* Hum Mol Genet, 2005. **14**(16): p. 2369-85.

128. Glynn, D., R.J. Sizemore, and A.J. Morton, *Early motor development is abnormal in complexin 1 knockout mice.* Neurobiol Dis, 2007. **25**(3): p. 483-95.

129. Yi, J.H., et al., *Early, transient increase in complexin I and complexin II in the cerebral cortex following traumatic brain injury is attenuated by N-acetylcysteine.* J Neurotrauma, 2006. **23**(1): p. 86-96.

130. Drew, C.J., R.J. Kyd, and A.J. Morton, *Complexin 1 knockout mice exhibit marked deficits in social behaviours but appear to be cognitively normal.* Hum Mol Genet, 2007. **16**(19): p. 2288-305.

131. Glynn, D., R.A. Bortnick, and A.J. Morton, *Complexin II is essential for normal neurological function in mice.* Hum Mol Genet, 2003. **12**(19): p. 2431-48.

132. Hazell, A.S. and C. Wang, *Downregulation of complexin I and complexin II in the medial thalamus is blocked by N-acetylcysteine in experimental Wernicke's encephalopathy.* J Neurosci Res, 2005. **79**(1-2): p. 200-7.

133. Zink, M., et al., *Perinatal exposure to alcohol reduces the expression of complexins I and II.* Neurotoxicol Teratol, 2009. **31**(6): p. 400-5.

134. Barr, A.M., et al., *Prenatal ethanol exposure in rats decreases levels of complexin proteins in the frontal cortex.* Alcohol Clin Exp Res, 2005. **29**(11): p. 1915-20.

135. Eastwood, S.L. and P.J. Harrison, *Decreased expression of vesicular glutamate transporter 1 and complexin II mRNAs in schizophrenia: further evidence for a synaptic pathology affecting glutamate neurons.* Schizophr Res, 2005. **73**(2-3): p. 159-72.

136. Halim, N.D., et al., *Presynaptic proteins in the prefrontal cortex of patients with schizophrenia and rats with abnormal prefrontal development.* Mol Psychiatry, 2003. **8**(9): p. 797-810.

137. Sommer, J.U., et al., *Differential expression of presynaptic genes in a rat model of postnatal hypoxia: relevance to schizophrenia.* Eur Arch Psychiatry Clin Neurosci, 2010. **260 Suppl 2**: p. S81-9.

138. Sawada, K., et al., *Hippocampal complexin proteins and cognitive dysfunction in schizophrenia.* Arch Gen Psychiatry, 2005. **62**(3): p. 263-72.

139. Radyushkin, K., et al., *Complexin2 null mutation requires a 'second hit' for induction of phenotypic changes relevant to schizophrenia.* Genes Brain Behav, 2010. **9**(6): p. 592-602.

140. Begemann, M., et al., *Modification of cognitive performance in schizophrenia by complexin 2 gene polymorphisms.* Arch Gen Psychiatry, 2010. **67**(9): p. 879-88.

141. Fung, S.J., S. Sivagnanasundaram, and C.S. Weickert, *Lack of change in markers of presynaptic terminal abundance alongside subtle reductions in markers of presynaptic terminal plasticity in prefrontal cortex of schizophrenia patients.* Biol Psychiatry, 2011. **69**(1): p. 71-9.

142. Chen, X., et al., *Three-dimensional structure of the complexin/SNARE complex.* Neuron, 2002. **33**(3): p. 397-409.

143. Pabst, S., et al., *Selective interaction of complexin with the neuronal SNARE complex. Determination of the binding regions.* J Biol Chem, 2000. **275**(26): p. 19808-18.

144. Yoon, T.Y., et al., *Complexin and Ca2+ stimulate SNARE-mediated membrane fusion.* Nat Struct Mol Biol, 2008. **15**(7): p. 707-13.

145. Tadokoro, S., M. Nakanishi, and N. Hirashima, *Complexin II regulates degranulation in RBL-2H3 cells by interacting with SNARE complex containing syntaxin-3.* Cell Immunol, 2010. **261**(1): p. 51-6.

146. Bajohrs, M., et al., *Promiscuous interaction of SNAP-25 with all plasma membrane syntaxins in a neuroendocrine cell.* Biochem J, 2005. **392**(Pt 2): p. 283-9.

147. Pabst, S., et al., *Rapid and selective binding to the synaptic SNARE complex suggests a modulatory role of complexins in neuroexocytosis.* J Biol Chem, 2002. **277**(10): p. 7838-48.

148. Bracher, A., et al., *X-ray structure of a neuronal complexin-SNARE complex from squid.* J Biol Chem, 2002. **277**(29): p. 26517-23.

149. Cai, H., et al., *Complexin II plays a positive role in Ca2+-triggered exocytosis by facilitating vesicle priming.* Proc Natl Acad Sci U S A, 2008. **105**(49): p. 19538-43.

150. Xue, M., et al., *Tilting the balance between facilitatory and inhibitory functions of mammalian and Drosophila Complexins orchestrates synaptic vesicle exocytosis.* Neuron, 2009. **64**(3): p. 367-80.

151. Xue, M., et al., *Distinct domains of complexin I differentially regulate neurotransmitter release.* Nat Struct Mol Biol, 2007. **14**(10): p. 949-58.

152. Martin, J.A., et al., *Complexin has opposite effects on two modes of synaptic vesicle fusion.* Curr Biol, 2011. **21**(2): p. 97-105.

153. Xue, M., et al., *Binding of the complexin N terminus to the SNARE complex potentiates synaptic-vesicle fusogenicity.* Nat Struct Mol Biol, 2010. **17**(5): p. 568-75.

154. Maximov, A., et al., *Complexin controls the force transfer from SNARE complexes to membranes in fusion.* Science, 2009. **323**(5913): p. 516-21.

155. Shata, A., et al., *Phosphorylated synaphin/complexin found in the brain exhibits enhanced SNARE complex binding.* Biochem Biophys Res Commun, 2007. **354**(3): p. 808-13.

156. Ono, S., et al., *Regulatory roles of complexins in neurotransmitter release from mature presynaptic nerve terminals.* Eur J Neurosci, 1998. **10**(6): p. 2143-52.

157. Tang, J., et al., *A complexin/synaptotagmin 1 switch controls fast synaptic vesicle exocytosis.* Cell, 2006. **126**(6): p. 1175-87.

158. Itakura, M., et al., *Transfection analysis of functional roles of complexin I and II in the exocytosis of two different types of secretory vesicles.* Biochem Biophys Res Commun, 1999. **265**(3): p. 691-6.

159. Liu, J., et al., *Overexpression of complexin in PC12 cells inhibits exocytosis by preventing SNARE complex recycling.* Biochemistry (Mosc), 2007. **72**(4): p. 439-44.

160. Abderrahmani, A., et al., *Complexin I regulates glucose-induced secretion in pancreatic beta-cells.* J Cell Sci, 2004. **117**(Pt 11): p. 2239-47.

161. Butterworth, M.B., et al., *PKA-dependent ENaC trafficking requires the SNARE-binding protein complexin.* Am J Physiol Renal Physiol, 2005. **289**(5): p. F969-77.

162. Archer, D.A., M.E. Graham, and R.D. Burgoyne, *Complexin regulates the closure of the fusion pore during regulated vesicle exocytosis.* J Biol Chem, 2002. **277**(21): p. 18249-52.

163. Cho, R.W., Y. Song, and J.T. Littleton, *Comparative analysis of Drosophila and mammalian complexins as fusion clamps and facilitators of neurotransmitter release.* Mol Cell Neurosci, 2010.

164. Xue, M., et al., *Complexins facilitate neurotransmitter release at excitatory and inhibitory synapses in mammalian central nervous system.* Proc Natl Acad Sci U S A, 2008. **105**(22): p. 7875-80.

165. Tsai, P.S., T. van Haeften, and B.M. Gadella, *Preparation of the cortical reaction: maturation-dependent migration of SNARE proteins, clathrin, and complexin to the porcine oocyte's surface blocks membrane traffic until fertilization.* Biol Reprod, 2011. **84**(2): p. 327-35.

166. Schaub, J.R., et al., *Hemifusion arrest by complexin is relieved by Ca2+-synaptotagmin I.* Nat Struct Mol Biol, 2006. **13**(8): p. 748-50.

167. Tokumaru, H., et al., *SNARE complex oligomerization by synaphin/complexin is essential for synaptic vesicle exocytosis.* Cell, 2001. **104**(3): p. 421-32.

168. Roggero, C.M., et al., *Complexin/synaptotagmin interplay controls acrosomal exocytosis.* J Biol Chem, 2007. **282**(36): p. 26335-43.

169. Tadokoro, S., M. Nakanishi, and N. Hirashima, *Complexin II facilitates exocytotic release in mast cells by enhancing Ca2+ sensitivity of the fusion process.* J Cell Sci, 2005. **118**(Pt 10): p. 2239-46.

170. Zhao, L., et al., *Complexin I is required for mammalian sperm acrosomal exocytosis.* Dev Biol, 2007. **309**(2): p. 236-44.

171. Huntwork, S. and J.T. Littleton, *A complexin fusion clamp regulates spontaneous neurotransmitter release and synaptic growth.* Nat Neurosci, 2007. **10**(10): p. 1235-7.

172. Strenzke, N., et al., *Complexin-I is required for high-fidelity transmission at the endbulb of held auditory synapse.* J Neurosci, 2009. **29**(25): p. 7991-8004.

173. Hobson, R.J., et al., *Complexin maintains vesicles in the primed state in C. elegans.* Curr Biol, 2011. **21**(2): p. 106-13.

174. Lu, B., S. Song, and Y.K. Shin, *Accessory alpha-helix of complexin I can displace VAMP2 locally in the complexin-SNARE quaternary complex.* J Mol Biol, 2010. **396**(3): p. 602-9.

175. Yang, X., et al., *Complexin clamps asynchronous release by blocking a secondary Ca(2+) sensor via its accessory alpha helix.* Neuron, 2010. **68**(5): p. 907-20.

176. Sun, J., et al., *A dual-Ca2+-sensor model for neurotransmitter release in a central synapse.* Nature, 2007. **450**(7170): p. 676-82.

177. Matthew, W.D., L. Tsavaler, and L.F. Reichardt, *Identification of a synaptic vesicle-specific membrane protein with a wide distribution in neuronal and neurosecretory tissue.* J Cell Biol, 1981. **91**(1): p. 257-69.

178. Perin, M.S., et al., *Structural and functional conservation of synaptotagmin (p65) in Drosophila and humans.* J Biol Chem, 1991. **266**(1): p. 615-22.

179. Yoshihara, M. and J.T. Littleton, *Synaptotagmin I functions as a calcium sensor to synchronize neurotransmitter release.* Neuron, 2002. **36**(5): p. 897-908.

180. Nalefski, E.A., et al., *C2 domains from different Ca2+ signaling pathways display functional and mechanistic diversity.* Biochemistry, 2001. **40**(10): p. 3089-100.

181. Craxton, M., *Evolutionary genomics of plant genes encoding N-terminal-TM-C2 domain proteins and the similar FAM62 genes and synaptotagmin genes of metazoans.* BMC Genomics, 2007. **8**: p. 259.

182. Nishiki, T. and G.J. Augustine, *Synaptotagmin I synchronizes transmitter release in mouse hippocampal neurons.* J Neurosci, 2004. **24**(27): p. 6127-32.

183. Maximov, A. and T.C. Sudhof, *Autonomous function of synaptotagmin 1 in triggering synchronous release independent of asynchronous release.* Neuron, 2005. **48**(4): p. 547-54.

184. Geppert, M., et al., *Synaptotagmin I: a major Ca2+ sensor for transmitter release at a central synapse.* Cell, 1994. **79**(4): p. 717-27.

185. Nishiki, T. and G.J. Augustine, *Dual roles of the C2B domain of synaptotagmin I in synchronizing Ca2+-dependent neurotransmitter release.* J Neurosci, 2004. **24**(39): p. 8542-50.

186. Littleton, J.T., et al., *Calcium dependence of neurotransmitter release and rate of spontaneous vesicle fusions are altered in Drosophila synaptotagmin mutants.* Proc Natl Acad Sci U S A, 1994. **91**(23): p. 10888-92.

187. DiAntonio, A. and T.L. Schwarz, *The effect on synaptic physiology of synaptotagmin mutations in Drosophila.* Neuron, 1994. **12**(4): p. 909-20.

188. Mackler, J.M., et al., *The C(2)B Ca(2+)-binding motif of synaptotagmin is required for synaptic transmission in vivo.* Nature, 2002. **418**(6895): p. 340-4.

189. Fernandez-Chacon, R., et al., *Synaptotagmin I functions as a calcium regulator of release probability.* Nature, 2001. **410**(6824): p. 41-9.

190. Perin, M.S., et al., *Phospholipid binding by a synaptic vesicle protein homologous to the regulatory region of protein kinase C.* Nature, 1990. **345**(6272): p. 260-3.

191. Sutton, R.B., et al., *Structure of the first C2 domain of synaptotagmin I: a novel Ca2+/phospholipid-binding fold.* Cell, 1995. **80**(6): p. 929-38.

192. Sutton, R.B., J.A. Ernst, and A.T. Brunger, *Crystal structure of the cytosolic C2A-C2B domains of synaptotagmin III. Implications for Ca(+2)-independent snare complex interaction.* J Cell Biol, 1999. **147**(3): p. 589-98.

193. Ubach, J., et al., *Ca2+ binding to synaptotagmin: how many Ca2+ ions bind to the tip of a C2-domain?* EMBO J, 1998. **17**(14): p. 3921-30.

194. Fernandez, I., et al., *Three-dimensional structure of the synaptotagmin 1 C2B-domain: synaptotagmin 1 as a phospholipid binding machine.* Neuron, 2001. **32**(6): p. 1057-69.

195. Mace, K.E., et al., *Synaptotagmin I stabilizes synaptic vesicles via its C(2)A polylysine motif.* Genesis, 2009. **47**(5): p. 337-45.

196. Stevens, C.F. and J.M. Sullivan, *The synaptotagmin C2A domain is part of the calcium sensor controlling fast synaptic transmission.* Neuron, 2003. **39**(2): p. 299-308.

197. Robinson, I.M., R. Ranjan, and T.L. Schwarz, *Synaptotagmins I and IV promote transmitter release independently of Ca(2+) binding in the C(2)A domain.* Nature, 2002. **418**(6895): p. 336-40.

198. Schiavo, G., et al., *Calcium-dependent switching of the specificity of phosphoinositide binding to synaptotagmin.* Proc Natl Acad Sci U S A, 1996. **93**(23): p. 13327-32.

199. Rhee, J.S., et al., *Augmenting neurotransmitter release by enhancing the apparent Ca2+ affinity of synaptotagmin 1.* Proc Natl Acad Sci U S A, 2005. **102**(51): p. 18664-9.

200. Arac, D., et al., *Close membrane-membrane proximity induced by Ca(2+)-dependent multivalent binding of synaptotagmin-1 to phospholipids.* Nat Struct Mol Biol, 2006. **13**(3): p. 209-17.

201. Choi, U.B., et al., *Single-molecule FRET-derived model of the synaptotagmin 1-SNARE fusion complex.* Nat Struct Mol Biol, 2010. **17**(3): p. 318-24.

CHAPTER TWO

FRET INTRODUCTION

My thesis project began as a validation of a crystal structure, which, in essence, means my aim is to determine interatomic distances. While either NMR or EPR might be able to determine distances, a much faster, and relatively accurate method of distance determination is FRET (Förster Resonance Energy Transfer). FRET is a method by which one fluorophore is excited and instead of emitting at its normal wavelength, its emission energy is transferred to a second fluorophore, in a distance-dependent manner. Based on the energy transfer, one can determine the proximity of two fluorphores. In addition to its speed, FRET is useful because it can be performed at low protein concentrations (1-2μM), which eases experimentation. It is worthwhile to discuss how FRET occurs, if only briefly, to help understand the principle thrust of my contributions to the following chapters.

THE PHYSICS OF FRET

The physics of fluorescence is well-established and reviewed in [1, 2], and is briefly presented here. The internal energy of a molecule in a stable state is, to a first approximation, a function of its electronic energy. However, there are two more contributions to a molecule's internal energy: vibrational and rotational energy. Possible energy states of a molecule in terms of electronic energy, vibrational energy, and rotational energy can be diagrammed (Figure 15). The differences between levels of electronic energy are larger than the differences between levels of vibrational energy, and those in turn are larger than the differences between levels of rotational energy; in fact,

rotational energy can be, and is often neglected in the diagrams and in everyday calculations. Absorption of a photon by a molecule imparts energy, hν, to the electron distribution and thus an oscillation at a frequency ν, to an electronic dipole of the molecule. This transition dipole will be shown to be a important soon.

First, one must consider the change in energy state of a molecule that has interacted with a photon. The Jablonski diagram in Figure 16 describes the increase in electronic energy after absorbing a photon and the relaxation from higher, excited energy states back to the ground state. The energy of the absorbed photon raises both electronic and vibrational energy to new levels, depending on the wavelength of the photon and its absorption probability. The excited-state molecule then loses energy to its surroundings, and the electronic energy relaxes back to the lowest vibrational state of the lowest energy excited state, the ground state (S_0 in Figure 16). This excited-state lifetime is referred to as the fluorescence lifetime, τ. It is defined as

$$\tau = \frac{1}{k_f + k_{nr}} \tag{1}$$

where k_f is the rate of relaxation from the lowest energy excited state to the ground state by emitting a photon (called fluorescence) and k_{nr} is the rate of relaxation to the ground state by all other processes, not involving emission of a photon (*nr* is for nonradiative).

The fluorescence lifetime can be derived from the decay of fluorescence intensity in a population of molecules excited simultaneously, a measureable parameter. The intensity of the population (I) decays exponentially as a function of time t and lifetime τ.

$$I = e^{-\frac{t}{\tau}} \tag{2}$$

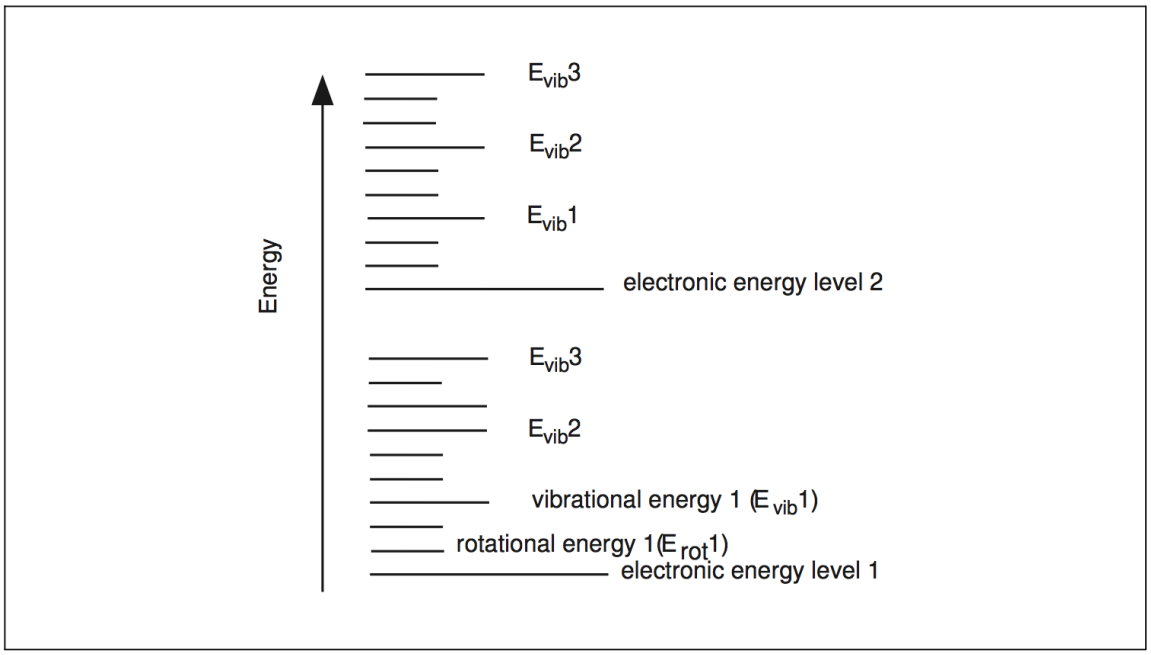

Figure 15: A simplified version of the energy levels a molecule can sample from [1]. The largest steps in energy differences are in electronic energies. These are bridged by both vibrationally (medium sized steps) and rotationally (smaller sized steps) determined energy states.

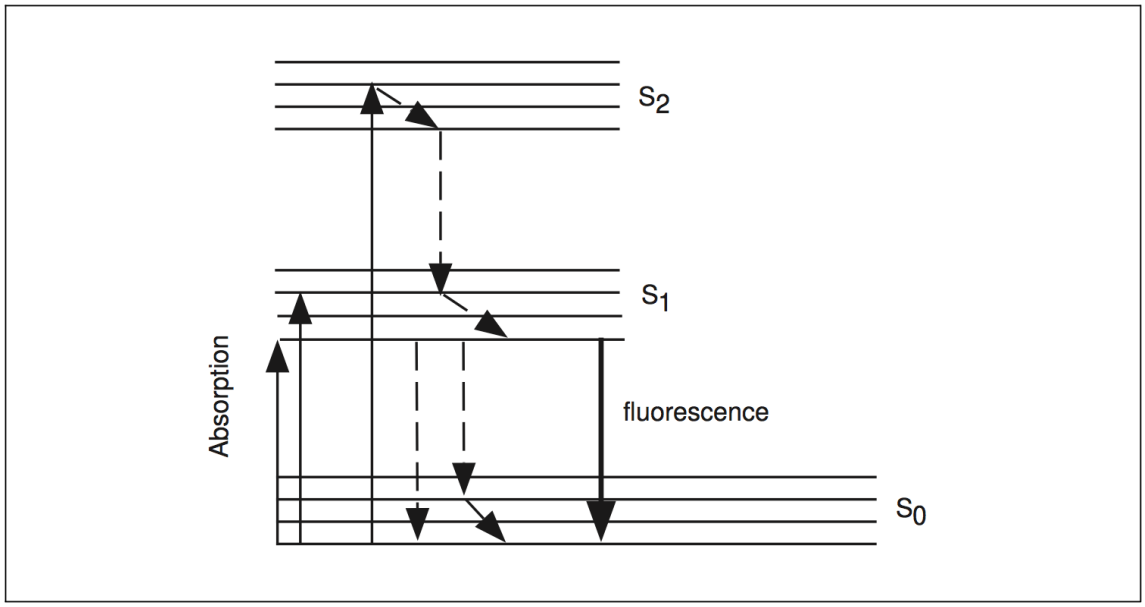

Figure 16: A sample Jablonski diagram. This Jablonski diagram from [1] depicts the absorption of energy by a molecule to a higher energy state, S_2, and successive relaxation events that can occur for that molecule so it can reach ground state, S_0, again. Fluorescence is one such process of energy release, in which a photon is released, bringing a molecule from a higher energy level to its ground state. FRET occurs when the energy absorption by one molecule is released by nonradiative transfer of the energy to a second molecule, exciting it instead, and bringing the initial molecule back to ground level without release of a photon.

One of the mechanisms for energy loss contained in k_{nr} is radiationless transfer of energy from the excited state dipole of one fluorescent molecule, the donor, to a transition dipole of another fluorescent molecule, the acceptor. This process is called Fluorescence Resonance Energy Transfer (FRET) and is the result of a distance dependent, through space, dipole-dipole interaction which occurs between an excited donor and an unexcited acceptor, and reviewed in [2, 3]. FRET theory predicts that energy could be transferred by the resonance dipole-dipole mechanism over a distance from ten to 100Å, depending on the spectroscopic parameters of the donor and acceptor. The rate of energy transfer, k_T is described by the following equation:

$$k_T = \frac{1}{\tau_D}\left(\frac{R_0}{R}\right)^6 \tag{3}$$

where τ_D is the donor lifetime in the absence of acceptor, R is the donor-acceptor distance, and R_0 (called the Förster critical distance) is a distance calculated from spectroscopic data and the mutual dipole orientation of the donor and acceptor. R_0 is an important intrinsic parameter between two fluorophores because it defines the distance between the donor and acceptor fluorophores at which the probability of donor de-excitation by energy transfer is equal to the sum of probabilities of all other deactivation processes that occur in the absence of the acceptor. That is, 50% of the energy from the donor is transferred to the acceptor. The Förster critical distance is defined by equation:

$$R_0^{\,6} = \frac{9(\ln 10)\kappa^2 Q_D J}{128\pi^5 n^4 N} \tag{4}$$

where κ^2 is the orientation factor for dipole-dipole interaction determined by the angle between the donor and acceptor dipoles, Q_D is the fluorescence quantum yield of the

donor in the absence of the acceptor, n is the refraction index of the medium between the donor and the acceptor, N is Avogadro's number, and J is the normalized spectral overlap integral, given by

$$J = \frac{\int F_D(\lambda)\varepsilon_A(\lambda)\lambda^4 d\lambda}{\int F_D(\lambda)d\lambda} \tag{5}$$

where $F_D(\lambda)$ is the fluorescence intensity of the donor in the absence of the acceptor at wavelength λ, and $\varepsilon_A(\lambda)$ is the molar absorption coefficient of the acceptor at λ.

The efficiency of transfer of the energy transfer, E_T, is a quantitative measure of the number of photons that are transferred from donor to acceptor. E_T is the ratio of the rate, k_T to the total sum of rate constants of all processes by which an excited donor molecule can return to its ground state, including k_T.

$$E_T = \frac{k_T}{k_T + \sum_{i \neq T} k_i} = k_T \tau_{DA} \tag{6}$$

where the subscript i refers to the different pathways of deactivation from the excited donor state, and τ_{DA} is the measured fluorescence lifetime of the excited state of donor in the presence of acceptor.

The energy transfer can be measured in several different ways: enhanced fluorescence of the acceptor, decreased fluorescence of the donor, decrease of the donor fluorescence lifetime, change in the anisotropy of the donor and the acceptor, and/or donor photobleaching. In my case, I chose donor fluorescence decrease out of sheer ease.

The distance between the donor and the acceptor may be calculated from the efficiency of energy transfer and using the following equation:

$$E_T = \frac{{R_0}^6}{{R_0}^6 + R^6} \tag{7}$$

The practical importance of R_0 is that it provides a handle for estimating the range of distances for which FRET can be observed for any given probe pair. Because of the strict distance dependence of energy transfer (it is a function of distance to the sixth power), steady state FRET measurements should be carried out within the value of ±50% of R_0.

In biomolecules, FRET can be utilized either via fluorophores native to the biomolecule such as tryptophan or tyrosine in proteins, naturally fluorescent fusion proteins like GFP or RFP, which can be engineered into the sequence of the protein, or via small organic fluorophores which can be specifically coupled to unique sites in these biomolecules, often through maleimide-cysteine chemistry in proteins. In general interchomophoric distance is greater than that of the alpha carbons of the amino acids to which they are attached by about 5-10Å. FRET occurs between delocalized electrons in the probes rather than between the side chains of the amino acid residues. Lankiewicz *et al.*[3] reviews the validity of this assumption and shows FRET compares to X-ray crystallography and NMR and that there is a general agreement among the three.

In addition to finding R_0 for a given FRET pair, the orientation factor, κ^2 must also be determined. It can vary from 0 to 4, but the actual value of κ^2 rarely assumes these values. In general, it is assumed that if the dyes are freely rotating, κ^2 is equals 2/3. In order to calculate κ^2, one must therefore determine whether one's dyes are freely rotating. A fluorescent molecule excited by plane-polarized light will emit polarized

fluorescence. The degree of polarization depends on the molecule's motion during the lifetime of its excited state. That is, if a molecule is freely rotating, it doesn't maintain its polarization as well as a rigid molecule. So, a measure of the emitted light's polarization can be used to determine the validity of the freely rotating assumption. The polarization of emitted fluorescence is usually read out as anisotropy, r,

$$r = \frac{I_{\parallel} - I_{\perp}}{I_{\parallel} + 2I_{\perp}} \tag{8}$$

where $I_{\parallel}$ is the intensity of the population when the emission filter is parallel to that of the excitation filter, and is the intensity when the two filters are perpendicular. FRET occurs, then r total fluorescence intensity I_{DA} (for a single species of fluorophore) or r_{donor} acceptor fluorescence, I_A (for different species of donor and acceptor). Anisotropy can therefore be used to determine the ability of the fluorophore to freely rotate, suggesting the goodness of 2/3 being chosen for κ^2.

FLUOROPHORE CHOICE

In cell biology systems, among the most common FRET partners include the family of GFP proteins [4-8]. Their value lies in their ability to be expressed as fusion proteins with the protein of interest, allowing direct visualization within a cell using confocal fluorescence microscopy [9]. In single molecule biophysics, the commonly used FRET fluorophores include the Cy dyes and the Alexa dyes [10-14], which are extremely bright dyes which can bind via maleimide-cysteine chemistry. These bright dyes have become more useful of late due to their brightness, and ability to be visualized in single-molecule experiments.

The benefits of both of these classes of fluorophores in many systems are actually detriments for my goals, however. Because they are so bright, they have relatively large overlap integrals (*J*), meaning they have large R_0 values, in the 50-60 nm range [11, 15], meaning they will be reliable for determination of distances from around 30-100Å. The distances I have to measure, though, are in the 20-40Å range. Commonly used FRET pairs for shorter distance measurements often involve engineered tryptophan residues paired with other relatively weak fluorphores. like EDANS (5-[(2-aminoethyl)amino]naphthalene-1-sulfonic acid), ANS (8-anilonaphthalene-1-sulfonate), or pyrene (reviewed in [16] and references contained therein), which have R_0 values on the order of 20-25Å, which would be perfect for the distance calculations I want to measure. Unfortunately VAMP2 has two native tryptophans in its C-terminus which are likely essential for its functioning [17]; in addition, the t-SNAREs also have native tryptophans as well, so to do experiments using tryptophan as my donor might affect how the SNAREs behave. Another problem with mutating native tryptophans out of proteins is that it renders the protein concentrations difficult to assay via standard UV_{280} spectroscopic methods. So, instead of mutating out the SNAREs' native tryptophans, I removed the few native cysteine residues where were in the proteins and used thiol-maleimide chemistry to bind fluorophore pairs with small R_0 values.

Unfortunately, there are not many of these fluorophores in existence [16], and the ones that do exist have problems such as low solubility in aqueous buffers and low labeling efficiency due to poor reactivity with the thiol group. In the course of my attempts, I tried (EDANS/NBD), (Bimane/NBD), (Pyrene/Bimane), among others. I

found NBD to be extremely insoluble in water, making it nearly impossible to work with for my proteins. Pyrene, on the other hand, forms homo-excimers [18], an interaction between the ground state of one pyrene molecule and the excited state of a second pyrene molecule. This would unnecessarily confound my data and would lead to no real benefit.

As none of these previously used short distance FRET pairs would work for me, I ended up developing a novel FRET pair. Stilbene has similar fluorescent properties to pyrene, so I chose to pair it with pyrene's partner, bimane [19], and carried out the tests to determine whether it would work. That is, I calculated its quantum yield (Q_D) to be 0.19, using tryptophan as the reference [16]. I also performed polarization measurements and determined that the anisotropy values were around 0.1, which suggests that the FRET probes have isotropic motion. This allowed me to use 2/3 for my orientation factor, κ^2. I also used a refractometer to measure the refractive index of my buffer ($\eta = 1.358$). From these values, I calculated R_0 to be 27.5Å for the Stilbene/Bimane FRET pair, which is well in the range to measure the distances I want to measure. As a control, and to validate my initial experiments, I also used a previously published Bimane/Oregon Green FRET pair [20] as validation.

FRET data were collected on a Perkin-Elmer LS55 luminescence spectrometer, operating at 25°C. Excitation and emission slits of 5 mm were used in all experiments. Both buffer alone and acceptor alone samples were subtracted from the scans to eliminate any fluorescence excitation due to the buffer or any excitation of the acceptor molecule at the donor molecule's excitation wavelength. Efficiency of transfer values were then

calculated by examining the decrease in the donor fluorescence as compared to a donor-only sample and using

$$E = 1 - \frac{f_{DA}}{f_D} \tag{9}$$

where f_D is the donor fluorescence intensity measured in the absence of acceptor and f_{DA} is the donor fluorescence intensity measured in the presence of acceptor and E is the efficiency of transfer. This value was then corrected for acceptor molecule percentage labeling using

$$E = 1 - \frac{f_{DA}}{f_D} \tag{10}$$

where the corrected efficiency was calculated by dividing the observed efficiency by the fraction of molecules labeled with acceptor, f_A. Distances were then calculated using formula (7) above.

REFERENCES

1. Edidin, M., *Fluorescence resonance energy transfer: techniques for measuring molecular conformation and molecular proximity.* Curr Protoc Immunol, 2003. **Chapter 18**: p. Unit 18 10.
2. Lakowicz, J.R., *Principles of Fluorescence Spectroscopy*. 3 ed. 2006, New York City: Springer. 954.
3. Lankiewicz, L., J. Malicka, and W. Wiczk, *Fluorescence resonance energy transfer in studies of inter-chromophoric distances in biomolecules.* Acta Biochim Pol, 1997. **44**(3): p. 477-89.
4. Chudakov, D.M., et al., *Fluorescent proteins and their applications in imaging living cells and tissues.* Physiol Rev, 2010. **90**(3): p. 1103-63.
5. Wang, Y. and N. Wang, *FRET and mechanobiology.* Integr Biol (Camb), 2009. **1**(10): p. 565-73.
6. Wiedenmann, J., F. Oswald, and G.U. Nienhaus, *Fluorescent proteins for live cell imaging: opportunities, limitations, and challenges.* IUBMB Life, 2009. **61**(11): p. 1029-42.
7. Sample, V., R.H. Newman, and J. Zhang, *The structure and function of fluorescent proteins.* Chem Soc Rev, 2009. **38**(10): p. 2852-64.
8. Tsien, R.Y., *The green fluorescent protein.* Annu Rev Biochem, 1998. **67**: p. 509-44.

9. Schmid, J.A. and A. Birbach, *Fluorescent proteins and fluorescence resonance energy transfer (FRET) as tools in signaling research.* Thromb Haemost, 2007. **97**(3): p. 378-84.

10. Gambin, Y. and A.A. Deniz, *Multicolor single-molecule FRET to explore protein folding and binding.* Mol Biosyst, 2010. **6**(9): p. 1540-7.

11. Roy, R., S. Hohng, and T. Ha, *A practical guide to single-molecule FRET.* Nat Methods, 2008. **5**(6): p. 507-16.

12. Rasnik, I., S.A. McKinney, and T. Ha, *Surfaces and orientations: much to FRET about?* Acc Chem Res, 2005. **38**(7): p. 542-8.

13. Jares-Erijman, E.A. and T.M. Jovin, *FRET imaging.* Nat Biotechnol, 2003. **21**(11): p. 1387-95.

14. Ha, T., *Single-molecule fluorescence resonance energy transfer.* Methods, 2001. **25**(1): p. 78-86.

15. Sabanayagam, C.R., J.S. Eid, and A. Meller, *Using fluorescence resonance energy transfer to measure distances along individual DNA molecules: corrections due to nonideal transfer.* Journal of Chemical Physics, 2005. **122**(6): p. 061103.

16. Wu, P. and L. Brand, *Resonance energy transfer: methods and applications.* Anal Biochem, 1994. **218**(1): p. 1-13.

17. Maximov, A., et al., *Complexin controls the force transfer from SNARE complexes to membranes in fusion.* Science, 2009. **323**(5913): p. 516-21.

18. Lehrer, S.S., *Intramolecular pyrene excimer fluorescence: a probe of proximity and protein conformational change.* Methods Enzymol, 1997. **278**: p. 286-95.

19. Borochov-Neori, H. and M. Montal, *Rhodopsin-G-protein interactions monitored by resonance energy transfer.* Biochemistry, 1989. **28**(4): p. 1711-8.

20. Buskiewicz, I., et al., *Domain rearrangement of SRP protein Ffh upon binding 4.5S RNA and the SRP receptor FtsY.* RNA, 2005. **11**(6): p. 947-57.

CHAPTER THREE

PREFACE

The model put forth in **GIRAUDO ET AL**, **figure x**, proposes that the Accessory Helix of Complexin clamps fusion by binding to the pre-zippered C-terminus of the t-SNARE preventing the binding of the VAMP2 C-terminus. We collaborated with the Reinisch lab at Yale University to examine this model crystallographically. The key to the solving of the crystal was twofold: first, we truncated the VAMP2 at residue 60 with the thought that, if it is not present, the C-terminus cannot zipper. Second, we used the superclaming mutant of Complexin (**residues**) to assist it in being able to bind better.

Once the crystal structure was solved, one major concern was that it was solely an artifact of either high concentration and crystal packing or truncation of the v-SNARE. In order to ensure that the observed crystal structure is real and not an artifact of crystallization, I developed a FRET-based assay to determine the positioning of the Accessory Helix in Complexin. After validating that the crystal structure was, in fact, real, we also examined its energetics via Isothermal Titration Calorimetry (ITC) as well as its functional consequences using both liposome fusion and cell-cell fusion assays and arrived at a model of the clamping process.

This paper provides an explanation of how Complexin, and specifically its Accessory helix can clamp fusion. My contribution of the FRET studies helped to prove that the crystal structure is valid.

Complexin cross-links pre-fusion SNAREs into a zig-zag array: a structure-based model for complexin clamping.

Daniel Kümmel[1], Shyam S. Krishnakumar[1] , Daniel T. Radoff[1,2], Feng Li[1], Claudio G. Giraudo[1], Frederic Pincet[1,3], James E. Rothman[1,*], Karin M. Reinisch[1,*]

[1]Department of Cell Biology, Yale University School of Medicine, New Haven, Connecticut 06520, USA.

[2]Department of Biochemistry and Molecular Biophysics, Columbia University New York, New York 10032, USA.

[3]Laboratoire de Physique Statistique, Unité Mixte de Recherche 8550, Centre National de la Recherche Scientifique associée aux Universités Paris VI et Paris VII, Ecole Normale Supérieure, 24 rue Lhomond, 75005 Paris, France.

*Correspondence should be addressed to JER james.rothman@yale.edu (203-737-5293) or KMR karin.reinisch@yale.edu (203-785-6469)

SUMMARY

Complexin prevents SNAREs from releasing neurotransmitters until an action potential arrives at the synapse. To understand the mechanism for this inhibition, we determined the structure of complexin bound to a mimetic of a pre-fusion SNAREpin that lacks the portion of the v-SNARE which zippers last to trigger fusion. The "central helix" of complexin is anchored to one SNARE complex while its "accessory helix" extends away at ~45º and bridges to a second complex, occupying the vacant v-SNARE binding site to inhibit fusion. That the accessory helix competes with the v-SNARE for t-SNARE binding was expected, but surprisingly, the interaction occurs inter-molecularly. Thus complexin organizes the SNAREs into a zig-zag topology which, when interposed between the vesicle and plasma membranes, is incompatible with fusion.

INTRODUCTION

Information processing in all nervous systems requires the correlation of events in the external world with internal representations, and therefore relies on transmission of signals between neurons that are precisely timed and that retain coherence. This, in turn, requires that the release of neurotransmitters at synapses also be precisely timed, following immediately the arrival of a nervous impulse. The physiological and anatomical mechanisms have long been known[1,2]. Synaptic vesicles containing neurotransmitter are already docked at the "active zones" of the pre-synaptic membrane, ready to respond to the elevated calcium levels that accompany an action potential by releasing neurotransmitter.

In recent years, much has also been learned about the molecular mechanisms underlying this physiology. The central players in neurotransmitter release are the SNARE proteins[3]. These are the engines that drive membrane fusion between cargo-carrying vesicles and the plasma membrane[4,5] as v-SNAREs (anchored in the vesicle membrane) zipper into a coiled-coil four helix bundle with cognate t-SNAREs (anchored in the plasma membrane)[3-6]. In synapses, a major v-SNARE is VAMP2, and the t-SNARE proteins are SNAP25 and syntaxin1, where VAMP2 and syntaxin1 each contribute one helix to the coiled-coil and SNAP25 contributes two[7]. Another vital component is synaptotagmin, a synaptic vesicle protein[8] that binds calcium ions[9] and is the immediate sensor and trigger for vesicle fusion[10-12]. How precisely synaptotagmin couples to SNAREs to trigger fusion remains unknown.

But whatever the mechanism, rapid and synchronous release of neurotransmitter requires that the fusion process by SNARE proteins be frozen in place, or "clamped"[3], when it is well advanced. This is because fusion by SNARE proteins is spontaneous[4,5] and must therefore be inhibited to prevent continuous release of neurotransmitters. This is also because neurotransmitter release takes place on a much shorter time scale than the entire process of vesicle docking and fusion complex assembly. For example, fusion of artificial vesicles bearing v-SNAREs to planar lipid bilayers containing t-SNAREs requires 10-100 msec following docking[13-15], whereas neurotransmitter release can take place in one millisecond or less after calcium entry. Thus, fusion must be clamped at a very late stage in synapses.

A combination of biochemical, genetic, and physiological results have clearly pinpointed complexin (CPX)[16,17] as the central component of this clamp[18-20]. Since CPX both facilitates and inhibits synaptic fusion[21-26], it has been proposed to act by catalyzing the initial stages of SNARE assembly, but then clamping further assembly until the arrival of an action potential (reviewed in[27]). The thermodynamic basis by which CPX can function both as an activator and a clamp for SNARE assembly is explored in a sister manuscript[28].

Structures of CPX bound to a post-fusion fully assembled SNAREpin[29,30] yielded first insights regarding the facilitatory mechanism, but did not resolve how CPX inhibits fusion. In the post-fusion/SNARE structures, CPX forms a continuous helix parallel to the SNAREpin coiled-coil, with a "central helix" portion of CPX (CPX_{cen}, residues 48-70 in hCPX1) contacting both the v-SNARE and t-SNARE in the membrane-distal portion

of the SNAREpin. This is the portion of the SNAREpin that zippers first, and it is thus possible that CPX facilitates initial assembly[30]. The remainder of the CPX helix, termed its "accessory helix" (CPX_{acc}, residues 26-47 in hCPX1), parallels the C-terminal membrane-proximal portion of the fully zippered SNARE complex, but does not interact with it.

Nonetheless, the accessory helix is needed to create the clamped, pre-fusion state[21,31] in which the membrane-distal N-terminal portions of the SNARE coiled-coil have zippered, but the membrane-proximal VAMP2 C-terminus has not yet associated with the corresponding regions of SNAP25 and syntaxin1[18,21,32-34]. Biochemical and spectroscopic experiments strongly support a mechanism whereby CPX_{acc} directly competes with the VAMP2 C-terminus for binding to the t-SNARE[19,35] - but how this happens has been unclear in the absence of structural studies with pre-fusion SNARE complexes.

We have therefore designed a half-zippered soluble mimetic of the pre-fusion synaptic SNAREpin, and we have solved its structure when bound to complexin. Remarkably, we find that the CPX accessory helix extends away from the SNAREpin, and binds a second SNAREpin to inhibit its assembly. Solution and functional studies confirm both the CPX conformation and the interaction between the accessory helix and pre-fusion SNAREpin observed in the structure. Our studies thus suggest that complexin cross-links pre-fusion SNARE complexes into a zig-zag array. This array, when interposed between the vesicle and plasma membrane, provides a further barrier to

fusion. Although cross-linking the CPX/SNARE array may block fusion, it also orients the SNAREs appropriately for fusion to proceed quickly upon clamp release.

RESULTS AND DISCUSSION

STRUCTURES OF A "PRE-FUSION" SNAREPIN AND ITS COMPLEX WITH CPX.

The pre-fusion form of the SNARE complex is a transient intermediate stabilized in part by the simultaneous insertion of SNAREpins into two membrane bilayers, and hence is not readily accessible for structural studies. Zippering up begins as the pre-folded N-terminal portions of VAMP2 associate with the pre-assembled t-SNARE complex[36-38]. In designing a soluble pre-fusion SNARE mimetic suitable for structural studies, we therefore prevented the completion of zippering by C-terminally truncating the VAMP2 SNARE motif. This SNARE complex (SNAREΔ60) also contains residues 190-253 of rSyntaxin1A and residues 10-82 and 141-203 of hSNAP25A.

We determined the structure of this truncated SNARE complex at 2.2 Å resolution (**Table 1**). Except for the absent VAMP2 C-terminus, the truncated SNARE complex in our studies superimposes well with fully assembled SNARE complexes studied previously (rmsd 0.77-0.97 Å)[7,30]. A notable finding is that the syntaxin1 and SNAP25 helices are almost fully formed even in the absence of the VAMP2 C-terminus

(**Figure 17A**), suggesting that the t-SNAREs may be almost fully folded when the v-SNARE is only half zippered.

		SNARE		scCPX/ SNARE		scCPX-F34M/ SNARE	
space group		P 1		C 2_1		P 1	
unit cell	a [Å]	27.6		75.9		53.7	
	b [Å]	39.8		52.7		127.4	
	c [Å]	102.3		128.7		142.7	
	α [°]	83.4		90		107.5	
	β [°]	89.9		95.2		90.0	
	γ [°]	89.9		90		90.1	
Resolution [Å] *		50-2.2	(2.28-2.2)	50-3.5	(3.63-3.5)	30-3.8	(3.94-3.8)
Unique reflections *#		20205	(1655)	6129	(576)	58784	(4948)
Redundancy *		3.7	(3.3)	3.4	(3.5)	1.9	(1.8)
I/σ *		19.7	(5.7)	15.7	(6.2)	9.1	(2.6)
Completeness [%] *#		91.9	(76.4)	94.8	(91.3)	83.5	(80.7)
R_{sym} [%] *		5.2	(20.4)	6.2	(23.4)	8.0	(25.3)
Refinement [Å]		50-2.2		25-3.5		30-3.8	
R_{work} / R_{free} [%]		22.7 / 26.8		27.0 / 31.6		30.3 / 34.6	
rmsd bond distances [Å]		0.017		0.054		0.035	
rmsd bond angles [°]		1.58		1.28		0.98	
mean B value [Å²]		56.9		99.8		116.1	
Ramachandran diagram [%] §							
most favored		98.8		91.7		98.4	
additionally allowed		0.2		8.3		1.6	

Table 1: Data processing and refinement statistics for the structures presented in this study.
* values in parenthesis refer to outer shell of reflections
# for reflections with I/σ greater than zero
§ from Molprobity[57]

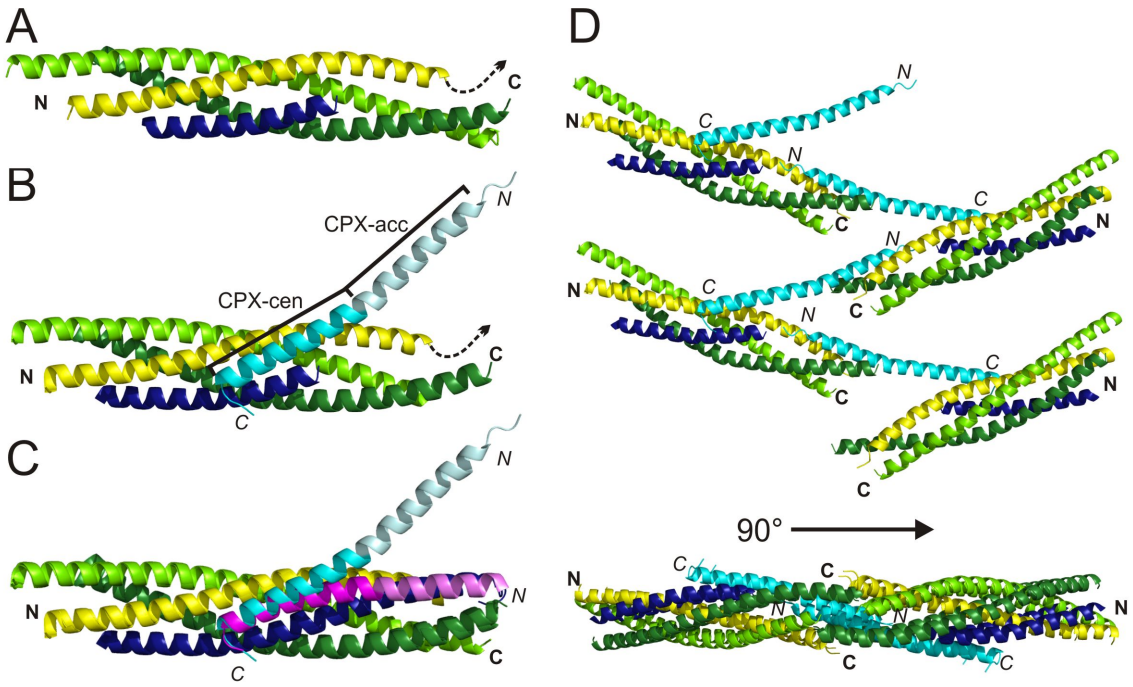

Figure 17: Structure of the pre-fusion CPX/SNARE complex. VAMP2 (residues 29-60) is blue, syntaxin yellow (residues 190-250), SNAP25 lime (N-terminal SNARE motif, residues 10-74) and green (C-terminal SNARE motif, residues 141-203) and CPX (residues 26-73) cyan. Model of (A) the truncated SNARE complex without and (B) with CPX bound. CPX_{cen} is cyan, and CPX_{acc} pale cyan. A dashed arrow indicates syntaxin membrane anchor. (C) Comparison of pre- and post-fusion CPX/SNARE complexes, with post-fusion CPX magenta (CPX_{acc} is pale magenta, PDB ID 1KIL). The arrow indicates the conformational change of CPX during clamp release. (D) Top and side views of the zig-zag array of post-fusion CPX/SNARE complexes observed in crystals. SNAREpins are related by 180° rotation and translation along the zig-zag midline, so that on different sides of the mid-line the linkers that connect syntaxins and VAMPs to their trans-membrane helices are on opposite sides of the zig-zag plane.

We next co-crystallized SNAREΔ60 with a CPX fragment (scCPX) consisting of its central and accessory helices (residues 26-83) and containing three "superclamp" mutations (D27L, E34F, R37A) that increase its clamping efficiency both *in vitro*[19] and *in vivo*[39]. The energy profile associated with clamping and clamp release is not altered, except that the superclamp binds more tightly to the pre-fusion SNARE complexes[28]. The structure was determined at 3.5 Å resolution using the truncated SNARE complex as a search model in the molecular replacement method (**Table 1**), and CPX was modeled into difference electron density. The final model includes residues 190-250 of syntaxin1, 10-74 and 141-203 of SNAP25, 29-60 of VAMP2, and 26-73 of CPX (**Figure 17B**).

To confirm the sequence alignment along CPX, we used selenomethionine substituted forms of scCPX, where residues L27 and F34 in the accessory helix were mutated to methionine (scCPX-L27M, scCPX-F34M). The selenomethionine-substituted forms of CPX were co-crystallized with the truncated SNARE complex, and anomalous data (**Table 1**) were used to calculate difference maps that unambiguously locate the position of residues 27 and 34 as well as 55, a methionine in the wild-type sequence (**Figure 18**). We also determined the structure of the selenomethionine-substituted scCPX-F34M bound to the truncated SNARE complex (**Table 1**). While the crystals of this complex belong to a different spacegroup (P1) from the scCPX/SNARE crystals we initially obtained (C2), our findings regarding CPX-SNARE interactions are similar.

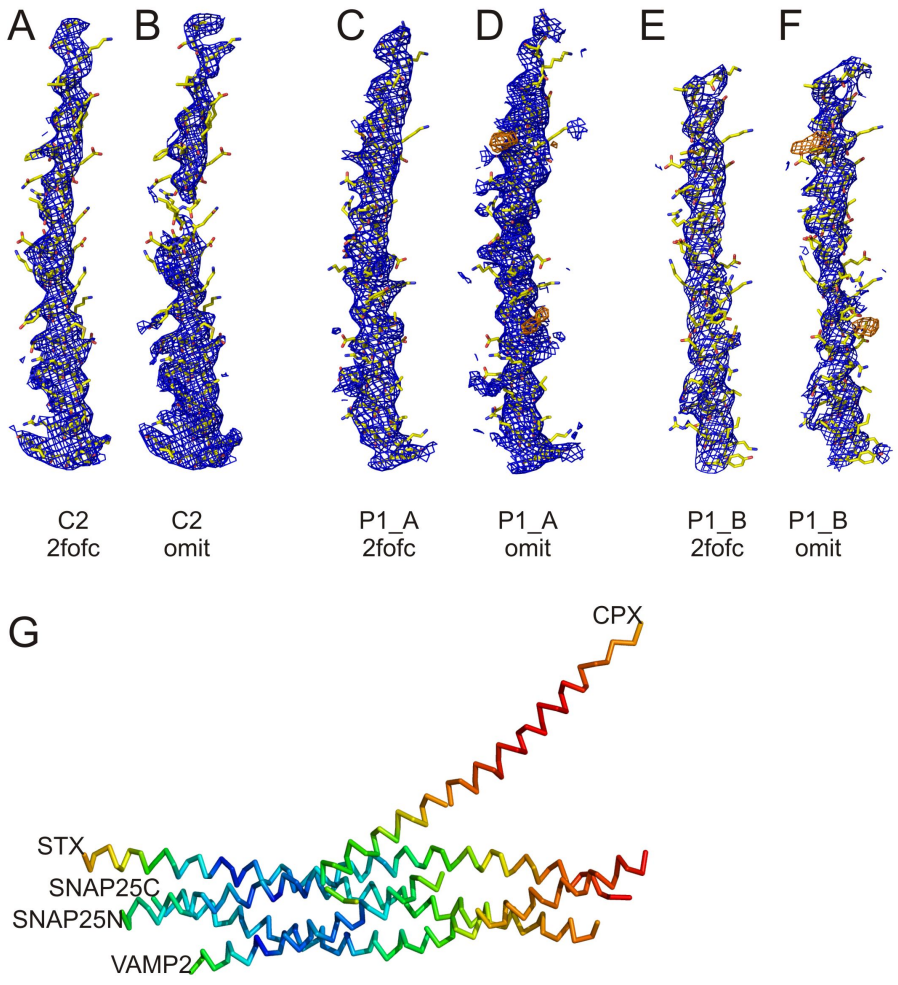

Figure 18: Electron density for CPX contoured at 1σ. (A) Weighted 2fo-fc electron density after refinement and (B) composite simulated annealed omit map for CPX in the C2 crystal form. (C) Weighted 2fo-fc electron density after refinement (D) and four-fold averaged composite simulated annealed omit map for CPX-F34M in binding mode A of the P1 crystal form. (E) Weighted 2fo-fc electron density after refinement (F) and four-fold averaged composite simulated annealed omit map for CPX-F34M in binding mode B of the P1 crystal form. There are two binding modes for CPX_{acc}-F34M and the t-SNARE groove in the P1 crystal form, "A" and "B". CPX and especially its accessory helix have high B-factors, and as seen in (A-F), solvent-exposed side-chains are not well ordered. We therefore used selenomethionine-substituted forms of CPX to confirm the sequence register. The anomalous difference maps used to located the positions of M55 and M34 are shown in orange in (D) and (F) and are contoured at 3.5 σ. (G) B-factor plot of CPX/SNARE complex in rainbow color scheme (blue to red, 17-185 $Å^2$).

The CPX/SNAREΔ60 structures resemble the fully-zippered, post-fusion structures observed previously in several aspects (**Figure 17C**). The conformations of the SNARE proteins are essentially unaltered (rmsd 0.83 Å). Further, as in the post-fusion forms of the CPX/SNARE complex[29,30] as well as alone in solution[40], CPX forms a continuous helix. The interactions between CPX_{cen} and the SNARE complex observed in the post-fusion structure are also largely unperturbed (small positional shifts in CPX_{cen} are detailed in **Table 2**; see also **Figure 17C**). CPX_{cen} binds in the groove between syntaxin1 and VAMP2, with key residues R59, R63, I66, Y70, and I72 inserted into two high affinity binding pockets observed in earlier studies[29,30]. A third previously identified binding interface involves residues D64, D65 and D68 in the VAMP2 C-terminus, which are missing in our construct. This interaction is not necessary for clamping[41], and so its absence in our structure likely will not affect conclusions regarding the CPX clamping mechanism.

CPXcen Cα	displacement [Å] post- vs. pre-fusion
59	2.6
60	1.5
61	1.2
62	1.1
63	0.9
64	0.5
65	0.7
66	1.0
67	0.5
68	0.4
69	0.4
70	0.3

Table 2: The central helix of Complexin is slightly differently anchored to the SNARE complex. The displacement for each Cα atom between the post-fusion and pre-fusion structure is listed.

Despite these similarities, the arrangement of CPX relative to the SNAREs in our structure differs markedly from that in post-fusion forms of the CPX/SNARE complex. The accessory helix undergoes a dramatic reorientation (rmsd of CPX as compared to PDB ID 1KIL[30] is 2.2 Å). Rather than running alongside the SNARE complex, CPX_{acc} now bends away at a ~ 45º angle (**Figure 17C**). The reorientation likely results from small differences in CPX_{cen} docking (**Table 2**) as well as small changes in phi/psi torsion angles in the transition region between CPX_{cen} and CPX_{acc} (**Table 3**). This result was unexpected given biochemical data indicating that CPX_{acc} should occupy the binding site for the VAMP2 C-terminus, since CPX and the VAMP2 C-terminus compete for binding to the t-SNAREs[19,35]. While CPX_{acc} does not interact with the same SNARE complex bound by CPX_{cen}, however, it does interact with a second, symmetry-related complex.

Overall, the crystal packing is such that CPX/SNARE complexes are arranged in a continuous zig-zag (**Figure 17D**), leaving the middle of the accessory helix entirely solvent exposed. This region has high thermal motion, as evidenced by high B-factors (**Figure 18**). SNAREpins on opposite sides of the zig-zag mid-line are related by a 180 degree rotation about (and a translation along) the mid-line. This means that on different sides of the mid-line, the linkers that connect the syntaxins and the VAMPs to their trans-membrane helices in the plasma membrane and the synaptic vesicle, respectively, are on opposite sides of the zig-zag plane. Although the CPX-F34M mutant crystallized in a different space group, it cross-links different SNARE complexes the same way, and the complexes are arranged in a zig-zag (**Figure 19**).

CPX position	Post-fusion phi [°]	Post-fusion psi [°]	Pre-fusion phi [°]	Pre-fusion psi [°]	Difference phi [°]	Difference psi [°]
45	-77.4	-35.2	-83.4	-36.1	6.0	0.9
46	-63.1	-27.8	-72.3	-31.8	9.2	4.0
47	-86.1	-35.4	-75.3	-49.5	-10.8	14.1
48	-65.4	-39.4	-54.2	-31.6	-11.2	-7.8
49	-68.7	-30.4	-69.1	-43.4	0.4	13.0
50	-73.3	-43.5	-65.9	-41.7	-7.4	-1.8
51	-64.9	-26.0	-62.3	-38.7	-2.6	12.7
52	-90.0	-19.9	-68.1	-33.2	-21.9	13.3
53	-78.2	-35.6	-63.4	-45.4	-14.8	9.8
54	-68.3	-35.9	-73.3	-35.0	5.0	-0.9
55	-65.2	-44.9	-66.3	-40.9	1.1	-4.0
56	-59.5	-47.4	-54.8	-54.8	-4.7	7.4
57	-58.2	-43.9	-54.2	-40.6	-4.0	-3.3
58	-63.1	-33.9	-82.4	-14.2	19.3	-19.7
average	-70.1	-35.7	-67.5	-38.4	-2.6	2.7

Table 3: The CPX helix twisted differently in the post- and pre-fusion structure. Peptide angles of the CPX region linking the central and accessory helix are listed.

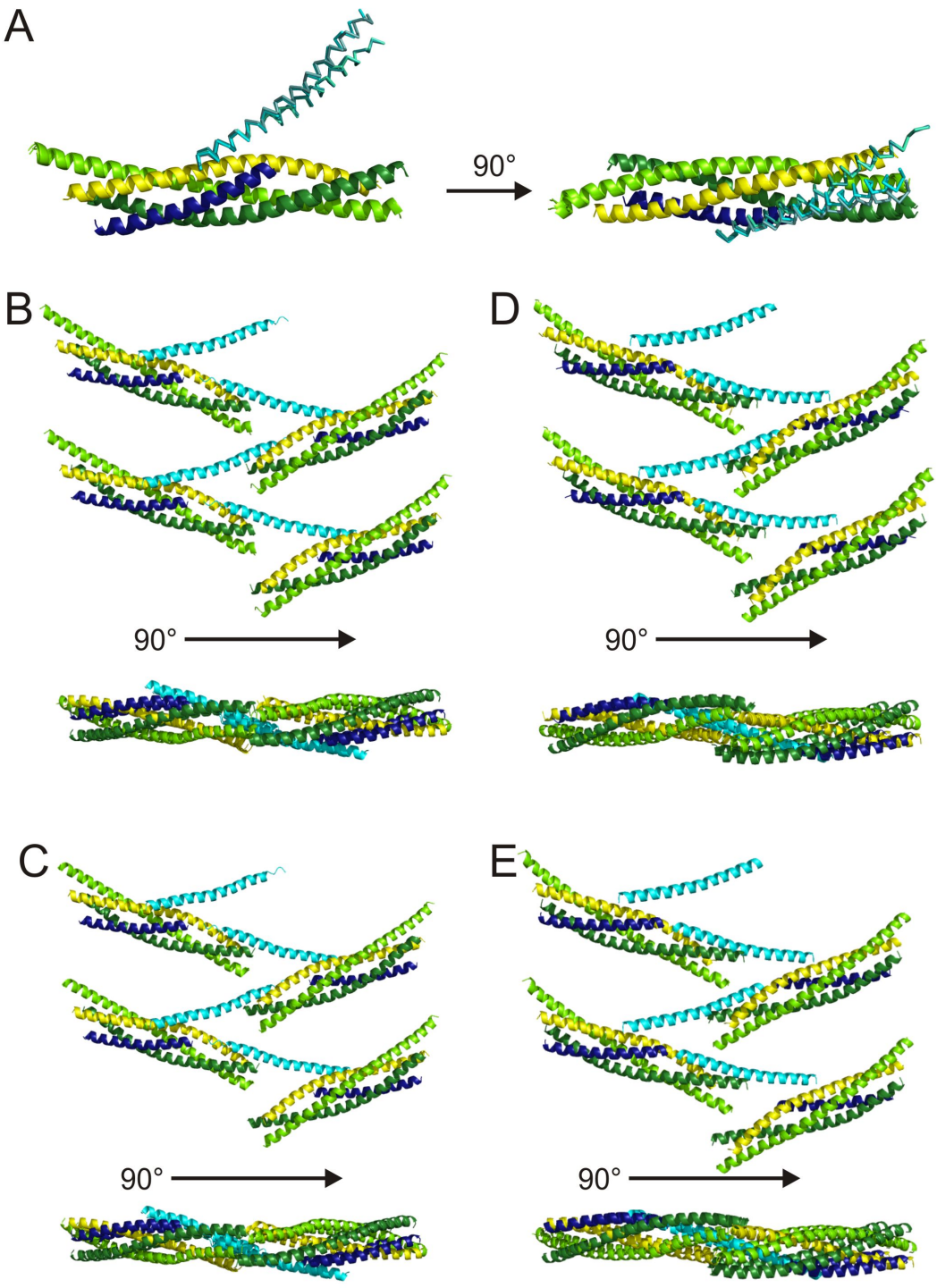

Figure 19: Zig-zag arrays in the P1 crystal form. (A) Superposition of CPX/SNARE complexes constituting four crystallographically distinct zig-zag arrangements in the P1 crystal form. (B)-(E) Top and side view of the four different lattices in the P1 crystal form.

Overall, the crystal packing is such that CPX/SNARE complexes are arranged in a continuous zig-zag (**Figure 17D**), leaving the middle of the accessory helix entirely solvent exposed. This region has high thermal motion, as evidenced by high B-factors (**Figure 18**). SNAREpins on opposite sides of the zig-zag mid-line are related by a 180 degree rotation about (and a translation along) the mid-line. This means that on different sides of the mid-line, the linkers that connect the syntaxins and the VAMPs to their trans-membrane helices in the plasma membrane and the synaptic vesicle, respectively, are on opposite sides of the zig-zag plane. Although the CPX-F34M mutant crystallized in a different space group, it cross-links different SNARE complexes the same way, and the complexes are arranged in a zig-zag (**Figure 19**).

Residues at the N-terminal end of CPX_{acc} (L27, A30, A31, F34, and A37) form a hydrophobic surface which binds to the t-SNARE in a second SNARE complex in a site normally occupied by the C-terminus of the VAMP2 helix in post-fusion state, which was deleted from the mimetic used here (**Figure 20A, Figure 21**). In crystals of scCPX-F34M/SNARE, the interactions between CPX_{acc} and the t-SNARE groove are as just described for the scCPX/SNARE crystals in four of eight crystallographically distinct complexes. In the remaining four complexes, the binding site on the t-SNARE is shifted by approximately two helical turns, so that the interface between CPX_{acc} and the t-SNARE is larger (~1000 $Å^2$ versus ~715 $Å^2$, **Figure 20B, Figure 21**), additionally involving CPX residues L41, A44 and R48. Because a single mutation in the CPX_{acc} sequence allows for two different binding modes, we expect that the high sequence variability in CPX_{acc} of different complexins (isoforms 1-4 and in different organisms)

results in slight variations of SNARE-bridging interactions and strength. The recurrence of the zig-zag arrangement of CPX/SNARE complexes in two different crystal forms, however, supports the notion that this arrangement may be physiologically relevant.

Notably, for both scCPX and scCPX-F34M, residues that were mutated to make the superclamp CPX (D27L, E34F/M, R37A) are an integral part of the hydrophobic interface with the SNARE complex. The ability to bind the t-SNARE surface via a more extended hydrophobic interface may explain why the superclamp sequences have a higher affinity for pre-fusion SNARE complexes than wild-type CPX (shown below) and why superclamp CPX_{acc} clamps more effectively *in vitro* and *vivo*[19,39].

SOLUTION STUDIES CONFIRM THE CPX_{ACC}/SNAREΔ60 INTERACTION.

Thus, in both the CPX/SNARE structures, we find CPX_{acc} interacting with the t-SNAREs in such a way that CPX, linked by its central helix to one SNARE complex, blocks binding of the VAMP2 C-terminus to another complex, cross-linking the SNARE complexes into an array in the process.

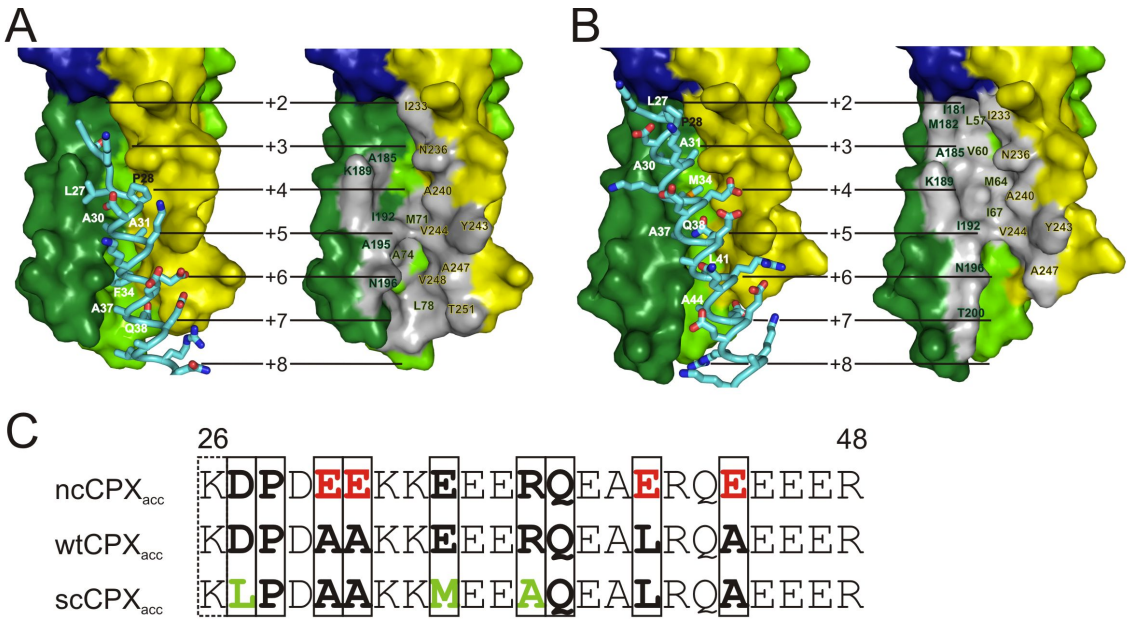

Figure 20: Interacting surfaces of CPX_{acc} and the t-SNAREs. (A) Interacting residues of scCPX are labeled in left panels; the binding site on the t-SNARE is outlined as grey patch and labeled on right panels. (B) For scCPX-F34M, CPX_{acc} can bind to the t-SNARE groove as in (A) or as shown here. (C) Sequence of the accessory helix of wild-type (wt) CPX and the non-clamping (nc) and superclamp (sc) mutants. Residues of CPX interacting with the t-SNARE in the crystal structures are boxed. The side chain of K26 is disordered in our structure, but functional data[19] suggest that it has a role in clamping. It may interact with the VAMP2 C-terminus absent in our structure.

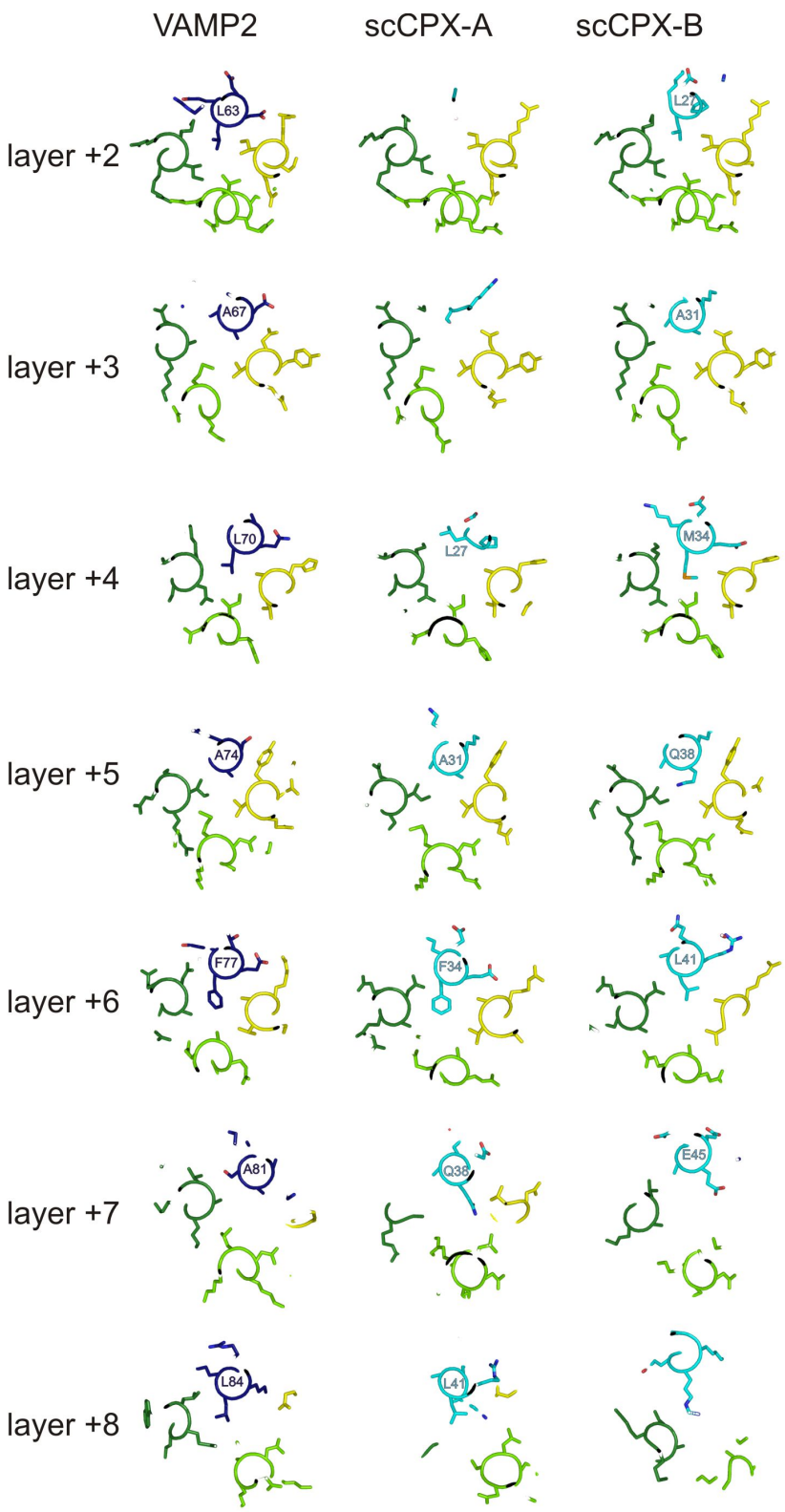
VAMP2
scCPX-A
scCPX-B
layer +2
L63
L27
layer +3
A67
A31
layer +4
L70
L27
M34
layer +5
A74
A31
Q38
layer +6
F77
F34
L41
layer +7
A81
Q38
E45
layer +8
L84
L41

Figure 21: Comparison of the hydrophobic layer interactions of the t-SNARE groove with VAMP2 (left panels) CPX in binding mode A (middle panels) and in binding mode B (right panels).

We used isothermal titration calorimetry (ITC) experiments to confirm that CPX_{acc} interacts with the t-SNARE in pre-fusion SNARE complexes. In these experiments, we used a complexin construct comprising both the central and accessory helices (residues 26-83) rather than a peptide corresponding to the accessory helix alone. Our rationale was that the accessory peptide does not fold into an alpha helix, as monitored by CD, and thus does not fold as in the full length protein, where it has high helical propensity (CD and ref. 40). The longer complexin construct was chosen to avoid complications in binding measurements resulting from folding energetics. To observe the interaction between only CPX_{acc} and the SNARE complex, we blocked the CPX_{cen} binding site on either a fully-assembled post-fusion SNARE or SNAREΔ60 by pre-binding CPX_{cen} (residues 48-134). Various CPX constructs were then titrated in to derive interaction affinities. As predicted from the post-fusion SNARE/CPX crystal structure, we find no additional interaction between wild-type complexin (wtCPX, residues 26-83) and the blocked post-fusion SNAREpin (**Figure 22A**). In contrast, wtCPX interacts with blocked SNAREΔ60 with Kd ~10 μM affinity, consistent with an additional binding site present only pre-fusion and the finding that CPX competes with the VAMP2 C-terminus for binding[19]. Further, the interaction affinity can be modulated by mutating residues in CPX_{acc}, as expected if CPX_{acc} participates in the interaction (**Figure 22B**). We used CPX mutants where residues at the CPX_{acc}/SNARE interface in the crystal structure were altered. In addition to scCPX (D27L, E34F, R37A) we designed a non-clamping CPX mutant (ncCPX: A30E, A31E, L41E, A44E), where hydrophobic residues at the

CPX_{acc}/t-SNARE interface in the crystal structure were replaced by charged residues (**Figure 20C**). As expected, the binding affinity for scCPX is ~8-fold stronger than wild-type, consistent with the difference in activity observed in both *in vitro* and *in vivo* assays[19,39], whereas ncCPX no longer interacts with blocked SNAREΔ60 (**Figure 22B**). Thus, binding studies corroborate an interaction between CPX_{acc} – both wild-type and superclamp – and the pre-fusion SNARE complex as observed in the crystal structure.

We used Förster resonance energy transfer (FRET) experiments to establish that the angled conformation of CPX also occurs in solution and therefore is not dictated by crystal packing. The donor dye (stilbene) was attached to SNAP-25 residue 193, with the acceptor dye (bimane) positioned either at residue 31 or 38 of superclamp CPX (**Figure 23A**). (Note that acceptor positions are placed so that they would interfere with CPX_{acc}/t-SNARE cross-linking interactions, enabling monodisperse CPX/SNARE complexes to be studied.) Distances estimated via quenching of donor fluorescence for CPX bound to the fully zippered SNARE complex correspond closely to distances observed in the crystal structure of the post-fusion CPX/SNARE complex (PDB 1KIL), where CPX_{acc} runs parallel to the SNARE complex (**Figure 23B,C, Table 4**).

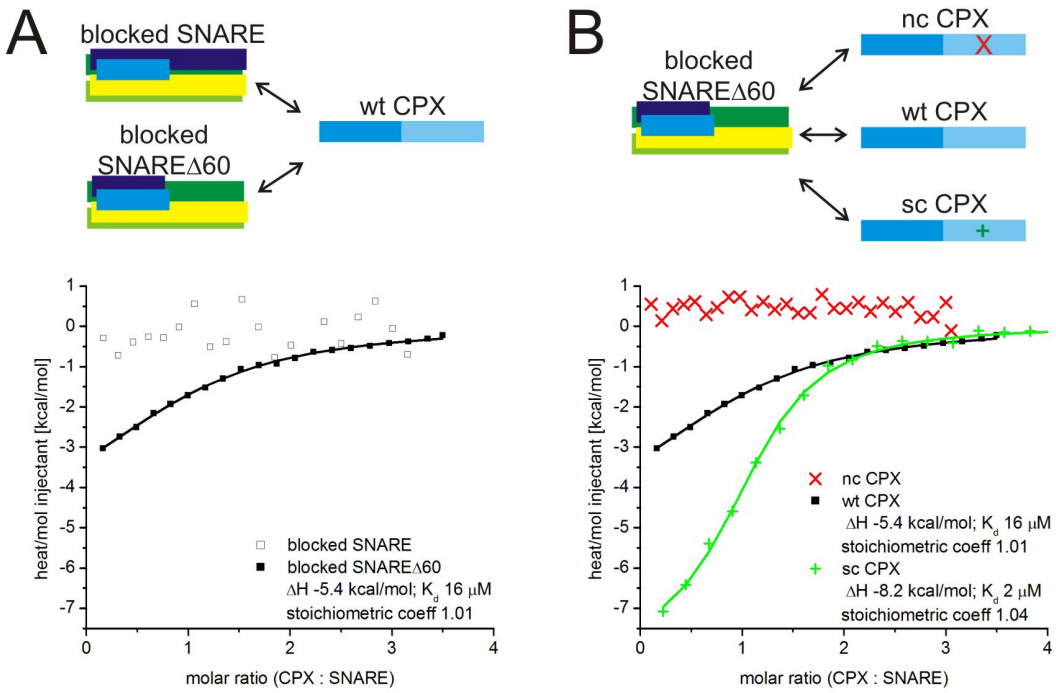

Figure 22: Characterization of the interaction of CPX_{acc} with SNARE complexes by isothermal titration calorimetry. (A) A groove in the t-SNARE is a second binding site for CPX distinct from the central helix binding site. When the central helix binding site on the SNARE complex is blocked, CPX still binds to the SNARE complex once the C-terminal half of VAMP2 is removed in the pre-fusion SNARE mimetic. (B) Binding to the t-SNARE groove is mediated by CPX_{acc}. Mutations in the accessory helix of CPX modulate the binding affinity to the t-SNARE positively (scCPX) or negatively (ncCPX) as expected from the crystal structure.

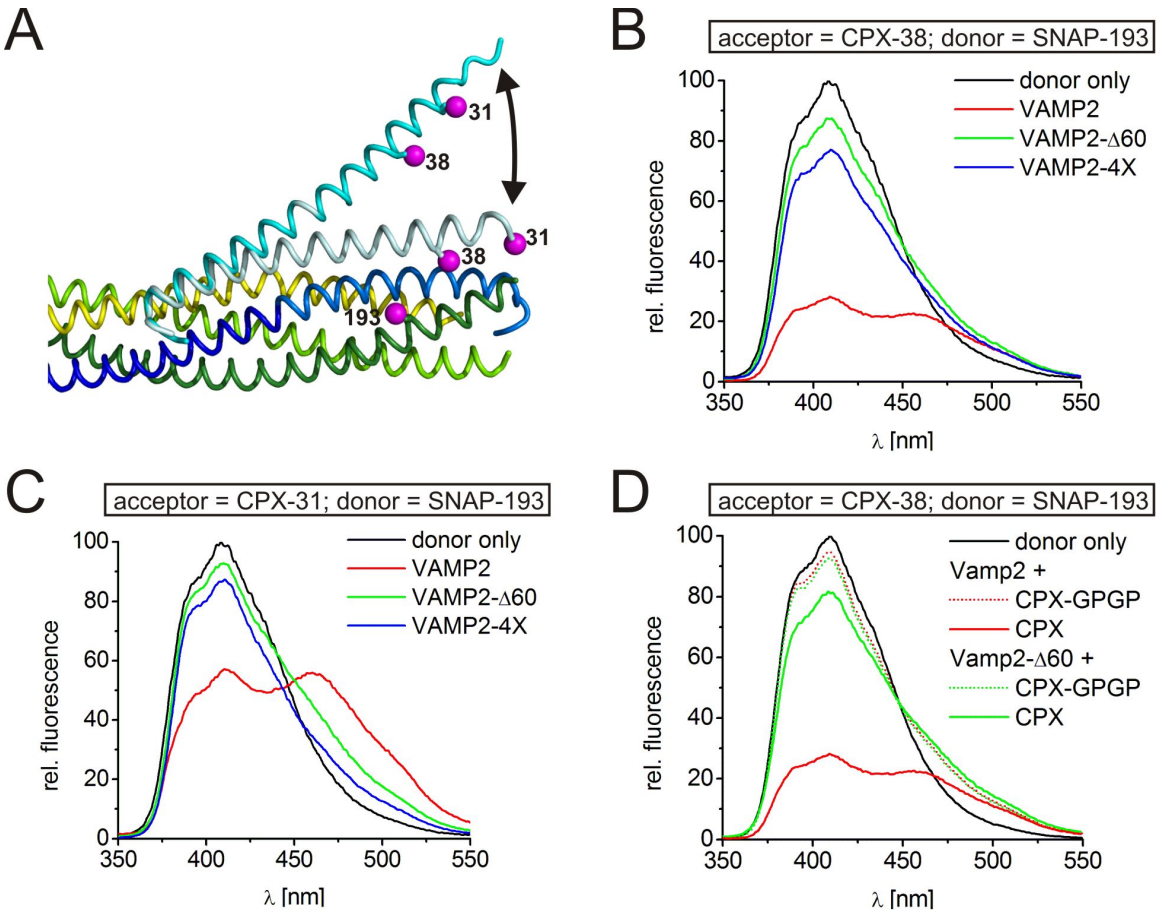

Figure 23: FRET experiments probing CPX orientation in pre- and post-fusion CPX/SNARE complexes. (A) Superposition of pre- and post-fusion CPX/SNARE complexes, where pre-fusion CPX is cyan and post-fusion CPX is pale cyan. As indicated (magenta), SNAP25 was labeled with stilbene at position 193, and CPX was labeled with bimane at positions 31 or 38. (B) Fluorescence emission spectra of stilbene only (black) and stilbene/bimane labeled CPX/SNARE complexes containing VAMP2 (residues 25-96, red), VAMP2-Δ60 (residues 25-60, green), or VAMP2-4X (residues 25-96 with mutations L70D, A74R, A81D, L84D to preclude zippering of the VAMP2 C-terminus, blue). CPX is labeled with bimane at residue 38. (C) As in (B), but CPX is labeled with bimane at residue 31. These data were used to calculate distances shown in Table 2. (D) FRET of a "flexible" CPX mutant (CPX-GPGP) in comparison to wt CPX when bound to pre-fusion (VAMP2-Δ60) or post-fusion (VAMP2) SNARE complexes. When the accessory helix is uncoupled from the central helix by a helix-breaking GPGP insertion, there is a complete loss of FRET signal with both SNARE complexes, different from the partial change in FRET observed with intact CPX. Thus, it is unlikely that differences between the FRET signals observed with intact CPX are due to random motion in CPX_{acc}.

	Distance* SNAP25-193 to	
	CPX-38 [Å]	CPX-31 [Å]
FRET measurements		
VAMP2 (25-96)	20 ± 1	27 ± 1
VAMP2-D60 (29-60)	34 ± 1	42 ± 1
VAMP2-4X (25-96; L70D,A74R,A81D,L84D)	33 ± 1	38 ± 1
Measured in crystal structure		
post-fusion (PDB 1KIL)	18	24
pre-fusion (C2 crystal form)	28	38
* Error bars reflect the reproducibility of the spectra rather than accuracy of the distance measurements.		

Table 4: FRET distances were determined from quenching of donor fluorescence between SNAP25 and CPX when bound to SNARE complexes in post-fusion (VAMP2) or pre-fusion (VAMP2-Δ60, VAMP2-4X) conformation. Error bars refer to n = 4-6 independent experiments. Values measured in the respective crystal structures are given for comparison.

In contrast, residues nearer the CPX_{acc} N-terminus appear to move increasingly away from the SNARED60 complex used for crystallization (so that the dye at CPX residue 31 is farther from the donor than the dye at CPX residue 38) and the distances estimated via quenching of donor fluorescence (see **Figure 24** for comparable data for acceptor fluorescence increase and with a second FRET pair) agree with the angled conformation in the crystal structure (**Table 4, Figure 23B,C**). Use of a "flexible" CPX construct (CPX-GPGP), where a helix-breaking GPGP linker was inserted between the central and accessory helices of CPX, discounts the possibility that the change in the FRET signal reflects random motion in CPX_{acc} due to increased CPX flexibility rather than a discrete change in CPX conformation (**Figure 23D**). In contrast to the experiments with the undisrupted CPX constructs, there was no detectable FRET signal for CPX-GPGP bound to either SNARED60 or to the post-fusion SNARE, consistent with random motion in CPX-GPGP but not for the intact CPX. To rule out that the angled conformation in solution results from VAMP2 truncation, we also studied and obtained similar results (**Table 4, Figure 23B,C**) for a complex containing the entire VAMP2 SNARE motif, but harboring mutations in its C-terminal hydrophobic layers (L70D, A74R, A81D, L84D) that prevent assembly of this region with syntaxin1 and SNAP25 and eliminate fusion activity[41]. These experiments indicate that when bound to a half-zippered form of the SNARE complex, it is the intrinsic property of CPX_{acc} to extend away from the complex. Because this conformation is maintained in solution, it determines how the complex crystallizes, and not *vice versa*.

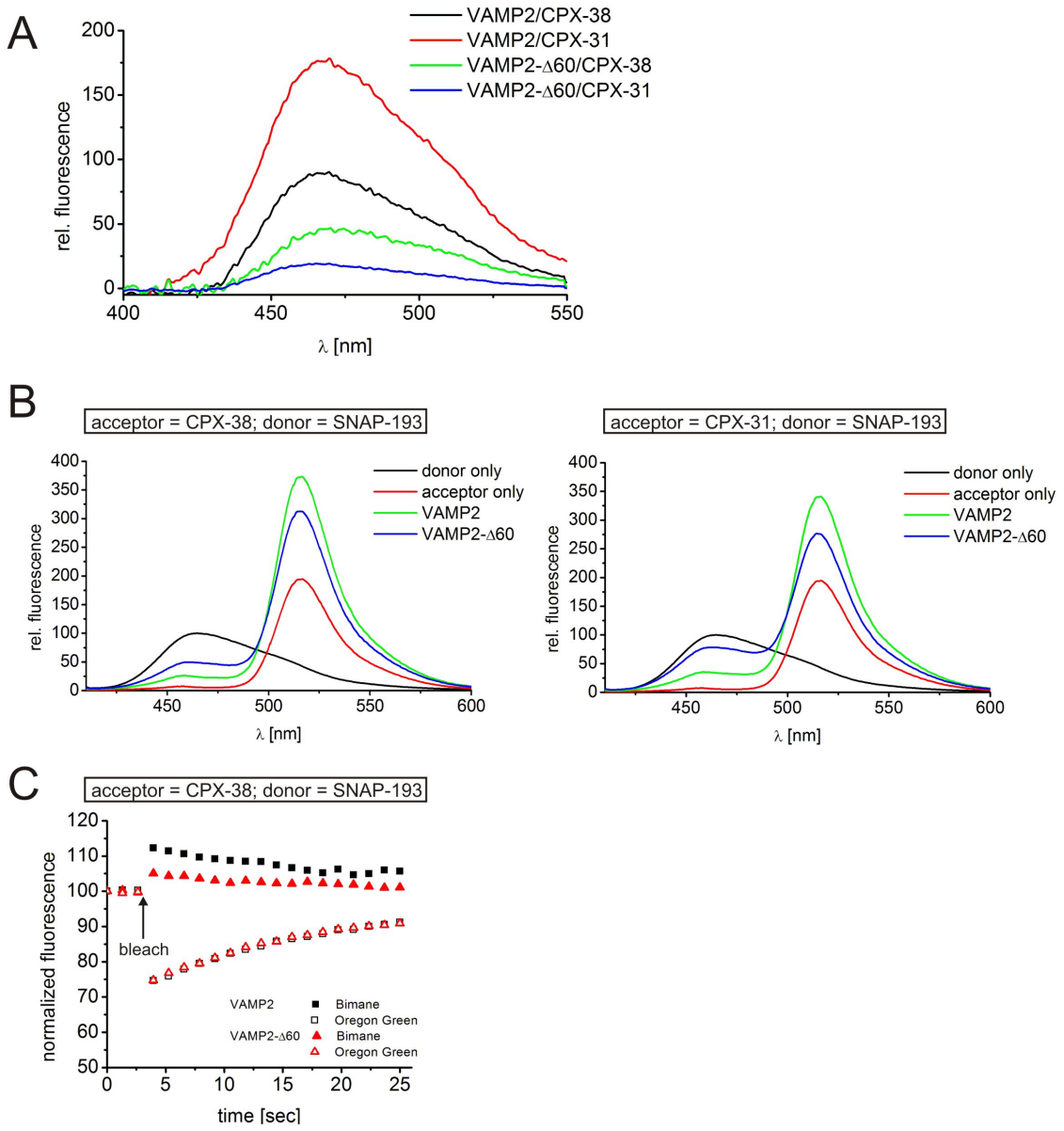

Figure 24: (A) Increase in the acceptor (Bimane) signal correlates with quenching of the donor (Stilbene) fluorescence confirming FRET. Acceptor (Bimane) emission was extracted from the Stilbene/Bimane emission scans (Figure 23) by subtracting the donor and buffer contributions. The corrected acceptor emission was then normalized with maximum acceptor fluorescence when excited at acceptor excitation wavelength (396 nm). We observe more FRET with the VAMP2 (residues 25-96) than with VAMP2-Δ60 (residues 25-60), with both CPX labeled on 38 (black vs. green, respectively) and 31 (red vs. blue, respectively) which shows that the CPX_{acc} helix is further away from the SNAREpin in the pre-fusion (VAMP2-Δ60) complex than the post-fusion VAMP2 (residues 25-96) complex. The acceptor fluorescence increase qualitatively matches the donor-quenching data except for CPX labeled at position 38 in the CPX/SNARE complex containing VAMP2. However, the acceptor emission is 1/3 weaker in this complex compared to the other CPX/SNARE complexes, even though the excitation properties are unaffected. This means the local environment possibly affects the acceptor emission in this case and could explain the

anomalous behavior. (B) Fluorescence emission spectra of Bimane alone (black), only Oregon green (red), and Bimane/Oregon labeled CPX/SNARE complex containing VAMP2 (residues 25-96, green), VAMP2-Δ60 (residues 25-60, blue) excited at 396 nm. SNAP25 D193C was labeled with donor, Bimane, and CPX was labeled with acceptor, Oregon green 488, at positions 38 (left panel) or 31 (right panel). The FRET measurements from this FRET pair are in good agreement with the results obtained with the Stilbene/Bimane FRET pair (Figure 23), confirming that the CPX_{acc} helix bends away from the SNAREs in the truncated SNARE complex compared to the fully-zippered SNARE complex. (C) Bleaching of acceptor (Oregon green) fluorescence results in donor (Bimane) fluorescence increase demonstrating FRET. Fluorescence recovery (FRAP) experiments were done on Bimane/Oregon labeled CPX/SNARE complexes containing VAMP2 (residues 25-96, black) or VAMP2-Δ60 (residues 25-60, red) in a Leica SP5 confocal setup. The acceptor fluorescence was bleached using a 488 nm laser and the fluorescence recovery was recorded in two different channels set at 440-480 nm (Bimane, filled symbols) and 500-540 nm (Oregon green, open symbols) respectively. The fluorescence intensity normalized with respect to the pre-bleach fluorescence is shown above. There is an increase of the donor fluorescence after bleaching of the acceptor and the effect is larger for VAMP2 compared to VAMP2-Δ60. This means CPX_{acc} helix is closer to the SNAREpin in the CPX/SNARE complex containing VAMP2 than in VAMP2-Δ60 complex corroborating our previous results.

Thus, as CPX rigidly extends away from the half-zippered SNARE complex, the only plausible way for both its central and accessory helices to interact with the SNAREpin is if CPX can interact with two different pre-fusion SNAREs, cross-linking SNAREs into an array like the zig-zag observed in the crystals.

MUTATIONS IN THE CPX_{ACC} BINDING SURFACE AFFECT CLAMPING.

Further support that the CPX_{acc}/t-SNARE binding interface observed in the crystal structure represents biologically relevant interactions comes from *in vitro* clamping assays. In these experiments, "flipped" SNARE proteins are expressed on the cell surface, and the effects of CPX and synaptotagmin constructs on cell-cell fusion are monitored. These flipped-SNARE cell-cell fusion assays were initially developed to demonstrate clamping by CPX and clamp release by synaptotagmin[4,18] and the effects of CPX mutations (including the superclamp mutations) in these assays are consistent with their effects in vivo[39].

We systematically tested the effect of the mutations introduced in CPX_{acc} and mapped residues that do or do not affect clamping onto the surface of CPX (**Figure 25A,B**). Mutations which are located at the CPX_{acc}/SNARE interface observed in the structure all alter clamping efficiency. As expected, clamping is affected positively by scCPX mutations and negatively by ncCPX mutations (**Figure 25**). As a control, mutations that are oriented away from the interface on the opposite side of CPX have no effect on clamping (**Figure 25**). These findings strongly support that the interface observed in the crystal contact is relevant for the physiological function of complexin and verify the rational of our mutant design for ITC.

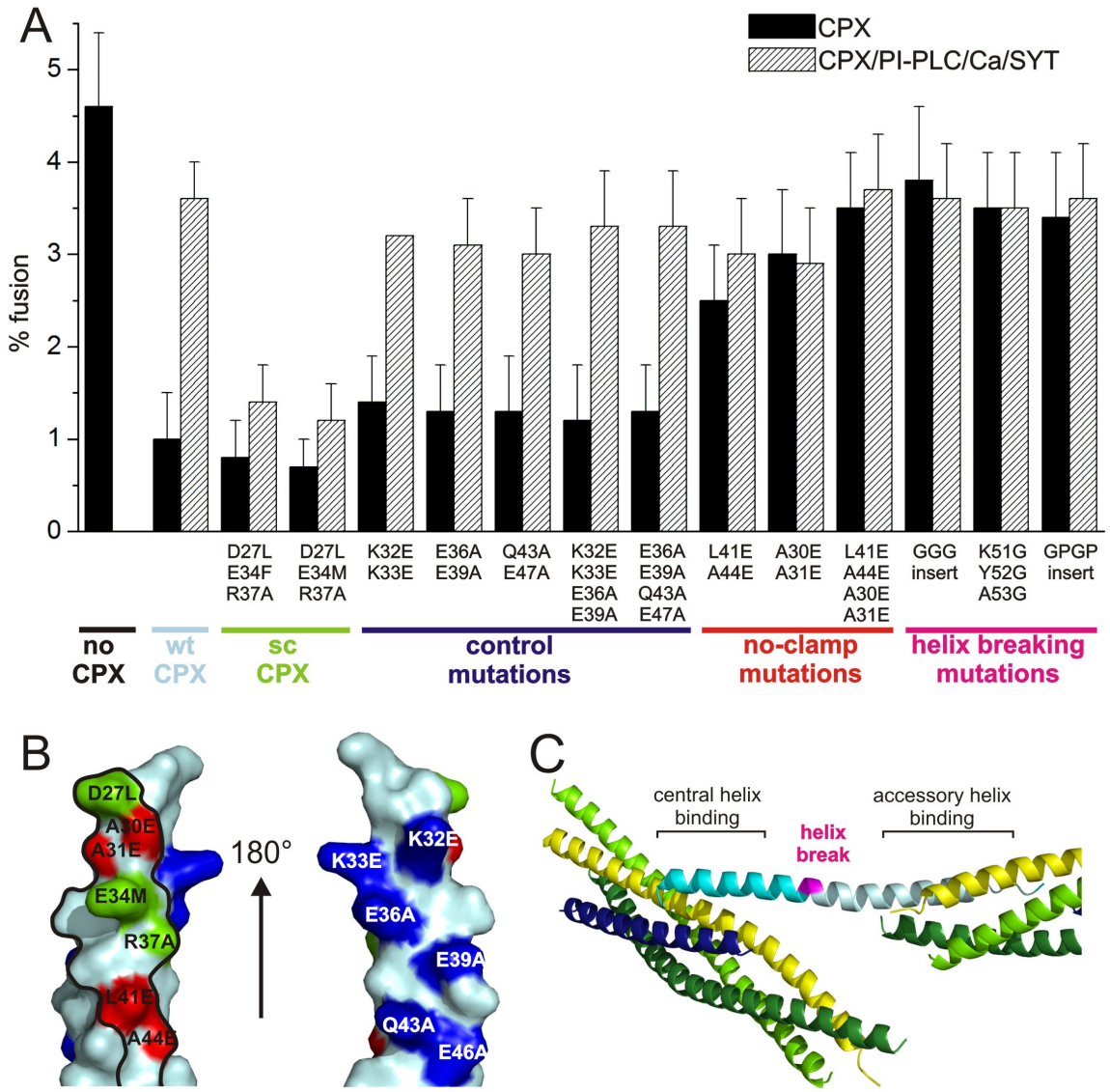

Figure 25: Effects of CPX and VAMP2 mutations on clamping in cell-cell fusion assays. (A) Mutational analysis of CPX accessory helix mutations in the cell-cell fusion assay. (B) Mapping of the mutational analysis of the CPX_{acc}/t-SNARE interface. CPX_{acc} is shown with the surface that interacts with the t-SNARE in the crystal structures outlined in black. Mutations in CPX that affect clamping positively (green) or negatively (red) are at the interface. Mutations that do not affect clamping (blue) are on the opposite side of CPX. (C) Location of the helix breaking mutations (magenta) between central and accessory helix in the CPX/SNARE pre-fusion crystal structure.

We note, however, that although ITC and the *in vitro* clamping assays validate that CPX_{acc} interacts with pre-fusion t-SNAREs using a surface similar to that identified from the crystal structure, it is likely—given the differences between the superclamp and wild-type sequences—that the *details* of the interaction differ for wild-type CPX. But as discussed earlier, due to low sequence conservation in the accessory helix, there may be also variability in the interactions of CPX_{acc} from different organisms.

The observations from the crystal structure and their agreement with FRET from mono-disperse solutions suggest that the CPX accessory helix rigidly bends away from the SNARE complex. To test whether the rigidity of CPX is important for clamping, we again used the flipped SNARE cell-cell fusion assays. We used CPX mutants (CPX-GPGP, CPX-GGG) which had a helix-breaking linkers (GPGP and GGG, respectively) inserted after residue 50, between CPX_{cen} and $CPX_{acc,}$ as well as a construct where residues 51-53 at the central-accessory helix junction were replaced by glycines to disrupt the long CPX helix (see **Figure 25C**). Clamping should be affected if the continuity and hence rigidity of the CPX helix is mechanistically important. We found that clamping indeed was reduced in all three cases, consistent with the requirement for a continuous helix (**Figure 25A**).

MODEL FOR CLAMPING

Binding, fluorescence and functional studies all corroborate the conformation of CPX as observed in the crystal structure as well the novel interaction identified between CPX_{acc} and the t-SNARE. Based on the crystal structure, we therefore propose that CPX directly cross-links pre-synaptic, pre-fusion SNARE complexes and further that the

arrangement of CPX/SNARE complexes in the clamped state is similar to the zig-zag observed in the crystal lattice. Such an arrangement is plausible given the length of linkers that anchor the t- and v-SNAREs to the membranes, as the linkers for syntaxin1 and the half-zippered VAMP2 are longer than 10 (~ 37 Å) and 30 residues (>100 Å), respectively (**Figure 26A**). The number of CPX/SNARE complexes in the zig-zag would be limited due to curvature in the vesicle, which increases the distance between the vesicle and plasma membranes with increasing distance from the fusion site (close to the zig-zag center), so that polymer extension beyond a certain distance is untenable. Experiments suggest that for optimal fusion rates, there are 5-10 SNARE complexes in a fusion pore[14], allowed by our model.

The crystal structure naturally suggests several synergistic mechanisms by which CPX might stabilize the pre-fusion state and inhibit fusion (**Figure 26**):

First, CPX_{acc} binds the t-SNAREs in a site occupied by C-terminal portions of the VAMP2 SNARE motif in post-fusion SNARE complexes, competitively blocking the completion of zippering by VAMP2 as proposed previously from biochemical studies[19,35], but with the critical modification that this interaction occurs inter-molecularly.

Second, close apposition of SNAREpins by cross-linking at their zippering ends should prevent further zippering which, if it occurred would cause them to sterically clash (~2 turns of the N-terminal SNAP25 SNARE motifs are not folded in our structure).

Third, the linker regions of Syntaxin1 and VAMP2 on different sides of the zig-zag mid-line emerge on opposite sides of the zig-zag plane, again sterically interfering

with complete zippering.

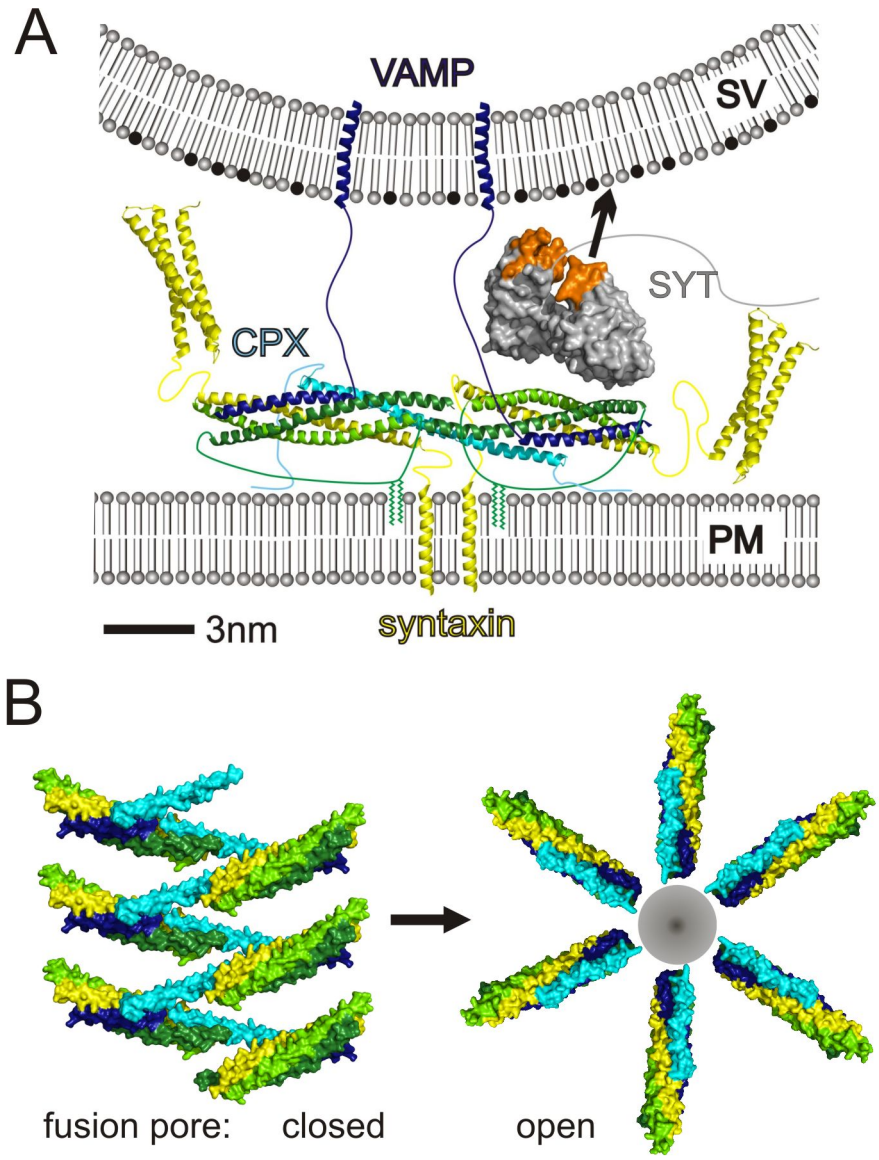

Figure 26: Molecular models for CPX clamping. (A) Model for the clamp at the synapse. CPX/SNARE complexes with half-zippered VAMP2 are cross-linked by CPX into a zig-zag topology incompatible with fusion (see text). The plane of the zig-zag is normal to the vertical direction. For clarity, only two of the CPX/SNARE complexes in the zig-zag are shown. Palmitoylation on SNAP25 is indicated and restrains the distance between the CPX/SNARE zig-zag and the plasma membrane (PM). The distance between the zig-zag plane and the vesicle (SV) must be less than ~110 Å, the maximum distance spanned by the v-SNARE linker. The calcium sensor synaptotagmin (grey with Ca^{2+}-binding loops orange), which relieves CPX clamping, is accommodated by this model and is positioned according to FRET analysis[46]. Its Ca^{2+}-binding loops are juxtaposed to the vesicle membrane, which is rich in anionic lipids like phosphatidyl-serine (black), well positioned for interactions with this membrane in response to Ca^{2+} stimulus. (B) Model of the CPX/SNARE assembly in the clamped state when the fusion pore is "closed" (left). The fusion pore can open only once the zig-zag clamped array has disassembled (right). Complexes in "open" state are modeled on PDBID 1KIL.

Fourth, the fusion pore cannot form as it is blocked by the CPX/SNARE zig-zag array, which is interposed between the vesicle and plasma membranes. Our finding from functional assays that flexibility in CPX interferes with clamping suggests that the CPX/SNARE zig-zag must be rigid at least to some extent. The requirement for rigidity is consistent with a role as a barrier between membranes that are poised for fusion.

And fifth, cross-linking the SNARE complexes into a zig-zag prevents them from forming the circular arrangement needed to accommodate either a hemi-fusion stem[42] or a fusion pore[43], precluding their formation. Notably, though, even in the zig-zag, the orientation of the SNAREs is very similar to that in a fusion-competent arrangement (compare panels in **Figure 26B**), except that the cross-links must dissolve in order for fusion to take place. As the zig-zag clamp disassembles and SNAREs zipper, steric repulsion would push the SNAREs radially away from the zig-zag mid-line to form a circular arrangement (**Figure 26B**), now enclosing a nascent fusion pore which opens progressively as zippering completes[44].

Though clearly vital for clamping[19], each pairwise interaction between CPX_{acc} and t-SNARE complexes seems of relatively low affinity (K_d ~ 10 μM, corresponding to ~6.8 kcal/mol). Nonetheless, binding with this affinity is likely to occur physiologically because the concentrations of CPX and SNARE proteins in the region local to fusion between apposed bilayers (~20 nm x ~20 nm x ~20 nm (**Figure 26A**) containing 5-10 CPX/SNARE complexes[14]) are likely to be in the 1-2 mM range (incidentally, an order of magnitude higher than their concentration in the crystallization mixture). And due to

entropy considerations, polymerization would be more favored for proteins constrained to two dimensions, as at the synapse, than in solution.

The clamp may be further stabilized by the CPX N-terminus, which is absent in our structure, and which can interact with membrane proximal portions of SNAREs[20,45]. And functional assays show that synaptotagmin (included in **Figure 26A** according to[46]), in its calcium-free conformation, stabilizes the clamped state produced by CPX[18,47], although how this occurs is currently unclear.

SNARE ACTIVATION

As noted previously, in addition to its inhibitory role, CPX also has an important positive role in promoting fusion[21,28]. Some of the domains shown to be required for this mode of action[21,24] are not present in our structure. It has been speculated, however, that one positive contribution may result from the binding of CPX_{cen} to the VAMP2/syntaxin1 interface, which would stabilize initial SNARE assembly and zippering[27,30]. Our studies now suggest a similar role for the accessory helix: its interaction with the t-SNARE groove newly identified by us indicates that CPX might facilitate t-SNARE folding by binding to the C-terminal part of their SNARE motifs prior to VAMP2 binding.

Most importantly, we note that the assembled clamp itself might promote fusion by simply setting the stage: multiple SNARE complexes are gathered in orientations close to that required for fusion pore formation (compare panels in **Figure 26B**) even as their cross-linking impedes it, and they are already half-zippered. This alone will allow for fast, efficient fusion as soon as the clamp is released upon stimulus.

The mechanism of clamp disassembly is further explored in an accompanying manuscript[41], as is the finding that clamp release is intrinsically coupled to a conformational change in CPX, where CPX switches from the angled conformation observed in the CPX/SNAREΔ60 structure to that in the post-fusion CPX/SNARE complex[29,30].

EXPERIMENTAL PROCEDURES

PROTEIN EXPRESSION, PURIFICATION AND COMPLEX ASSEMBLY.

Recombinant fusion proteins were expressed in *E.coli* BL21 (DE3) cells by induction with 0.5 mM IPTG for 4 h at 37 °C. Selenomethionine substituted CPX-L27M and CPX-F34M were expressed according to Doublie[48]. Proteins were purified with either glutathione-Sepharose (GE) or Ni-NTA-agarose (Qiagen) resin and tags were cleaved according to manufacturers' instructions. Complexes were reconstituted by mixing proteins, followed by gel filtration on a HiLoad Superdex 75 (16/60, GE Healthcare). See Supplementary Methods for detailed protocols.

CRYSTALLIZATION AND DATA COLLECTION.

Peak fractions were pooled and concentrated to ~10 mg/ml for crystallization. Crystals were obtained at 20 °C using the hanging drop vapor diffusion method. The best crystals were obtained when the SNARE complex was mixed with 6-fold molar excess of CPX_{acc} peptide (residues 26-35, purchased from Biosynthesis) and equilibrated against 0.05 M calcium acetate, 27% 2-methyl-2,4-pentanediol (MPD), 0.1 M sodium cacodylate pH 6.5-7.0. The crystals were loop-mounted from the mother liquor and plunged into liquid nitrogen for cryopreservation.

Crystals of the CPX/SNARE complex were obtained by equilibration against a solution containing 13-15% polyethyleneglycol (PEG) 5000MME, 0.2 M ammonium sulfate, 0.01 M EDTA, and 0.1 M Tris pH 7.5. Crystallization conditions for the CPX-L27M/SNARE and CPX-F34M/SNARE complexes were similar. Crystals were transferred into buffer supplemented with 15% PEG 400 prior to flash-freezing in liquid nitrogen.

Data were collected at NSLS (National Synchrotron Light Source, Brookhaven) beamline X29 and APS (Advanced Photon Source, Argonne) beamline ID-24C processed with HKL2000[49].

STRUCTURE DETERMINATION

For all crystals, phases were obtained by the molecular replacement method as implemented in Phaser[50]. Models were build in Coot[51] and refined with Refmac[52]. For the truncated SNARE complex we used a search model based on PDB 1KIL. TLS groups and non-crystallographic symmetry (NCS) restraints were used in refinement and led to a high resolution model of the truncated SNARE complex. The CPX_{acc} peptide (26-35) in the crystallization solution is not bound to the SNARE complex.

Crystals of the CPX/SNARE complex belong to space group C2 and diffract to 3.5 Å resolution. The truncated SNARE complex served as the search model. Complexin was manually built into difference density as a continuous α-helix. For refinement, TLS groups and H-bond restraints for α-helical secondary structure derived from the high resolution SNARE complex structure were used.

The selenomethionine substituted CPX-F34M/SNARE crystals diffract to 3.8 Å resolution. The crystals have $P2_1$ pseudosymmetry but we were able to refine to reasonable R values only in P1. As there are eight CPX-F34M/SNARE complexes in the P1 asymmetric unit, we used the thin shell method in choosing the R_{free} set in order to avoid bias from non-crystallographic symmetry (NCS)[53]. The truncated SNARE complex structure was used as a search model in molecular replacement. A Fourier anomalous difference map was calculated using CNS[54], allowing us to unambiguously locate the positions of the Se atoms of residues 34 as well as 55, a methionine in the wild-type sequence in CPX-F34M. NCS restraints were used in refinement.

Composite simulated-annealed omit maps were calculated in CNS[54] to confirm the CPX/SNARE models (**Figure 18**).

Crystals of the selenomethionine substituted CPX-L27M/SNARE complex belong to space group P1 and diffract to 4.5 Å. A molecular replacement solution using the CPX/SNARE complex as search model was found, identifying 4 complexes in the asymmetric unit. Although data resolution did not allow us to refine the structure, we could determine the position of the CPX Se atoms of residues 27 and 55, a methionine in the wild-type sequence, in an anomalous difference map calculated using phases from the molecular replacement solution[54]. The positions are consistent with register in the CPX/SNARE complex.

All figures were prepared with Pymol[55]. Data collection and refinement statistics are summarized in Table 1.

ISOTHERMAL TITRATION CALORIMETRY (ITC) ANALYSIS.

The ITC analysis is described in more detail in the Supplementary Methods. Briefly, measurements were carried out with a Microcal ITC200 instrument. Proteins were in PBS buffer supplemented with 0.25 mM TCEP. The CPX constructs (200-600 μM) were titrated into a solution of SNARE complexes in the sample cell (10-30 μM), and thermodynamic parameters were calculated using the Microcal Origin ITC200 software package and assuming a "one-set-of-sites" binding model.

FRET ANALYSIS.

Positions D193 on SNAP25 and Q38 or A31 on scCPX (hCpx1 residues1-134 carrying superclamp mutations D27L, E34F and R37A) were mutated into cysteines using the Stratagene QuikChange Kit. SNAP25 D193C was labeled with the donor probe, Stilbene (4-acetamido-4'-((iodoacetyl)amino)-stilbene-2,2'-disulfonic acid, disodium salt, Invitrogen) and either CPX Q38C or A31C was labeled with the acceptor Bimane (Monochlorobimane, Invitrogen), using 10X molar excess of dye overnight at 4°C in 50 mM Tris Buffer, pH 7.4, containing 150 mM NaCl, 10 % Glycerol and 1 mM TCEP. Excess dye was separated from the labeled proteins using a NAP desalting column (GE Healthcare). The double-labeled CPX/SNARE complexes were assembled overnight at 4°C and purified by gel-filtration on a Superdex 75 (10/30, GE Healthcare) gel filtration column. All fluorescence data were obtained on a Perkin-Elmer LS55 luminescence spectrometer at 25°C. Excitation and emission slits of 5 nm were used in all measurements. Fluorescence emission spectra were measured over the range of 350-550 nm with the excitation wavelength set at 335 nm. The donor probe concentration was

adjusted to 2 μM in all samples. We used fluorescence resonance energy transfer (FRET) to calculate the distance between the two fluorophores with a R_0 of 27.5 Å for the Stilbene-Bimane FRET pair[56]. See Supplementary Methods for more detailed experimental procedures.

CELL-CELL FUSION ASSAY.

The flipped SNARE cell-cell fusion assay was performed as described before[4,18,19,31]. In brief, HeLa cell lines were transiently transfected with flipped VAMP2 (wt or 3xDA), DsRed2-NES and either with or without CPX mutants and synaptotagmin as indicated (v-cells). After one day, transfected v-cells were seeded onto glass coverslips containing cells stably co-expressing flipped syntaxin1, flipped SNAP-25 and CFP-NLS (t-cells). The following day, cells were fixed with 4% paraformaldehyde directly or after treatment with recovery solution (1 U/ml Phosphatidylinositol Specific Phospholipase-C, 20 μg/ml laminin, with or without 1.8 mM EGTA), washed and mounted with Prolong Antifade Gold mounting medium (Molecular Probes). Confocal images were acquired on a Zeiss 510-Meta confocal microscope and processed using Adobe Photoshop software.

ACCESSION CODES

Coordinates and structure factors for the structures described in this manuscript have been submitted to the PDB (accession codes XXXX and YYYY).

ADDITIONAL DATA

This paper contains data on a helix-breaking motif without demonstrating that the motif actually disrupts the helicity of the Complexin. Here I present circular dichroism (CD) data which demonstrate that this is, in fact, the case.

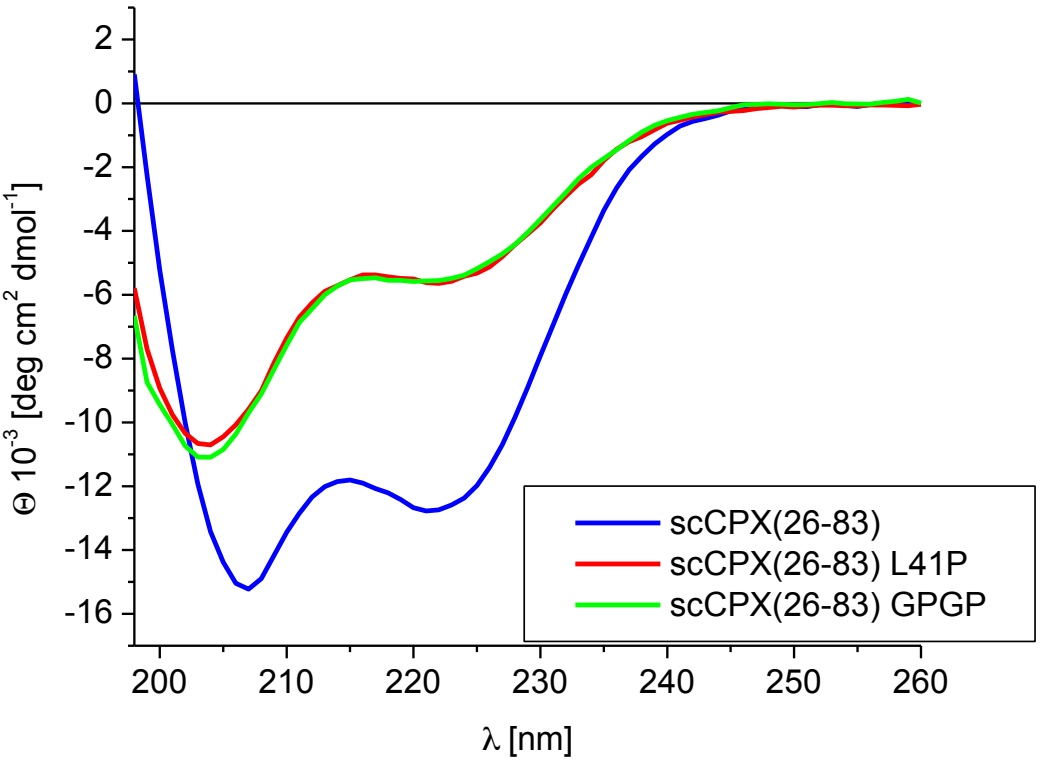

Figure 27: Circular Dichroism data shows that the insertion of helix breaking motifs between the Central and Accessory Helices in Complexin actually does disrupt the helices.

REFERENCES

1. Fatt, P. & Katz, B. Spontaneous subthreshold activity at motor nerve endings. *J Physiol* **117**, 109-28 (1952).

2. Palade, G.E. & Palay, S.L. Electron microscope observations of interneuronal and neuromuscular synapses. *Anat. Record* **118**, 335-336 (1954).

3. Sollner, T. et al. SNAP receptors implicated in vesicle targeting and fusion. *Nature* **362**, 318-24 (1993).

4. Hu, C. et al. Fusion of cells by flipped SNAREs. *Science* **300**, 1745-9 (2003).

5. Weber, T. et al. SNAREpins: minimal machinery for membrane fusion. *Cell* **92**, 759-72 (1998).

6. McNew, J.A. et al. Compartmental specificity of cellular membrane fusion encoded in SNARE proteins. *Nature* **407**, 153-9 (2000).

7. Sutton, R.B., Fasshauer, D., Jahn, R. & Brunger, A.T. Crystal structure of a SNARE complex involved in synaptic exocytosis at 2.4 A resolution. *Nature* **395**, 347-53 (1998).

8. Perin, M.S., Fried, V.A., Mignery, G.A., Jahn, R. & Sudhof, T.C. Phospholipid binding by a synaptic vesicle protein homologous to the regulatory region of protein kinase C. *Nature* **345**, 260-3 (1990).

9. Brose, N., Petrenko, A.G., Sudhof, T.C. & Jahn, R. Synaptotagmin: a calcium sensor on the synaptic vesicle surface. *Science* **256**, 1021-5 (1992).

10. Fernandez-Chacon, R. et al. Synaptotagmin I functions as a calcium regulator of release probability. *Nature* **410**, 41-9 (2001).

11. Geppert, M. et al. Synaptotagmin I: a major Ca2+ sensor for transmitter release at a central synapse. *Cell* **79**, 717-27 (1994).

12. Pang, Z.P., Shin, O.H., Meyer, A.C., Rosenmund, C. & Sudhof, T.C. A gain-of-function mutation in synaptotagmin-1 reveals a critical role of Ca2+-dependent soluble N-ethylmaleimide-sensitive factor attachment protein receptor complex binding in synaptic exocytosis. *J Neurosci* **26**, 12556-65 (2006).

13. Domanska, M.K., Kiessling, V., Stein, A., Fasshauer, D. & Tamm, L.K. Single vesicle millisecond fusion kinetics reveals number of SNARE complexes optimal for fast SNARE-mediated membrane fusion. *J Biol Chem* **284**, 32158-66 (2009).

14. Karatekin, E. et al. A fast, single-vesicle fusion assay mimics physiological SNARE requirements. *Proc Natl Acad Sci U S A* **107**, 3517-21 (2010).

15. Liu, T., Tucker, W.C., Bhalla, A., Chapman, E.R. & Weisshaar, J.C. SNARE-driven, 25-millisecond vesicle fusion in vitro. *Biophys J* **89**, 2458-72 (2005).

16. Ishizuka, T., Saisu, H., Odani, S. & Abe, T. Synaphin: a protein associated with the docking/fusion complex in presynaptic terminals. *Biochem Biophys Res Commun* **213**, 1107-14 (1995).

17. McMahon, H.T., Missler, M., Li, C. & Sudhof, T.C. Complexins: cytosolic proteins that regulate SNAP receptor function. *Cell* **83**, 111-9 (1995).

18. Giraudo, C.G., Eng, W.S., Melia, T.J. & Rothman, J.E. A clamping mechanism involved in SNARE-dependent exocytosis. *Science* **313**, 676-80 (2006).

19. Giraudo, C.G. et al. Alternative zippering as an on-off switch for SNARE-mediated fusion. *Science* **323**, 512-6 (2009).

20. Maximov, A., Tang, J., Yang, X., Pang, Z.P. & Sudhof, T.C. Complexin controls the force transfer from SNARE complexes to membranes in fusion. *Science* **323**, 516-21 (2009).

21. Xue, M. et al. Tilting the balance between facilitatory and inhibitory functions of mammalian and Drosophila Complexins orchestrates synaptic vesicle exocytosis. *Neuron* **64**, 367-80 (2009).

22. Cho, R.W., Song, Y. & Littleton, J.T. Comparative analysis of Drosophila and mammalian complexins as fusion clamps and facilitators of neurotransmitter release. *Mol Cell Neurosci* (2010).

23. Huntwork, S. & Littleton, J.T. A complexin fusion clamp regulates spontaneous neurotransmitter release and synaptic growth. *Nat Neurosci* **10**, 1235-7 (2007).

24. Xue, M. et al. Distinct domains of complexin I differentially regulate neurotransmitter release. *Nat Struct Mol Biol* **14**, 949-958 (2007).

25. Hobson, R.J., Liu, Q., Watanabe, S. & Jorgensen, E.M. Complexin Maintains Vesicles in the Primed State in C. elegans. *Curr Biol* **21**, 106-13 (2011).

26. Martin, J.A., Hu, Z., Fenz, K.M., Fernandez, J. & Dittman, J.S. Complexin has opposite effects on two modes of synaptic vesicle fusion. *Curr Biol* **21**, 97-105 (2011).

27. Sudhof, T.C. & Rothman, J.E. Membrane fusion: grappling with SNARE and SM proteins. *Science* **323**, 474-7 (2009).

28. Li, F. et al. Complexin: How Can the Same Protein Both Activate and Clamp Membrane Fusion? *in preparation* (2011).

29. Bracher, A., Kadlec, J., Betz, H. & Weissenhorn, W. X-ray structure of a neuronal complexin-SNARE complex from squid. *J Biol Chem* **277**, 26517-23 (2002).

30. Chen, X. et al. Three-dimensional structure of the complexin/SNARE complex. *Neuron* **33**, 397-409 (2002).

31. Giraudo, C.G. et al. Distinct domains of complexins bind SNARE complexes and clamp fusion in vitro. *J Biol Chem* **283**, 21211-9 (2008).

32. Hua, S.Y. & Charlton, M.P. Activity-dependent changes in partial VAMP complexes during neurotransmitter release. *Nat Neurosci* **2**, 1078-83 (1999).

33. Reim, K. et al. Complexins regulate a late step in Ca2+-dependent neurotransmitter release. *Cell* **104**, 71-81 (2001).

34. Tang, J. et al. A complexin/synaptotagmin 1 switch controls fast synaptic vesicle exocytosis. *Cell* **126**, 1175-87 (2006).

35. Lu, B., Song, S. & Shin, Y.K. Accessory alpha-helix of complexin I can displace VAMP2 locally in the complexin-SNARE quaternary complex. *J Mol Biol* **396**, 602-9 (2010).

36. Melia, T.J. et al. Regulation of membrane fusion by the membrane-proximal coil of the t-SNARE during zippering of SNAREpins. *J Cell Biol* **158**, 929-40 (2002).

37. Walter, A.M., Wiederhold, K., Bruns, D., Fasshauer, D. & Sorensen, J.B. Synaptobrevin N-terminally bound to syntaxin-SNAP-25 defines the primed vesicle state in regulated exocytosis. *J Cell Biol* **188**, 401-13 (2010).

38. Ellena, J.F. et al. Dynamic structure of lipid-bound synaptobrevin suggests a nucleation-propagation mechanism for trans-SNARE complex formation. *Proc Natl Acad Sci U S A* **106**, 20306-11 (2009).

39. Yang, X., Kaeser-Woo, Y.J., Pang, Z.P., Xu, W. & Sudhof, T.C. Complexin clamps asynchronous release by blocking a secondary Ca(2+) sensor via its accessory alpha helix. *Neuron* **68**, 907-20 (2010).

40. Pabst, S. et al. Selective interaction of complexin with the neuronal SNARE complex. Determination of the binding regions. *J Biol Chem* **275**, 19808-18 (2000).

41. Krishnakumar, S.S. et al. A Conformational Switch in Complexin Required for Synaptotagmin to Trigger Calcium-Dependent Fusion by Synaptic SNARE Proteins. *in preparation* (2011).

42. Kuzmin, P.I., Zimmerberg, J., Chizmadzhev, Y.A. & Cohen, F.S. A quantitative model for membrane fusion based on low-energy intermediates. *Proc Natl Acad Sci U S A* **98**, 7235-40 (2001).

43. Chernomordik, L.V., Zimmerberg, J. & Kozlov, M.M. Membranes of the world unite! *J Cell Biol* **175**, 201-7 (2006).

44. Stein, A., Weber, G., Wahl, M.C. & Jahn, R. Helical extension of the neuronal SNARE complex into the membrane. *Nature* **460**, 525-8 (2009).

45. Xue, M. et al. Binding of the complexin N terminus to the SNARE complex potentiates synaptic-vesicle fusogenicity. *Nat Struct Mol Biol* **17**, 568-75 (2010).

46. Choi, U.B. et al. Single-molecule FRET-derived model of the synaptotagmin 1-SNARE fusion complex. *Nat Struct Mol Biol* **17**, 318-24 (2010).

47. Chicka, M.C., Hui, E., Liu, H. & Chapman, E.R. Synaptotagmin arrests the SNARE complex before triggering fast, efficient membrane fusion in response to Ca2+. *Nat Struct Mol Biol* **15**, 827-35 (2008).

48. Doublie, S. Preparation of selenomethionyl proteins for phase determination. *Methods Enzymol* **276**, 523-30 (1997).

49. Otwinowski, Z. & Minor, W. Processing of X-ray Diffraction Data Collected in Oscillation Mode. in *Methods in Enzymology* Vol. 276 (eds. Carter Jr., C.W. & Sweet, R.M.) 307-326 (Academic Press, New York, 1997).

50. McCoy, A.J. et al. Phaser Crystallography Software. *J. Appl. Chrystallog.* **40**, 658-674 (2007).

51. Emsley, P. & Cowtan, K. Coot: model-building tools for molecular graphics. *Acta Crystallogr D Biol Crystallogr* **60**, 2126-32 (2004).

52. Murshudov, G.N., Vagin, A.A. & Dodson, E.J. Refinement of macromolecular structures by the maximum-likelihood method. *Acta Crystallogr D Biol Crystallogr* **53**, 240-55 (1997).

53. Kleywegt, G.J. & Jones, T.A. Where freedom is given, liberties are taken. *Structure* **3**, 535-40 (1995).

54. Brunger, A.T. et al. Crystallography & NMR system: A new software suite for macromolecular structure determination. *Acta Crystallogr D Biol Crystallogr* **54**, 905-21 (1998).

55. DeLano, W.L. The PyMOL Molecular Graphics System. . *DeLano Scientific LLC* (2003).

56. Lakowicz, J.R. *Principles of fluorescence spectroscopy*, xxvi, 954 p. (Springer, New York ; Berlin, 2006).

57. Chen, V.B. et al. MolProbity: all-atom structure validation for macromolecular crystallography. *Acta Crystallogr D Biol Crystallogr* **66**, 12-21 (2010).

ACKNOWLEDGEMENTS

We wish to thank the staffs of X29 at the NSLS and of NE-CAT at APS for their help in data collection, Lavan Khandan and Stephanie Baguley for technical assistance, and Dr. Jeff Coleman for advice. We are grateful to Dr. E. Karatekin and Professor David W. Rodgers for discussions regarding this manuscript. This work was supported by grants from the NIH to KMR (R01GM080616) and to JER, an ANR PCV grant to FP, and a grant from the DFG to DK.

SUPPLEMENTARY EXPERIMENTAL PROCEDURES

PROTEIN EXPRESSION, PURIFICATION AND COMPLEX ASSEMBLY.

Recombinant fusion proteins were expressed in *E.coli* BL21 (DE3) cells by induction with 0.5 mM IPTG for 4 h at 37 °C. The constructs used for crystallization are GST-PreScission-VAMP2Δ60 (containing human VAMP2 residues 29-60), GST-TEV-syntaxin1A (containing rat syntaxin1a residues 191-253), oligohistidine-MBP-Thrombin-

SNAP25N (containing human SNAP25A residues 7-82 and a C-terminal tryptophan), GST-TEV-SNAP25C (containing human SNAP25A residues 141-203) and GST-PreScission-CPX (containing human complexin1 residues 26-83 with the following "superclamp" mutations: D27L, E34F, R37A). To make CPX-L27M and CPX-F34M, positions 27 or 34 of CPX were mutated to methionine using QuikChange mutagenesis (Stratagene).

Cells were harvested and resuspended in buffer S (140 mM NaCl, 1 mM DTT, 20 mM Tris pH 7.5) supplemented with protease inhibitors (Complete EDTA-free, Roche), DNaseI (Sigma) and lysozyme (American Bioanalytical), then lysed using a cell disruptor (Avestin). Proteins were purified with either glutathione-Sepharose (GE) or Ni-NTA-agarose (Qiagen) resin according to manufacturers' instructions. Tags were cleaved with TEV, PreScission or thrombin (Sigma) protease overnight at 4 °C. The proteins were collected, concentrated and purified by size exclusion chromatography on a HiLoad Superdex 75 (16/60, GE Healthcare) column equilibrated with buffer S. Selenomethionine substituted CPX-L27M and CPX-F34M were expressed according to Doublie [48] and purified as described above.

To reconstitute the truncated SNARE complex, VAMP2-Δ60, SNAP25C, SNAP25N and synatxin1 were mixed at 1:1:1:1 molar ration and incubated for 2 h before gel filtration on a HiLoad Superdex 75 (16/60, GE Healthcare) column equilibrated with buffer S. CPX was added to the truncated SNARE complex at 1.2 molar excess and incubated over night. The sample was supplemented with imidazole (20 mM final concentration) and passed over 0.5 ml Ni-NTA resin three times to remove TEV and

PreScission proteases, which are oligohistidine tagged. The mixture was loaded on a HiLoad Superdex 75 (16/60, GE Healthcare) column equilibrated with buffer S, and peak fractions were pooled and concentrated to ~10 mg/ml for crystallization.

ISOTHERMAL TITRATION CALORIMETRY (ITC) ANALYSIS

Syntaxin1A, SNAP25C, SNAP25N and VAMP2-Δ60 were mixed together at a 1:1.2:1.2:1.2 molar ratio and incubated at 4^{o}C overnight to form the SNARE-Δ60 complex. Before ITC experiments, SNARE-Δ60 and CPX variants (CPX48-134, wtCPX, scCPX, ncCPX) were purified by gel filtration using a HiLoad Superdex 75 column (GE Healthcare Life Sciences) and PBS (phosphate buffered saline, pH 7.4: 137 mM NaCl, 3 mM KCl, 10 mM sodium phosphate dibasic, 2 mM potassium phosphate monobasic) with 0.25 mM TCEP as the running buffer, respectively. Peak fractions were pooled and concentrated. CPX 48-134 was added into SNARE-Δ60 at about 1.5:1 molar ratio and incubate overnight at 4^{o}C to form blocked SNARE-Δ60. CPX variants and blocked SNARE-Δ60 were then dialyzed in the same flask against 3 liters of PBS buffer with 0.25 mM TCEP for 4 hours at 4^{o}C and then dialyzed against another 3 liters of fresh PBS buffer with 0.25 mM TCEP overnight at 4^{o}C. The concentrations of dialyzed proteins were determined by using the Thermo Scientific Pierce Bicinchoninic Acid (BCA) protein assay kit with BSA as the standard and/or Bradford assay.

ITC experiments were performed on a Microcal ITC200 instrument. Typically, about 200 μL of blocked SNARE solution (10 to 30 μM) was loaded into the sample cell and about 40 μL of CPX solution (200 to 600 μM) was loaded into the syringe. An initial 0.2 μL injection was followed by several injections of constant volume. 180-

second equilibration time was used after each injection to ensure complete binding. The heat change from each injection was integrated, and then normalized by the moles of CPX in the injection. All ITC experiments were carried out at 37°C and at least twice. Microcal Origin ITC200 software package was used to analyze the titration calorimetric data and obtain the stoichiometric number (*N*), the molar binding enthalpy (*ΔH*), and the association constant (K_a). "One-set-of-sites" binding mode was used. The equilibrium dissociation constant (K_d), the binding free energy (*ΔG*), and the binding entropy (*ΔS)* were calculated using the thermodynamic equations (11-13):

$$K_d = \frac{1}{K_a} \tag{11}$$

$$\Delta G = -RT \ln K_a \tag{12}$$

$$\Delta G = -RT \ln K_a \tag{13}$$

Samples as used in the ITC experiments were re-analyzed by size exclusion chromatography using the HiLoad Superdex 75 column to control that VAMP-60 does not dissociate from the t-SNARE complex during the measurements.

FRET ANALYSIS.

Positions D193 on SNAP25 and Q38 or A31 on CPX (hCpx1 residues1-134 carrying superclamp mutations D27L, E34F and R37A was used in all FRET experiments) were mutated into cysteines using the Stratagene QuikChange Kit. SNAP25 D193C was labeled with the donor probe, Stilbene (4-acetamido-4'-((iodoacetyl)amino)-stilbene-2,2'-disulfonic acid, disodium salt, Invitrogen) and either CPX Q38C or A31C was labeled with the acceptor Bimane (Monochlorobimane, Invitrogen). Stilbene has

improved solubility compared to the established FRET dye Pyrene, and in conjunction with Bimane, it can be used to measure small changes at small distances. The proteins were labeled using 10X molar excess of dye overnight at 4°C in 50 mM Tris Buffer, pH 7.4, containing 150 mM NaCl, 10 % Glycerol and 1 mM TCEP. Following overnight incubation at 4°C, the excess dye was separated from the labeled proteins using a NAP desalting column (GE Healthcare). The labeling efficiency was calculated using ε_{335} = 35,000 L $m^{-1}cm^{-1}$ for Stilbene and ε_{396} = 5,300 L $m^{-1}cm^{-1}$ for Bimane, and the protein concentration was measured by Bradford assay using BSA as the standard. Typically, the labeling efficiency was >90% for Stilbene-SNAP25 and ~75% for Bimane-CPX. The double-labeled CPX/SNARE complexes were assembled overnight at 4°C and purified by gel-filtration on a Superdex 75 (10/30, GE Healthcare) gel filtration column. All fluorescence data were obtained on a Perkin-Elmer LS55 luminescence spectrometer operating at 25°C. Excitation and emission slits of 5 nm were used in all measurements. Fluorescence emission spectra were measured over the range of 350-550 nm with the excitation wavelength set at 335 nm. Background fluorescence from the buffer was subtracted to calculate the reported fluorescence values. The donor probe concentration was adjusted to 2 μM in all samples. Fluorescence resonance energy transfer (FRET) was used to calculate the distance between the two fluorophores [56]. According to the FRET theory, the efficiency of energy transfer (E) is related to the distance (R) between the two fluorophores by equation:

$$E = \frac{R_0^6}{R_0^6 + R^6} \qquad (14)$$

R_0, the distance at the transfer efficiency equals 50% is given by the following equation:

$$R_0 = 9.78 \cdot 10^3 \left(\kappa^2 \eta^{-4} Q_D J\right)^{1/6} \tag{15}$$

The spectral overlap integral (J) between the donor emission spectrum and acceptor absorbance spectrum was approximated by using the summation

$$J = \frac{\int F_D(\lambda)\varepsilon_A(\lambda)\lambda^4 d\lambda}{\int F_D(\lambda)d\lambda} \tag{16}$$

Where, $F_d(\lambda)$ and $\varepsilon_A(\lambda)$ represent the fluorescence intensity of the donor and the molar extinction coefficient of the acceptor at the wavelength λ. The overlap integral was calculated to be 1.34 X 10^{-14}. The quantum yield ($K_d = \frac{1}{K_a}$) of the Stilbene-SNAP25 was calculated to be 0.19 using tryptophan in solution ($\Delta G = -RT \ln K_a$= 0.14) as the reference[58]. Polarization studies of SNAP25 193-Stilbene, CPX38-Bimane and CPX31-Bimane in both full-length and truncated SNARE complexes gave anisotropy values around 0.1 showing that the FRET probes have isotropic motion, so value of 2/3 was used for orientation factor (κ^2). The refractive index of the medium (η) was measured to 1.358. Using these values, R_0 for the Stilbene-Bimane FRET pair was calculated to be 27.5 Å.

The energy transfer data were obtained by measuring the change in donor fluorescence (donor quenching) in the presence of the acceptor. The donor fluorescence intensity was measured in the absence (f_d) and presence (f_a) of acceptor. The efficiency of transfer (E) was calculated using the equation $E = 1 - f_a/f_d$. Since the labeling efficiency was not 100%, the observed transfer efficiency (E_{obs}) was corrected for the acceptor

stoichiometry. The corrected efficiency (E_{cor}) is given as $E_{cor} = E_{obs}/f_a$, where f_a is the fraction of assembly with acceptor [56].

REFERENCES FOR SUPPLEMENTARY MATERIAL

1. Fatt, P. & Katz, B. Spontaneous subthreshold activity at motor nerve endings. *J Physiol* **117**, 109-28 (1952).
2. Palade, G.E. & Palay, S.L. Electron microscope observations of interneuronal and neuromuscular synapses. *Anat. Record* **118**, 335-336 (1954).
3. Sollner, T. et al. SNAP receptors implicated in vesicle targeting and fusion. *Nature* **362**, 318-24 (1993).
4. Hu, C. et al. Fusion of cells by flipped SNAREs. *Science* **300**, 1745-9 (2003).
5. Weber, T. et al. SNAREpins: minimal machinery for membrane fusion. *Cell* **92**, 759-72 (1998).
6. McNew, J.A. et al. Compartmental specificity of cellular membrane fusion encoded in SNARE proteins. *Nature* **407**, 153-9 (2000).
7. Sutton, R.B., Fasshauer, D., Jahn, R. & Brunger, A.T. Crystal structure of a SNARE complex involved in synaptic exocytosis at 2.4 A resolution. *Nature* **395**, 347-53 (1998).
8. Perin, M.S., Fried, V.A., Mignery, G.A., Jahn, R. & Sudhof, T.C. Phospholipid binding by a synaptic vesicle protein homologous to the regulatory region of protein kinase C. *Nature* **345**, 260-3 (1990).
9. Brose, N., Petrenko, A.G., Sudhof, T.C. & Jahn, R. Synaptotagmin: a calcium sensor on the synaptic vesicle surface. *Science* **256**, 1021-5 (1992).
10. Fernandez-Chacon, R. et al. Synaptotagmin I functions as a calcium regulator of release probability. *Nature* **410**, 41-9 (2001).

11. Geppert, M. et al. Synaptotagmin I: a major Ca2+ sensor for transmitter release at a central synapse. *Cell* **79**, 717-27 (1994).

12. Pang, Z.P., Shin, O.H., Meyer, A.C., Rosenmund, C. & Sudhof, T.C. A gain-of-function mutation in synaptotagmin-1 reveals a critical role of Ca2+-dependent soluble N-ethylmaleimide-sensitive factor attachment protein receptor complex binding in synaptic exocytosis. *J Neurosci* **26**, 12556-65 (2006).

13. Domanska, M.K., Kiessling, V., Stein, A., Fasshauer, D. & Tamm, L.K. Single vesicle millisecond fusion kinetics reveals number of SNARE complexes optimal for fast SNARE-mediated membrane fusion. *J Biol Chem* **284**, 32158-66 (2009).

14. Karatekin, E. et al. A fast, single-vesicle fusion assay mimics physiological SNARE requirements. *Proc Natl Acad Sci U S A* **107**, 3517-21 (2010).

15. Liu, T., Tucker, W.C., Bhalla, A., Chapman, E.R. & Weisshaar, J.C. SNARE-driven, 25-millisecond vesicle fusion in vitro. *Biophys J* **89**, 2458-72 (2005).

16. Ishizuka, T., Saisu, H., Odani, S. & Abe, T. Synaphin: a protein associated with the docking/fusion complex in presynaptic terminals. *Biochem Biophys Res Commun* **213**, 1107-14 (1995).

17. McMahon, H.T., Missler, M., Li, C. & Sudhof, T.C. Complexins: cytosolic proteins that regulate SNAP receptor function. *Cell* **83**, 111-9 (1995).

18. Giraudo, C.G., Eng, W.S., Melia, T.J. & Rothman, J.E. A clamping mechanism involved in SNARE-dependent exocytosis. *Science* **313**, 676-80 (2006).

19. Giraudo, C.G. et al. Alternative zippering as an on-off switch for SNARE-mediated fusion. *Science* **323**, 512-6 (2009).

20. Maximov, A., Tang, J., Yang, X., Pang, Z.P. & Sudhof, T.C. Complexin controls the force transfer from SNARE complexes to membranes in fusion. *Science* **323**, 516-21 (2009).

21. Xue, M. et al. Tilting the balance between facilitatory and inhibitory functions of mammalian and Drosophila Complexins orchestrates synaptic vesicle exocytosis. *Neuron* **64**, 367-80 (2009).

22. Cho, R.W., Song, Y. & Littleton, J.T. Comparative analysis of Drosophila and mammalian complexins as fusion clamps and facilitators of neurotransmitter release. *Mol Cell Neurosci* (2010).

23. Huntwork, S. & Littleton, J.T. A complexin fusion clamp regulates spontaneous neurotransmitter release and synaptic growth. *Nat Neurosci* **10**, 1235-7 (2007).

24. Xue, M. et al. Distinct domains of complexin I differentially regulate neurotransmitter release. *Nat Struct Mol Biol* **14**, 949-958 (2007).

25. Hobson, R.J., Liu, Q., Watanabe, S. & Jorgensen, E.M. Complexin Maintains Vesicles in the Primed State in C. elegans. *Curr Biol* **21**, 106-13 (2011).

26. Martin, J.A., Hu, Z., Fenz, K.M., Fernandez, J. & Dittman, J.S. Complexin has opposite effects on two modes of synaptic vesicle fusion. *Curr Biol* **21**, 97-105 (2011).

27. Sudhof, T.C. & Rothman, J.E. Membrane fusion: grappling with SNARE and SM proteins. *Science* **323**, 474-7 (2009).

28. Li, F. et al. Complexin: How Can the Same Protein Both Activate and Clamp Membrane Fusion? *in preparation* (2011).

29. Bracher, A., Kadlec, J., Betz, H. & Weissenhorn, W. X-ray structure of a neuronal complexin-SNARE complex from squid. *J Biol Chem* **277**, 26517-23 (2002).

30. Chen, X. et al. Three-dimensional structure of the complexin/SNARE complex. *Neuron* **33**, 397-409 (2002).

31. Giraudo, C.G. et al. Distinct domains of complexins bind SNARE complexes and clamp fusion in vitro. *J Biol Chem* **283**, 21211-9 (2008).

32. Hua, S.Y. & Charlton, M.P. Activity-dependent changes in partial VAMP complexes during neurotransmitter release. *Nat Neurosci* **2**, 1078-83 (1999).

33. Reim, K. et al. Complexins regulate a late step in Ca2+-dependent neurotransmitter release. *Cell* **104**, 71-81 (2001).

34. Tang, J. et al. A complexin/synaptotagmin 1 switch controls fast synaptic vesicle exocytosis. *Cell* **126**, 1175-87 (2006).

35. Lu, B., Song, S. & Shin, Y.K. Accessory alpha-helix of complexin I can displace VAMP2 locally in the complexin-SNARE quaternary complex. *J Mol Biol* **396**, 602-9 (2010).

36. Melia, T.J. et al. Regulation of membrane fusion by the membrane-proximal coil of the t-SNARE during zippering of SNAREpins. *J Cell Biol* **158**, 929-40 (2002).

37. Walter, A.M., Wiederhold, K., Bruns, D., Fasshauer, D. & Sorensen, J.B. Synaptobrevin N-terminally bound to syntaxin-SNAP-25 defines the primed vesicle state in regulated exocytosis. *J Cell Biol* **188**, 401-13 (2010).

38. Ellena, J.F. et al. Dynamic structure of lipid-bound synaptobrevin suggests a nucleation-propagation mechanism for trans-SNARE complex formation. *Proc Natl Acad Sci U S A* **106**, 20306-11 (2009).

39. Yang, X., Kaeser-Woo, Y.J., Pang, Z.P., Xu, W. & Sudhof, T.C. Complexin clamps asynchronous release by blocking a secondary Ca(2+) sensor via its accessory alpha helix. *Neuron* **68**, 907-20 (2010).

40. Pabst, S. et al. Selective interaction of complexin with the neuronal SNARE complex. Determination of the binding regions. *J Biol Chem* **275**, 19808-18 (2000).

41. Krishnakumar, S.S. et al. A Conformational Switch in Complexin Required for Synaptotagmin to Trigger Calcium-Dependent Fusion by Synaptic SNARE Proteins. *in preparation* (2011).

42. Kuzmin, P.I., Zimmerberg, J., Chizmadzhev, Y.A. & Cohen, F.S. A quantitative model for membrane fusion based on low-energy intermediates. *Proc Natl Acad Sci U S A* **98**, 7235-40 (2001).

43. Chernomordik, L.V., Zimmerberg, J. & Kozlov, M.M. Membranes of the world unite! *J Cell Biol* **175**, 201-7 (2006).

44. Stein, A., Weber, G., Wahl, M.C. & Jahn, R. Helical extension of the neuronal SNARE complex into the membrane. *Nature* **460**, 525-8 (2009).

45. Xue, M. et al. Binding of the complexin N terminus to the SNARE complex potentiates synaptic-vesicle fusogenicity. *Nat Struct Mol Biol* **17**, 568-75 (2010).

46. Choi, U.B. et al. Single-molecule FRET-derived model of the synaptotagmin 1-SNARE fusion complex. *Nat Struct Mol Biol* **17**, 318-24 (2010).

47. Chicka, M.C., Hui, E., Liu, H. & Chapman, E.R. Synaptotagmin arrests the SNARE complex before triggering fast, efficient membrane fusion in response to Ca2+. *Nat Struct Mol Biol* **15**, 827-35 (2008).

48. Doublie, S. Preparation of selenomethionyl proteins for phase determination. *Methods Enzymol* **276**, 523-30 (1997).

49. Otwinowski, Z. & Minor, W. Processing of X-ray Diffraction Data Collected in Oscillation Mode. in *Methods in Enzymology* Vol. 276 (eds. Carter Jr., C.W. & Sweet, R.M.) 307-326 (Academic Press, New York, 1997).

50. McCoy, A.J. et al. Phaser Crystallography Software. *J. Appl. Chrystallog.* **40**, 658-674 (2007).

51. Emsley, P. & Cowtan, K. Coot: model-building tools for molecular graphics. *Acta Crystallogr D Biol Crystallogr* **60**, 2126-32 (2004).

52. Murshudov, G.N., Vagin, A.A. & Dodson, E.J. Refinement of macromolecular structures by the maximum-likelihood method. *Acta Crystallogr D Biol Crystallogr* **53**, 240-55 (1997).

53. Kleywegt, G.J. & Jones, T.A. Where freedom is given, liberties are taken. *Structure* **3**, 535-40 (1995).

54. Brunger, A.T. et al. Crystallography & NMR system: A new software suite for macromolecular structure determination. *Acta Crystallogr D Biol Crystallogr* **54**, 905-21 (1998).

55. DeLano, W.L. The PyMOL Molecular Graphics System. . *DeLano Scientific LLC* (2003).

56. Lakowicz, J.R. *Principles of fluorescence spectroscopy*, xxvi, 954 p. (Springer, New York ; Berlin, 2006).

57. Chen, V.B. et al. MolProbity: all-atom structure validation for macromolecular crystallography. *Acta Crystallogr D Biol Crystallogr* **66**, 12-21 (2010).

58. Wu, P. & Brand, L. Resonance energy transfer: methods and applications. *Anal Biochem* **218**, 1-13 (1994).

CHAPTER FOUR

PREFACE

In the last paper, we demonstrated how the Complexin Accessory Helix is capable of clamping fusion; namely by extending away from the four-helix bundle. We modeled that it binds in an intermolecular alternate four-helix bundle, preventing the zippering of the VAMP2, not of its own SNARE complex, but of its neighbors. The next obvious question to answer is how this clamp is released.

In this paper, we investigate the mechanism behind the unclamping of Complexin by Synaptotagmin and calcium. Based on observations that the Complexin sticks out at a 45° angle in the pre-fusion, clamped state (modeled by VAMP60) and runs alongside the SNARE complex in the post-fusion state (modeled by VAMP96), it is evident that certain residues in VAMP2 are responsible for bringing the Complexin Accessory helix closer to the SNARE complex. By extending the VAMP2 by a few residues at a time, I was able to pinpoint a region of the VAMP (aspartates 64, 65, and 68) responsible for this switch in position.

In combination with Isothermal Titration Calorimetry (ITC) data, liposome fusion data, and cell-cell fusion data, my FRET data demonstrate that this aspartate patch is responsible for allowing Synaptotagmin to release the clamp.

A Conformational Switch in Complexin is Required for Synaptotagmin to Trigger Calcium-Dependent Fusion by Synaptic SNARE Proteins

Shyam S. Krishnakumar[1,5] , Daniel T. Radoff[1,2,5], Daniel Kümmel[1], Claudio G. Giraudo[1], Feng Li[1], Lavan Khandan[1], Stephanie Baguley[1], Karin M. Reinisch[1], Frederic Pincet[1,3] and James E. Rothman[1,4]

[1]Department of Cell Biology, Yale University School of Medicine, New Haven, CT 06520, USA.

[2]Department of Biochemistry and Molecular Biophysics, Columbia University New York, NY 10032, USA.

[3]Laboratoire de Physique Statistique, Unité Mixte de Recherche 8550, Centre National de la Recherche Scientifique associée aux Universités Paris VI et Paris VII, Ecole Normale Supérieure, 24 rue Lhomond, 75005 Paris, France.

[4] Corresponding author: james.rothman@yale.edu; Tel: (203)-737-5293

[5]These authors contributed equally.

SUMMARY

Complexin clamps synaptic SNARE-mediated membrane fusion by creating and stabilizing a new intermediate state, in which the v-SNARE is only ~50% zippered. The crystal structure of this clamped state reveals that the Complexin accessory helix extends away from the SNAREpin in an "open" conformation, binding another SNAREpin, and inhibiting its assembly to clamp fusion. In contrast, the accessory helix in the post-fusion complex parallels the SNARE complex in a "closed" conformation. Here we use targeted mutations, FRET spectroscopy, and a functional assay that reconstitutes Ca^{2+}-triggered exocytosis to test and confirm the hypothesis that the conformational switch from open to closed in Complexin is needed for Synaptotagmin-Ca^{2+} to trigger fusion. Triggering fusion requires the zippering of three key Asp residues located in a "switch" region (64-68) of the v-SNARE. Conformational switching in Complexin is integral to clamp release and is likely triggered when its accessory helix is released from its *trans*-binding to the neighboring SNAREpin, allowing the v-SNARE to complete zippering and open a fusion pore.

INTRODUCTION

SNARE proteins are the core machinery driving membrane fusion between cargo-carrying vesicles and their target membranes[1-4] as v-SNAREs (anchored in the vesicle membrane) zipper into a coiled-coil four helix bundle[5] with cognate t-SNAREs (anchored in the target membrane). In neuronal synapses, the principal SNAREs responsible for neurotransmitter release are the v-SNARE, VAMP2, localized to the synaptic vesicle, and the t-SNARE, a binary complex of SNAP25 with Syntaxin1, localized to the pre-synaptic plasma membrane. VAMP2 and Syntaxin1 each contribute one helix to the coiled-coil, and SNAP25 contributes the other two. Fusion by the isolated synaptic SNAREs is rapid and spontaneous[6] implying that in the synapse, additional protein machinery is needed to arrest exocytosis until the signal to secrete is provided by the entry of calcium ions.

One such protein is the calcium- and SNARE-binding protein Synaptotagmin[7,8], which is the immediate sensor for synchronous vesicle fusion[9-11]. The SNARE complex binding protein Complexin[12,13] (CPX) is equally required for synaptic transmission, functioning both positively as an activator of fusion and negatively as a clamp, to prevent fusion prior to the calcium signal[14-19]. We established on energetic grounds how CPX can be both a clamp and an activator of SNAREpins in an accompanying manuscript[20].

In a second manuscript, we established the precise nature of the clamped state using X-ray crystallography together with confirmatory solution and functional studies[21]. To capture this intermediate, we used a SNARE complex containing a C-terminally truncated VAMP (termed VAMP2-60) to mimic the half-zippered v-SNARE that is trapped in the clamped state[14,18,20,22-24]. In the structure, CPX binds one partially-zippered

SNARE complex via its central helix (CPXcen, residues 48-75) while its accessory helix (CPXacc, residues 26-48) extends away from this SNARE complex at ~45° to bridge to a second SNAREpin, binding its C-terminal three helix bundle so as to sterically block that SNAREpin's own v-SNARE from completing its zippering. As a result of repeating these *trans*-interactions, the clamped SNAREpins are cross-linked into a rigid zig-zag array[21], which is itself topologically incompatible with the opening of a fusion pore.

In this paper we address the question: how is fusion switched "on" from the clamped state? A novel feature of the pre-fusion mimetic structure is that in the clamped state, CPXacc angles away from the SNAREpin to which its central helix is attached, a conformation that we refer to as "open" (**Figure 28**, cyan). This differs markedly from that observed in the fully-zippered post-fusion structure, where the CPXacc nearly parallels the SNARE complex[25,26] which we refer to as "closed" (**Figure 28**, light cyan). Taken together, the two structures suggest that CPXacc undergoes a dramatic re-orientation as part of the mechanism (requiring calcium binding to Synaptotagmin) that switches fusion "on" from the clamped state. In this paper, we show that the switch from the open to closed state is a molecular switch required to activate fusion from the clamped state. We report that three closely clustered Aspartate residues (positions 64, 65, and 68) in the C-terminal half of VAMP2 (termed the "Asp switch region") must zipper into t-SNARE for CPX to move its accessory helix from the open (clamped) to the closed (post-fusion) conformation. Mutating these residues inhibits activation of fusion from the clamped state by de-stabilizing the open conformation.

RESULTS

ZIPPERING ONE TURN OF THE VAMP2 HELIX TRIGGERS COMPLEXIN TO SWITCH FROM THE OPEN TO THE CLOSED CONFORMATION

We utilize here a Förster Resonance Energy Transfer (FRET) analysis with a Stilbene/Bimane donor/acceptor pair to monitor the conformational state of CPXacc in CPX-SNARE complexes[21]. In this assay, residue 193 of SNAP25 is labeled with the donor dye (Stilbene), and the acceptor dye (Bimane) is attached at residue 38 of CPXacc (**Figure 28**). This pair was chosen because of its sensitivity to changes in separations in the range of interest. When CPXacc adopts the open conformation, the fluorescent probes are far apart, resulting in low FRET, but when CPXacc moves to the closed conformation, the FRET probes are in close proximity, resulting in a larger FRET signal. Distances obtained in solution from FRET analysis of VAMP2 constructs used in crystallization (VAMP2-60 or VAMP2) were in excellent agreement with the distances observed in the respective crystals (**Table 5**).

This FRET assay allows us to readily distinguish the open conformation (complexes with VAMP2 truncated at residue 60) from the closed conformation (complexes in which the cytoplasmic domain of VAMP is nearly complete, truncated at residue 96) (**Figure 29**). To explore what happens in complexes with VAMP2 truncations in between these two extremes, we assembled full length CPX-SNARE complexes in which the VAMP2 C-terminus was progressively extended beyond residue 60 (VAMP2-65, VAMP2-69, VAMP2-73 and VAMP2-77) to mimic the progressive zippering of the VAMP2 C-terminus.

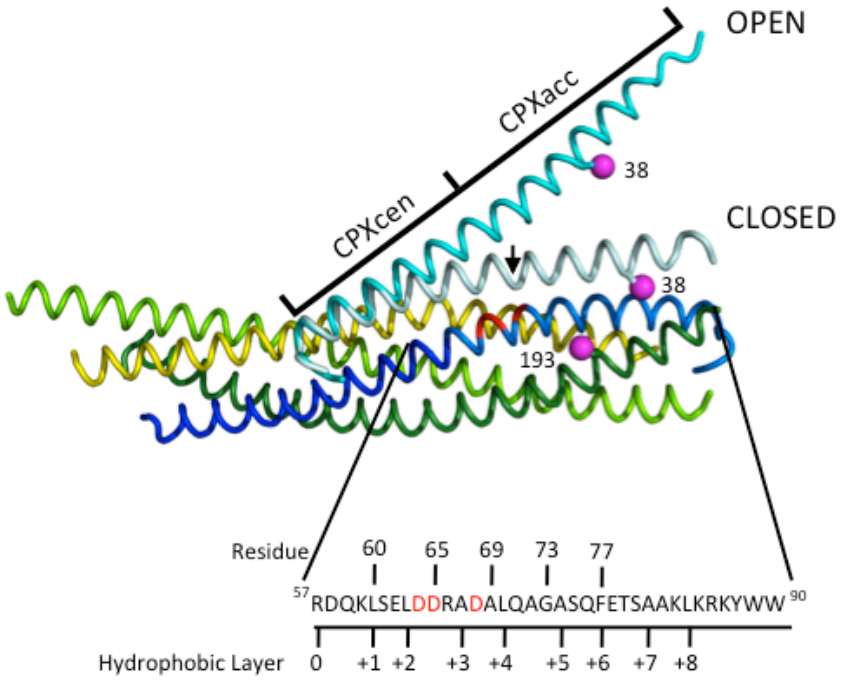

Figure 28: Superposition of the structures of the pre- and post-fusion CPX/SNARE complexes[21,25], showing the FRET label positions. Syntaxin1 (residues 190-250) is in yellow, SNAP 25 N-terminal SNARE motif (residues 10-74) is in lime, SNAP 25 C-terminal SNARE motif (residues 141-203) is in green and VAMP2 is in blue (residues 25-60 dark blue; residues 61-96 in light blue). The "switch" residues (D64, D65 and D68) are marked in red. The Complexin (residues 26-73) in the pre-fusion complex is in cyan, while in the post-fusion complex is in light cyan. The FRET label positions, residue 193 on SNAP25 and 38 on Complexin, are marked in magenta. The sequence of the C-terminal hydrophobic layer of VAMP2 (residues 57-90) with the C-terminal truncations tested in this paper (denoted by the residue number) is also shown. The black arrow in the post-fusion structure references CPX residue 48, the demarcation line between CPXcen and CPXacc.

Constructs	Distance between SNAP25 D193 and CPX Q38 (Å)
VAMP2 Deletions	
VAMP2-60	34 ± 1 Å
VAMP2-65	33 ± 2 Å
VAMP2-69	34 ± 1 Å
VAMP2-73	21 ± 2 Å
VAMP2-77	24 ± 1 Å
VAMP2 and VAMP2 Mutants (Residues 1-96)	
VAMP2	20 ± 1 Å
VAMP-4X	33 ± 1 Å
VAMP-3xDA	32 ± 3 Å
Measured in Crystal Structure	
Pre-fusion (VAMP2-60)	28 Å
Post-fusion (VAMP2)	18 Å

Table 5: FRET distances were determined from quenching of donor fluorescence between SNAP25 D193 and CPX Q38 in CPX-SNARE complexes with VAMP2 deletions and mutants. The distances measured in the pre-fusion and post-fusion crystal structures[21,25] are given for comparison. Standard deviations are reported from n = 4-6 independent experiments and they reflect the reproducibility of the spectra rather than accuracy of the distance measurements.

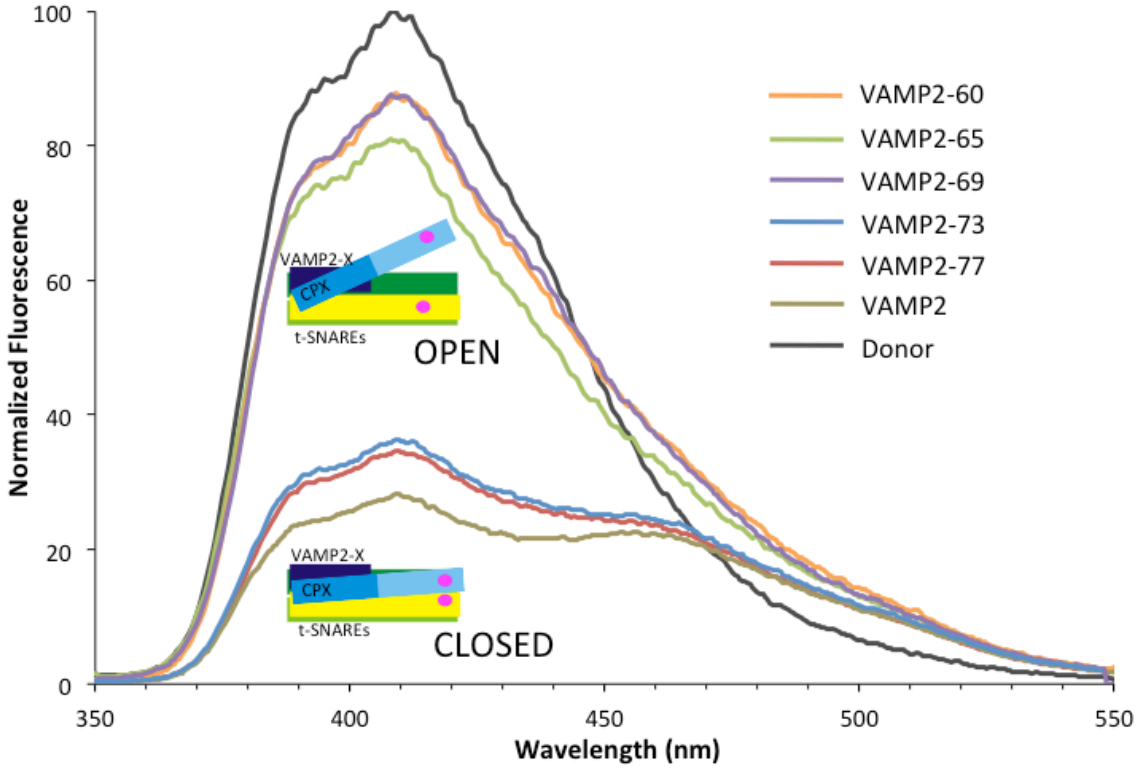

Figure 29: FRET experiments with C-terminal truncations of VAMP2. Fluorescence emission spectra of Stilbene/Bimane labeled CPX/SNARE complexes containing VAMP2-60 (residues 25-60, orange), VAMP2-65 (residues 25-65, green), VAMP2-69 (residues 25-69, purple), VAMP2-73 (residues 25-73, blue), VAMP2-77 (residues 25-77, red), and VAMP2 (residues 1-96, olive). A representative emission spectrum of a Stilbene (Donor)-only CPX-SNARE complex is shown in black. The donor-only spectrum was identical in all CPX-SNARE complexes.

The FRET spectra show that CPXacc adopts the open conformation in truncated CPX-SNARE complexes when the VAMP2 C-terminus was extended to the +2 (VAMP2-65) or +3 (VAMP2-69) hydrophobic layers (**Figure 29**). In these complexes, we observe low FRET efficiency, and the distance between the probes as measured by quenching of the donor fluorescence, is consistent with the distances observed in the crystal structure of the CPX-SNARE-60 complex (**Figure 29** & **Table 5**).

In contrast, when the VAMP2 C-terminus was extended only about one turn of the helix further, to the +4 hydrophobic layer (VAMP2-73) or beyond (VAMP2-77), high FRET efficiency is observed, quantitatively corresponding to the closed conformation, in which CPXacc runs parallel to the SNARE complex (**Figure 29**). In these complexes, the distance between donor and acceptor probes calculated from the FRET spectra is consistent with distances observed in the post-fusion CPX-SNARE structure (**Table 5**).

Remarkably, there is an all-or-none, discrete switch from open to closed conformation when one more turn of the helix is added between VAMP2 residues 69 and 73, without hybrid spectra of the two states. This shows that zippering of VAMP2 to at least the +4 hydrophobic layer is required for the switch in CPX conformation, indicating that a discrete 'switch region' is located in this stretch of VAMP2. Please note that the full-length "superclamp" CPX (scCPX) was used in these and later studies in this paper for consistency and direct comparability with the crystal structure which also employed mutations in the CPXacc (D27L, E34F, R37A) that increase binding to the t-SNARE.

AN 'ASP SWITCH REGION' IN THE CRITICAL REGION OF VAMP2 THROWS THE SWITCH

In the post-fusion structure[25], CPX binds the SNARE complex in the groove between VAMP2 and Syntaxin1, and the CPXcen makes three distinct contacts with VAMP2. Two of these interactions, a hydrophobic contact with VAMP2 V50/L54 and a salt-bridge with VAMP2 D57 are found in both the pre-fusion, clamped CPX-SNARE complex[21] and the post-fusion fully-zippered CPX-SNARE complex[25] structures.

We observed that a third, distinct contact region involving VAMP2 residues D64, D65 and D68 is present in the post-fusion complex only[25] (**Figure 30**), because the VAMP C-terminus was truncated at residue 60 in the pre-fusion complex[21]. These three Asp residues are located within the +2 to +4 hydrophobic layers of VAMP2, which we identified (**Figure 29**) as minimal 'switch region' required to switch CPXacc from the open to the closed conformation. They form hydrogen bonds and salt bridges to CPXcen which serve to anchor the accessory helix parallel (but without making any contacts) to the four helix SNARE bundle in the closed, post-fusion conformation (**Figure 30**).

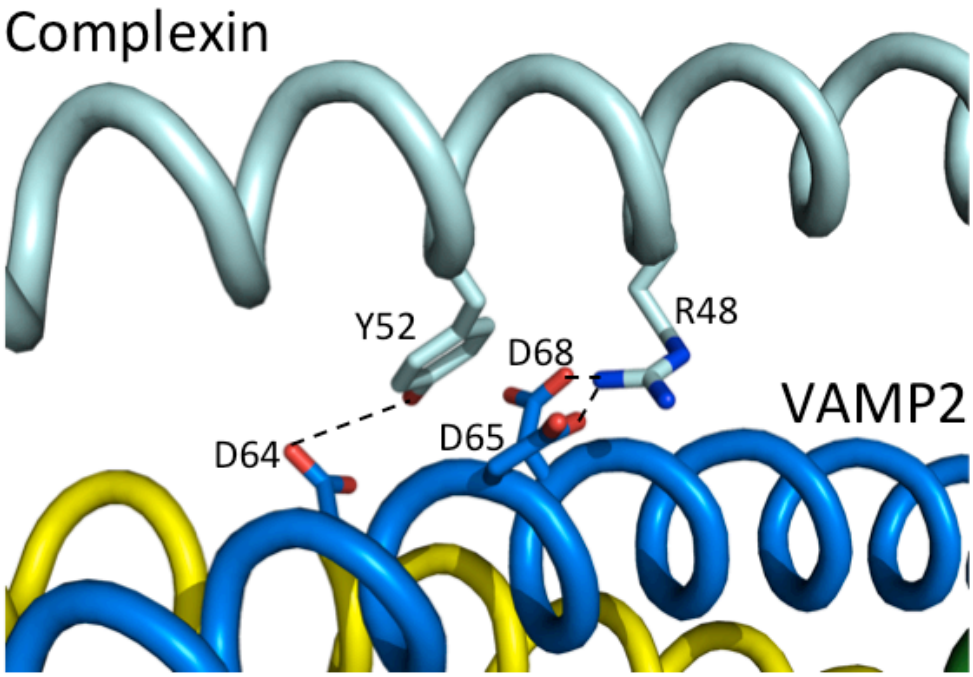

Figure 30: Hydrogen bonding and salt bridge interactions between the switch Asp residues (D64, D65, and D68) with CPXcen helix in the post-fusion complex[25].

To test the hypothesis that these contacts are needed to stabilize the closed conformation, we mutated all three switch Aspartate residues to Alanines in an otherwise complete VAMP2 cytoplasmic domain (residues 1-96) containing all of the VAMP residues that assemble into the four helix SNARE bundle[5], a construct referred to as VAMP-3xDA (VAMP2 with D64A/D65A/D68A mutations). As expected, VAMP-3xDA fully zippers into t-SNARE, as shown by resistance to cleavage by Tetanus and Botulinum-B neurotoxins (**Figure 31**) and the fact that VAMP-3xDA (when produced in a full-length form, containing its membrane anchor) retains its capacity to mediate fusion with its cognate synaptic t-SNARE in the liposome fusion assay (**Figure 31**).

As predicted by our hypothesis, CPXacc adopts the open conformation in the fully-zippered CPX-SNARE-3xDA complex, and its FRET spectrum corresponds closely to those of the pre-fusion mimetics of CPX-SNARE in which the switch region of VAMP is physically removed (**Figure 32** and **Table 5**, raw data in **Figure 33**). Mutating the individual switch Asp's reveals that all three Asp residues are required for the full-switching of the CPXacc, as mutation of any of the three Asp residues (VAMP2-D64A, VAMP2-D65A and VAMP2-D68A) destabilizes the closed conformation (**Figure 32**, raw data in **Figure 34**). Mutating residue 64 (VAMP2-D64A) has the maximum destabilizing effect, so it might act as the internal trigger for the switch (**Figure 32**).

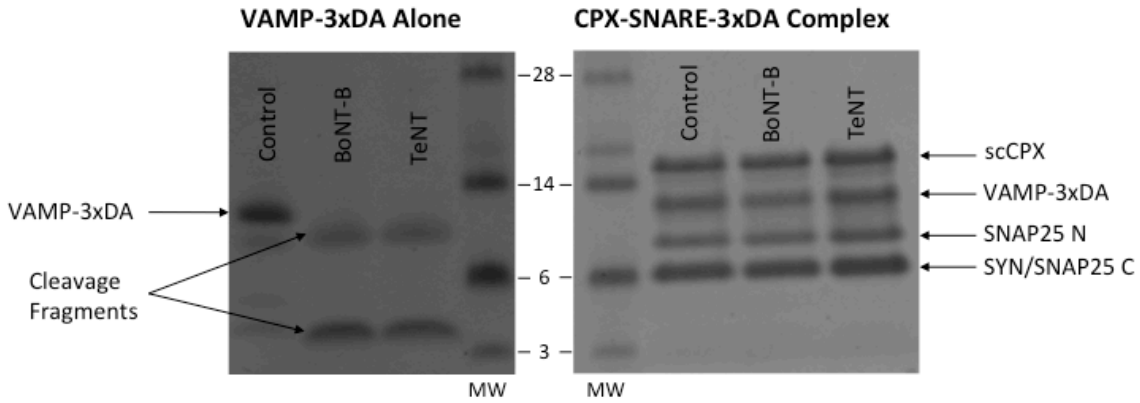

Figure 31: VAMP2 is the natural substrate for both Botulism-B (BoNT-B) and Tetanus (TeNT) neurotoxin. Neither toxin can bind nor cleave if the binding residues on VAMP2 (41-45 for TeNT and 63-67 for BoNT-B) are zippered into t-SNARE[1]. The free VAMP-3xDA is readily cleaved by both the neurotoxins (left panel) but is fully protected from cleavage in the presence of t-SNARE and CPX (right panel). This shows that VAMP-3xDA can assemble into a stable CPX-SNARE complex.

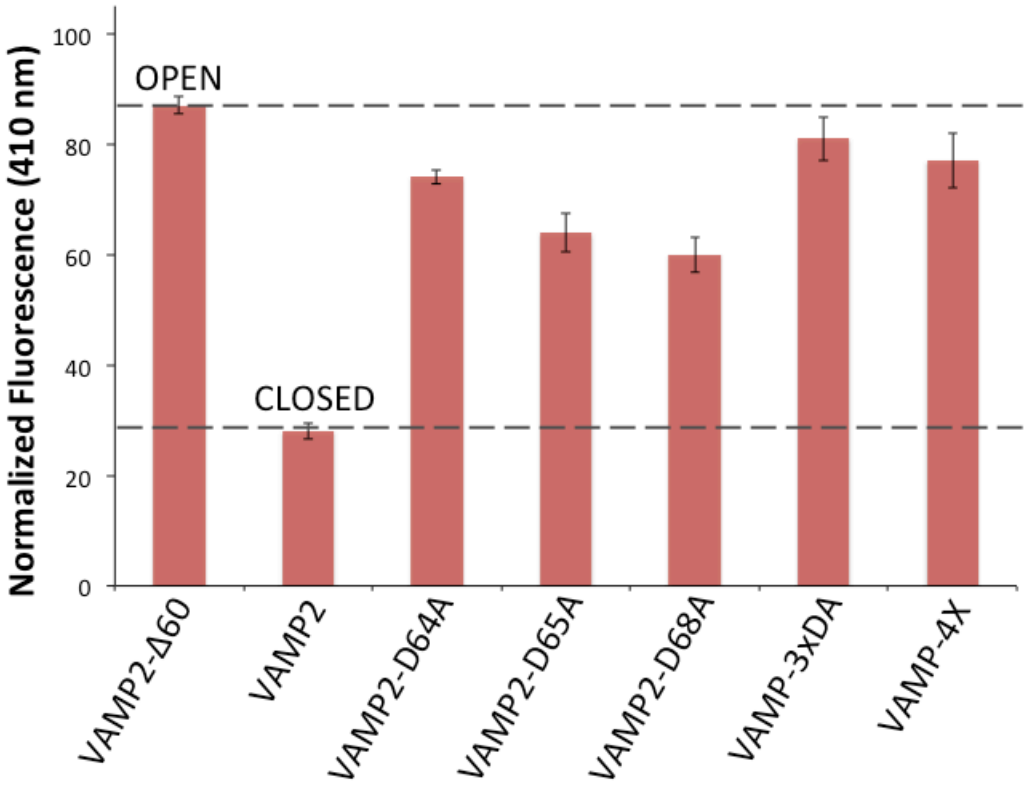

Figure 32: Complexin adopts an open conformation in CPX-SNARE complexes containing either VAMP-3xDA or VAMP-4X. Donor fluorescence at 410 nm (normalized to a Donor-only sample) for Stilbene/Bimane labeled CPX-SNARE complexes containing VAMP2-D64A, VAMP2-D65A, VAMP2-D68A, VAMP-3xDA, or VAMP-4X is shown. (The raw fluorescence emission curves are shown in **Figure 32** and **33**.) The donor fluorescence (at 410 nm) for VAMP2-60 ("open") and VAMP2 ("closed") are shown for comparison. Averages and standard deviations for 3-4 independent experiments are shown.

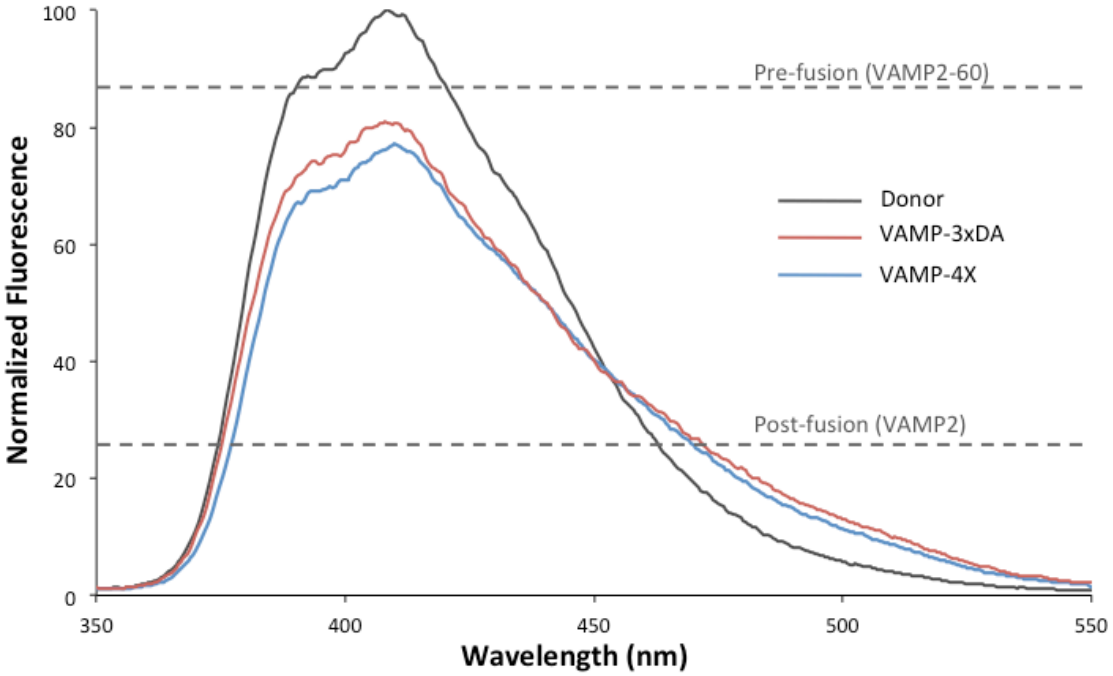

Figure 33: Zippering in of all three Asp residues (D64, D65, and D68) in the VAMP2 C-terminus into t-SNARE is required for full switching of the CPXacc position. Fluorescence emission spectra of Stilbene/Bimane labeled CPX-SNARE complexes containing VAMP-3xDA (VAMP2 with D64A, D65A, & D68A mutations, red) and VAMP-4X (VAMP2 with mutations L70D, A74R, A81D, and L84D, blue) A representative emission spectrum of Stilbene (Donor)-only CPX-SNARE complex is shown in black. The donor fluorescence level at 410 nm for the pre-fusion (VAMP2-60) and the post-fusion (VAMP2) CPX/SNARE complexes are shown as reference (dashed lines).

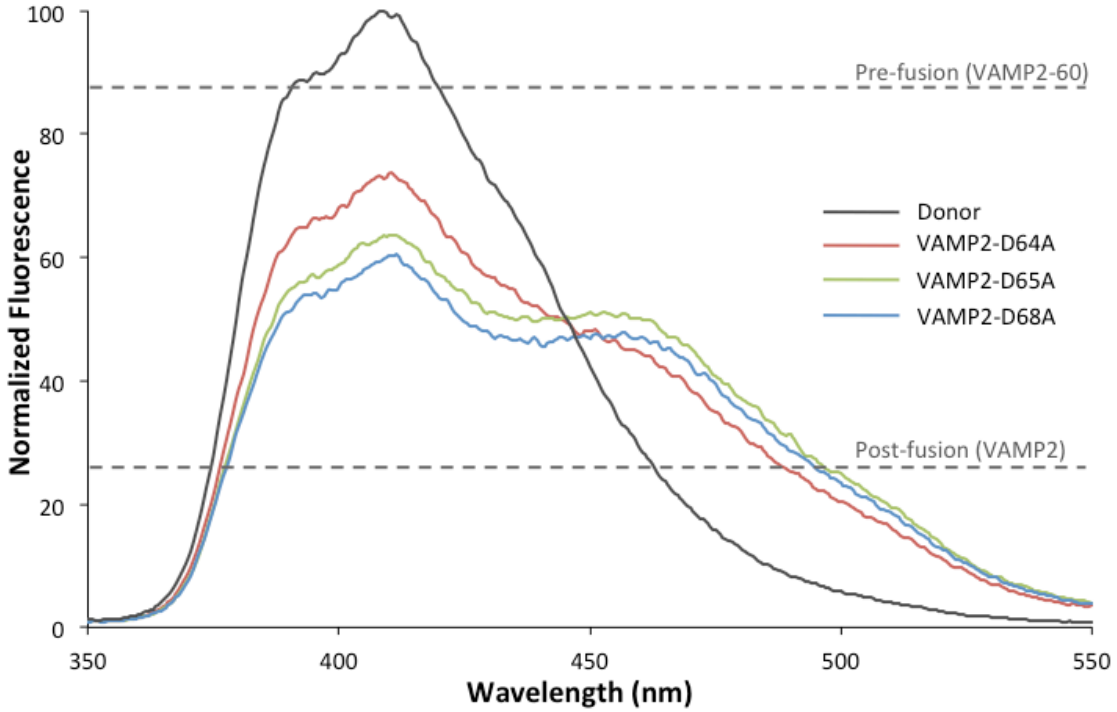

Figure 34: Zippering in of all three Asp residues (D64, D65, and D68) in the VAMP2 C-terminus into t-SNARE is required for full switching of the CPXacc position. Fluorescence emission spectra of Stilbene/Bimane labeled CPX-SNARE complexes containing VAMP2-D64A(red), VAMP2-D65A (green), and VAMP2-D68A (blue). A representative emission spectrum of Stilbene (Donor)-only CPX-SNARE complex is shown in black. The donor fluorescence level at 410 nm for the pre-fusion (VAMP2-60) and the post-fusion (VAMP2) CPX/SNARE complexes are shown as reference (dashed lines).

As predicted by our hypothesis, CPXacc adopts the open conformation in the fully-zippered CPX-SNARE-3xDA complex, and its FRET spectrum corresponds closely to those of the pre-fusion mimetics of CPX-SNARE in which the switch region of VAMP is physically removed (**Figure 32** and **Table 5**, raw data in **Figure 33**). Mutating the individual switch Asp's reveals that all three Asp residues are required for the full-switching of the CPXacc, as mutation of any of the three Asp residues (VAMP2-D64A, VAMP2-D65A and VAMP2-D68A) destabilizes the closed conformation (**Figure 32**, raw data in **Figure 34**). Mutating residue 64 (VAMP2-D64A) has the maximum destabilizing effect, so it might act as the internal trigger for the switch (**Figure 32**).

ZIPPERING OF THE ASP SWITCH RESIDUES IS REQUIRED TO SWITCH THE CPX_{ACC} POSITION

So far, we know that CPXacc is trapped in the open conformation when the switch Asp's are absent from VAMP (due either to point mutations or deletion). What about when the switch Asp's are present but not able to zipper? This would correspond more closely to what occurs physiologically before these residues have zippered. To mimic this state, we employed a VAMP construct in which the normal switch Asp's are present but carry point mutations in the C-terminal (membrane-proximal) region of VAMP that prevent full zippering.

Specifically, we used the entire VAMP2 cytoplasmic domain (residues 1-96) and introduced mutations in its C-terminal half (L70D, A74R, A81D & L84D; termed VAMP-4X) that prevent assembly of this region with Syntaxin1 and SNAP25 and

eliminate fusion activity (**Figure 29**). However, the N-terminal half of VAMP-4X still zippers because VAMP-4X forms stable complexes with t-SNARE and CPX (**Figure 35**). The FRET spectrum of the CPX-SNARE-4X complex (**Figure 32** and **Table 5**, raw data in **Figure 33**) was nearly identical to the open conformation observed in CPX-SNARE complex with VAMP-60 or when the switch Asp's were mutated or deleted by truncations. (**Figure 32** and **Table 5**)

Importantly, this experiment establishes that the mere presence of the VAMP2 residues D64, D65 and D68 is not sufficient for switching: they must also be zippered with the t-SNARE in the helical bundle in order to throw the switch from open to closed. This strongly suggests that zippering of the switch region of the v-SNARE (*i.e.*, progression of fusion beyond the clamped state) and movement of CPXacc from its open to its closed arrangement are thermodynamically coupled *i.e.* one cannot occur without the other.

This also could explain why CPXacc adopts an open conformation in the CPX-VAMP-69 complex (**Figure 29** and **Table 5**). Even though the key residues required for the switch (D64, D65 and D68) are present in this complex, they are at the end of the truncated VAMP2, and they may not be properly zippered into the t-SNARE. Extending the VAMP2 C-terminus one rung on the helix to the next hydrophobic layer (VAMP2-73) could then allow the switch region to stably zipper into the t-SNARE, and switch CPXacc to the closed conformation (**Figure 29** and **Table 5**).

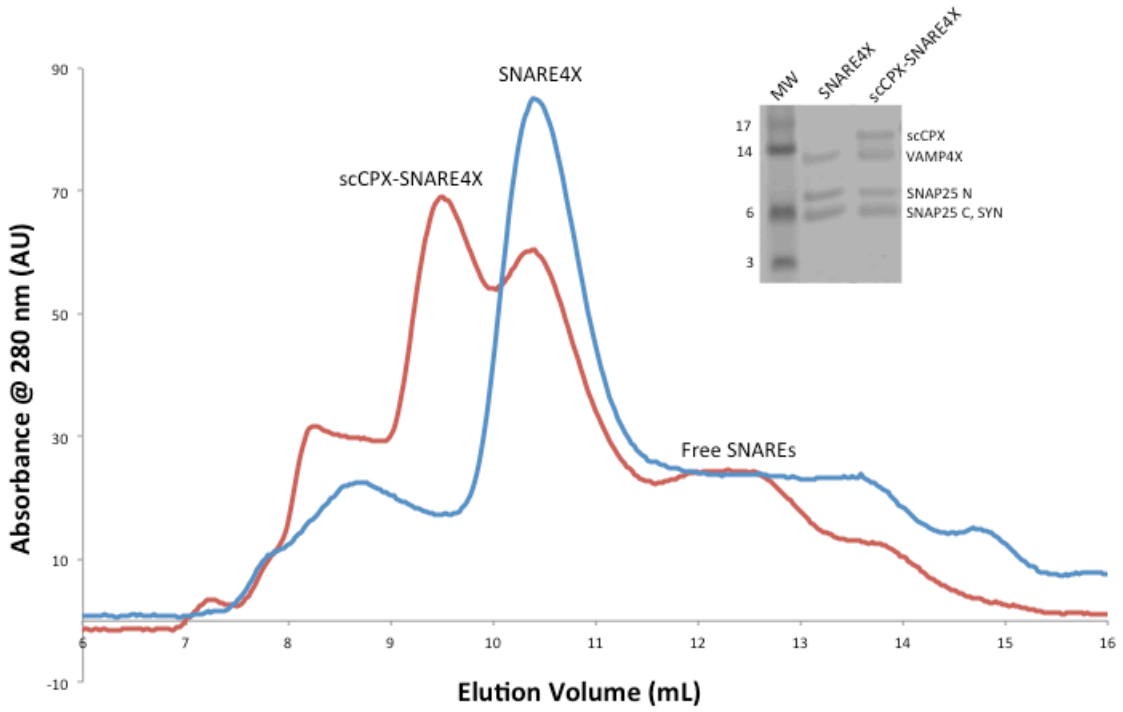

Figure 35: VAMP4X forms stable SNARE complexes. A representatitive Superdex 75 elution profile for SNARE4X (blue) and CPX-SNARE4X (red) complex are shown. **Inset**: Coomassie stained SDS-PAGE gel of the SNARE4X and CPX-SNARE-4X complex peak is shown.

THERMODYNAMICS OF THE COMPLEXIN CONFORMATIONAL SWITCH

We used Isothermal Titration Calorimetry (ITC) to determine the energetics of the contributions of the switch Asp residues to the open-to-closed conformational switch. To this effect, we compared the thermodynamics of binding of CPX to SNARE complexes assembled with either VAMP2 or VAMP-3xDA (**Figure 36**). Complexin binds the VAMP2 SNARE complex with 1:1 stoichiometry and high affinity (K_d = 83 nM). Mutating the switch Asp residues (VAMP-3xDA) does not alter the binding stoichiometry, but results in 8-fold decrease in the binding affinity (K_d = 670 nM) (**Figure 36** and **Table 6**), corresponding to a free energy difference of -1.3 kCal/mole. The enthalpy of the interaction of CPX with the SNARE complex was greatly reduced, -15 kCal/mole for the VAMP-3xDA SNARE complex as compared to -37.5 kCal/mole for the wild-type VAMP2 sequence. So the difference in the enthalpy ($\Delta\Delta H$ = -22.5 kCal/mole), is mainly from the interaction of CPXcen with the switch Asp residues on VAMP2.

In control experiment, when we blocked the CPXcen binding site on VAMP-3xDA SNARE complex by pre-binding CPXcen (residues 48-134), we see no further interaction with CPX (**Figure 36**). This shows that the interaction of CPX with the SNARE-3xDA complex is mediated solely by CPXcen. In addition, this confirms that SNARE-3xDA complex is fully-zippered since the additional binding site for CPXacc *i.e.,* the C-terminal t-SNARE groove is not available for binding.

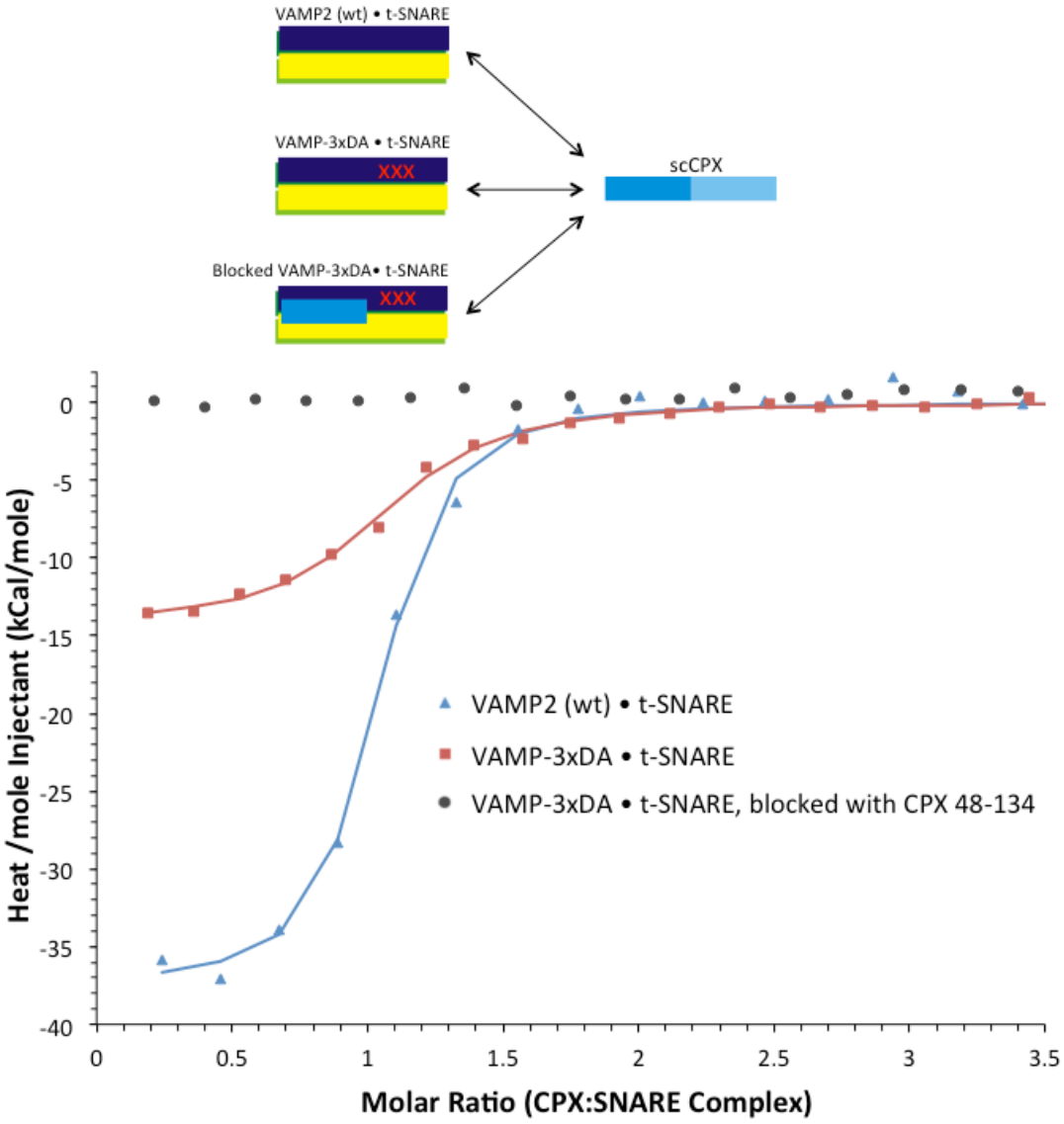

Figure 36: Interaction of CPX central helix with Asp residues (D64, D65, D68) on VAMP2 provides thermodynamic driving force for the switch. Calorimetric titrations of scCPX (residues 1-134 carrying superclamp mutations D27L, E34F, R37A, scCPX) into assembled SNARE complexes containing t-SNAREs and either VAMP2 (blue triangles), VAMP2-3xDA (red squares), or VAMP-3xDA with the CPXcen binding site blocked by CPX 48-13 (black circles). The solid lines represent the best fit to the corresponding data points using a nonlinear least squares fit with a one-set-of-sites model. The results of the fits are given in **Table 6**. All experiments were performed in triplicate at 37^{o}C, and a representative thermogram is shown.

Titrant	In sample cell	Stoichiometric Coefficient (N)	K_d (nM)	ΔH (kCal/mol)	ΔS (Cal/mol/K)	ΔG (kCal/mol)
scCPX	SNARE complex with VAMP2-wt	0.95 ± 0.01	83 ± 17	-37.5 ± 0.7	-88.6 ± 2.7	-10.1 ± 0.2
scCPX	SNARE complex with VAMP-3xDA	0.99 ± 0.04	670 ± 90	-15.0 ± 1.0	-20.1 ± 3.6	-8.8 ± 0.2
CPX^{48-134}	SNARE complex with VAMP-3xDA	0.98 ± 0.01	620 ± 110	-14.0 ± 1.1	-16.6 ± 3.8	-8.8 ± 0.1

Table 6: Thermodynamic parameters of CPX binding to SNAREs measured by Isothermal Titration Calorimetry. Superclamp CPX (scCPX, residues 1-134 carrying superclamp mutation D27L, E34F, R37A, scCPX) or CPX^{48-134} were titrated into assembled SNARE complexes containing VAMP2 (residues 1-96) or VAMP-3xDA (residues 1-96 with mutations D64A, D65A, & D68A). The thermodynamic parameters were calculated by nonlinear least squares fit with a one-set-of-sites model from the binding isotherms shown in **Figure 36**. Average and standard deviations of a minimum of three independent experiments are shown.

THE CONFORMATIONAL SWITCH IN COMPLEXIN OCCURS WHEN CALCIUM BINDS TO SYNAPTOTAGMIN TO TRIGGER FUSION

To the extent that the open-to-closed conformational switch in CPX is needed to activate fusion from the clamped state, locking CPXacc in the open state will prevent activation of fusion and result in a persistent clamped state, which should inhibit activation of fusion by Synaptotagmin and calcium ions.

To test this, we utilized the 'flipped' SNARE system in which cells expressing either VAMP2 or Syntaxin1-SNAP25 proteins on their surface are mixed and the rate of cell-to-cell fusion is scored using light microscopy[3]. In this system, fusion occurs spontaneously, unless CPX is added either as an exogenous pure protein or by endogenous gene expression and secretion. In the presence of CPX, fusion is blocked when the SNAREs are approximately half-zippered, as judged by the pattern of Botulinum and Tetanus neurotoxin resistance[14]. When Synaptotagmin is either added back to the medium (cytoplasmic domain only) or endogenously expressed as a flipped protein, fusion is then re-activated upon addition of Ca^{2+} ions[14]. The physiological relevance of this minimal system was established by several criteria[14]. For example, mutations in Synaptotagmin that alter calcium sensitivity in mice, correspondingly alter sensitivity in this reconstituted system, toxin sensitivity in the clamped state reproduces the pattern found at the neuromuscular junction and most recently, super-clamp mutations of CPXacc that increase clamping potency in neurons [27]also do so in this *in vitro* system[15]

We tested the activation of fusion mediated by VAMP-3xDA (VAMP2 with D64A/65A/68A) from the clamped state by Synaptotagmin and calcium and confirmed

the prediction that clamp release would be impaired when the v-SNARE lacked the switch Asp residues (**Figure 37**, VAMP-3xDA, green bar). The limited extent of activation that was observed with VAMP-3xDA and wild-type CPX was similar to the essentially permanent clamped state that results when wild-type SNAREs are frozen with super-clamp CPX (**Figure 37**, scCPX, green bar). In the latter case, the open state is stabilized by stronger binding of CPXacc to *trans*-t-SNARE, whereas in the former case it is the closed state that is de-stabilized by weaker binding of CPXcen to the SNARE bundle due to switch Asp mutations. As expected, mutating individual Asp residues in the switch region partially compromised activation in a manner reflecting their relative contributions to stabilizing the closed conformation measured by FRET (**Figure 32**).

As a control, we tested VAMP-3xDA in the absence of any CPX to confirm that it is intrinsically fusion competent (**Figure 37**, blue bars). Furthermore, we found that the clamping of fusion by wild-type CPX was identical for cells expressing VAMP2 or VAMP-3xDA (**Figure 37**, red bars). Because the mutations of the switch Asp's lock CPXacc in the open state, the fact that we see functional clamping in VAMP-3xDA is consistent and confirmatory that the accessory helix exerts clamping in the open conformation[21].

To further characterize the VAMP-3xDA mutation, we analyzed the kinetics of the activation of fusion by Synaptotagmin and calcium from the clamped state. We found the overall kinetics of clamp release was similar in cells expressing VAMP-3xDA or VAMP2 (**Figure 38**), but the extent of activation of fusion by Ca^{2+}-Synaptotagmin was limited at all time points (**Figure 38**). These activation curves have the same calcium

requirement (EC_{50} ~ 100 μM, **Figure 39**) indicating that the effect is mainly due to an intrinsic property of the VAMP-3xDA mutation rather an impairment in Synaptotagmin. These results clearly demonstrate that the conformational switch in CPX position is essential for Synaptotagmin to trigger fusion upon arrival of the Ca^{2+} signal.

To further characterize the VAMP-3xDA mutation, we analyzed the kinetics of the activation of fusion by Synaptotagmin and calcium from the clamped state. We found the overall kinetics of clamp release was similar in cells expressing VAMP-3xDA or VAMP2 (**Figure 38**), but the extent of activation of fusion by Ca^{2+}-Synaptotagmin was limited at all time points (**Figure 38**). These activation curves have the same calcium requirement (EC_{50} ~ 100 μM, **Figure 39**) indicating that the effect is mainly due to an intrinsic property of the VAMP-3xDA mutation rather an impairment in Synaptotagmin. These results clearly demonstrate that the conformational switch in CPX position is essential for Synaptotagmin to trigger fusion upon arrival of the Ca^{2+} signal.

DISCUSSION

The data presented establish that a region near the middle of the VAMP2 SNARE motif must be folded with the t-SNARE in order for CPX to assume the closed conformation. This positions the key Aspartate residues (D64, D65, D68) to correctly interact with the CPX central helix (**Figure 30**), driving CPX from its open into its closed conformation. The data also reveal that accessing the closed conformation is not required for clamping, but it is required for calcium-bound Synaptotagmin to release the clamp.

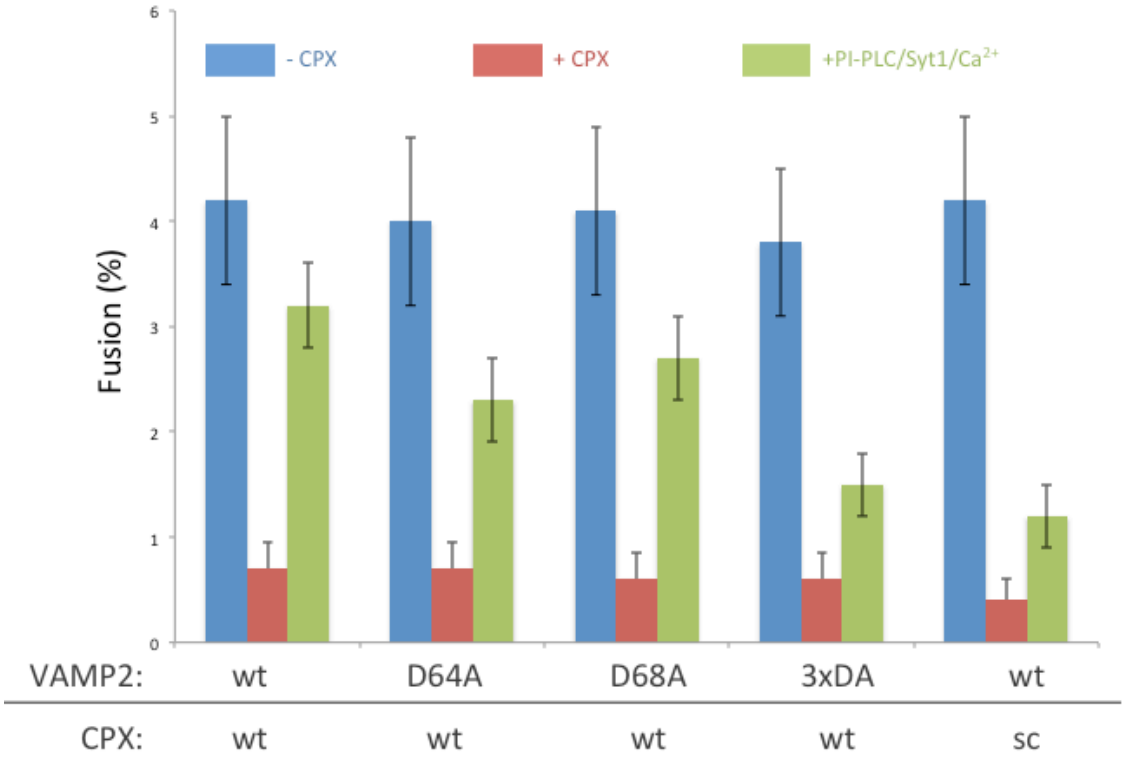

Figure 37: The switch in CPXacc position is necessary for Synaptotagmin/Ca^{2+} to trigger fusion. Clamping of SNARE-mediated fusion by CPX and the reversal of the clamp by Synaptotagmin/Ca^{2+} in wild-type VAMP2, VAMP2-D64A, VAMP2-D65A and VAMP-3xDA as measured in a cell-cell fusion assay. The effect of the superclamp CPX (scCPX; CPX D27L, E34F, R37A) on wild-type VAMP2 is shown for comparison.

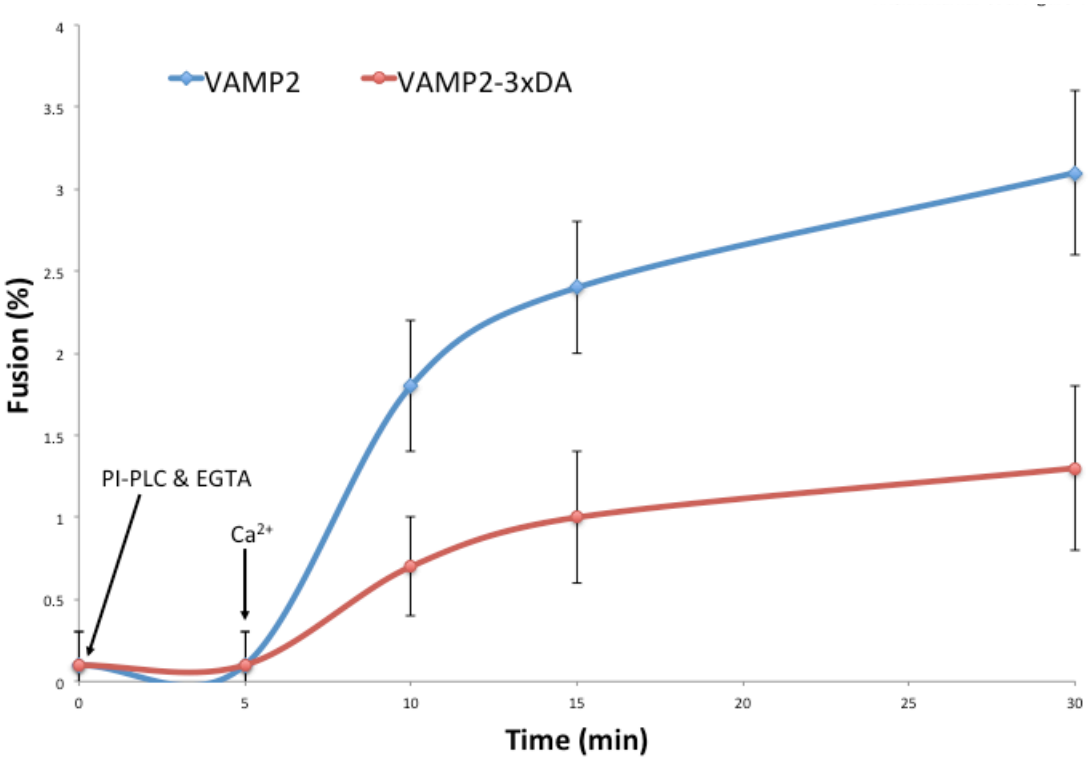

Figure 38: Kinetics of the reversal of the CPX clamp by Syanptotagmin/Ca^{2+}. The cell fusion recovery was carried out at 1mM free Ca^{2+} and the samples were fixed at the indicated time point after the addition of Ca^{2+}.

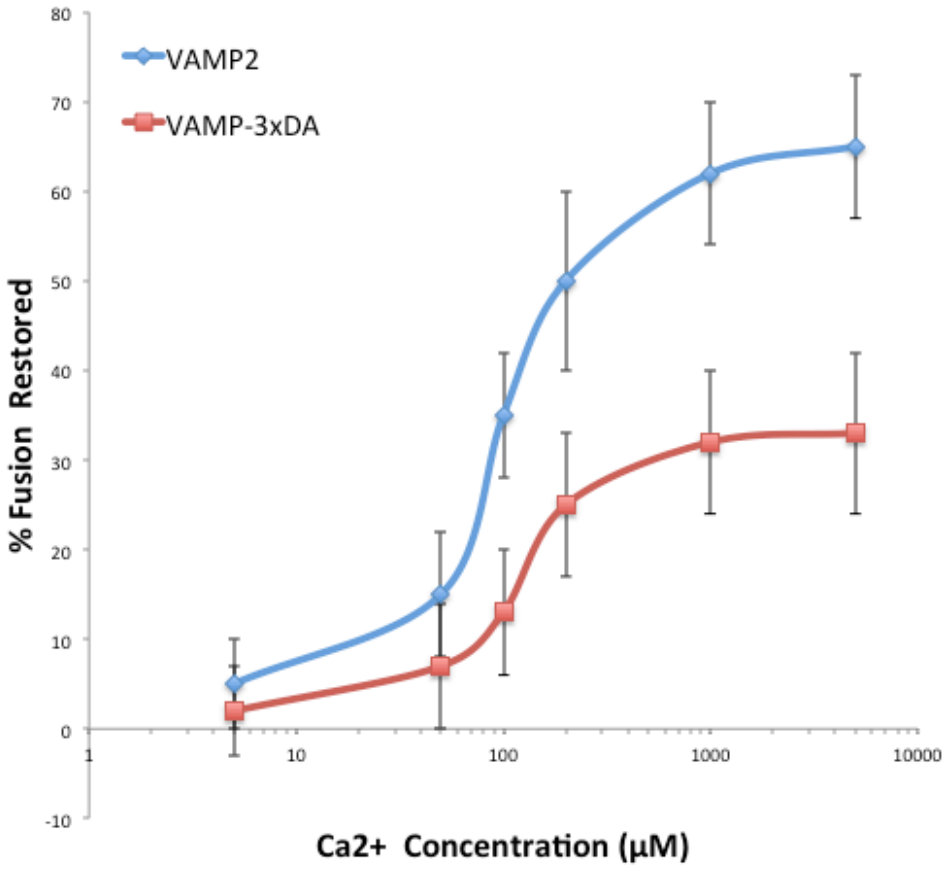

Figure 39: Ca^{2+}/Synaptotagmin sensitivity of the VAMP-3xDA mutation. Calcium titration experiment using cells expressing VAMP2 or VAMP3x-DA. 5 min after the addition of PI-PLC/EGTA, the free Ca^{2+} concentration was raised to the indicated concentration (ranging from 5 to 5000µM) and the cells were incubated at 37°C for 30 min. Cells were then fixed and the data quantified as the percentage of the fusion restored.

Clamp release entails removing CPXacc from its *trans*-t-SNARE binding site so that the *trans*-SNAREpin can complete zippering and thereby fuse the bilayers. In light of the network of interactions constituting the zig-zag array[21] (**Figure 40**), it is hard to imagine how this could occur as an isolated event. For example, if any one CPX in the array (example, the CPX emanating from SNAREpin 3 in **Figure 40**) were to flip from open to closed, in so doing, it would necessarily pull its CPXacc out of the binding pocket of its *trans*-SNAREpin across the midline of the array (number 2), where it had up until then been bound (**Figure 40**). But, in actuality this could not happen unless the switch region of the v-SNARE within SNAREpin 3 had somehow zippered up to create the binding site needed to anchor its emanating CPXacc. However, this in turn, is prohibited by yet another CPXacc (emanating from SNAREpin 4) which plugs the path of the v-SNARE within SNAREpin 3 (**Figure 40**). This suggests that the zippering of the VAMP2 c-terminus and the conformational switch in CPX must both occur in the short interval corresponding to clamp release, probably concomitantly. In essence, the zig-zag array seems designed either to remain as it is or to disassemble in a nearly simultaneous cascade, ideally suited for the synchronous activation of synaptic transmission. How could this be triggered?

The structure suggests an appealingly simple hypothesis. Removing any individual SNAREpin from the zig-zag entails breaking contacts with two other SNAREpins, one before and the other after it in the array (SNAREpin 3 in **Figure 40**). This fracture will almost always break the CPXacc bonds rather than the CPXcen bonds,

because the former (ΔG = -6.8 kCal/mole) are much weaker than the latter (ΔG = -9.1 kCal/mole)[21]. When this occurs, the cascade outlined in the last paragraph could be spontaneously triggered (see discussion below), and the SNAREpins located across the midline of the zig-zag would zipper away from each other to form the fusion pore and release neurotransmitter.

If our speculative hypothesis that fusion is triggered by perturbing a single SNAREpin in the array is correct, the activation energy that needs to be provided to enable this triggered fusion will be the energy required to disrupt the two CPXacc-t-SNARE binding sites in which that SNAREpin is engaged, totaling ~14 kCal/mole (corresponding to ~20 k_BT) [21]. The source of this energy must be from Synaptotagmin binding to calcium, the event that triggers release from the clamped state[8]. When Synaptotagmin binds calcium, it undergoes a conformational change[28] and as a result, ~21 kCal/mole of free energy (corresponding to ~33 k_BT) is made available to do work beyond that which is needed for the conformational change itself[29] as the sum of the individual ΔG values for sites 1-3 in C2A/B, excluding site 4 because it binds calcium well above the physiological range). In addition, the calcium-Synaptotagmin complex binds acidic phospholipid-containing bilayers with a K_{eq} of ~2 μM[29], corresponding to ~12 k_BT. The total energy potentially available to perturb the zig-zag array when a single Synaptotagmin binds its complement of calcium ions is thus ~45 k_BT, greatly exceeding the energy needed to remove its attached SNAREpin (~ 20 k_BT in our model).

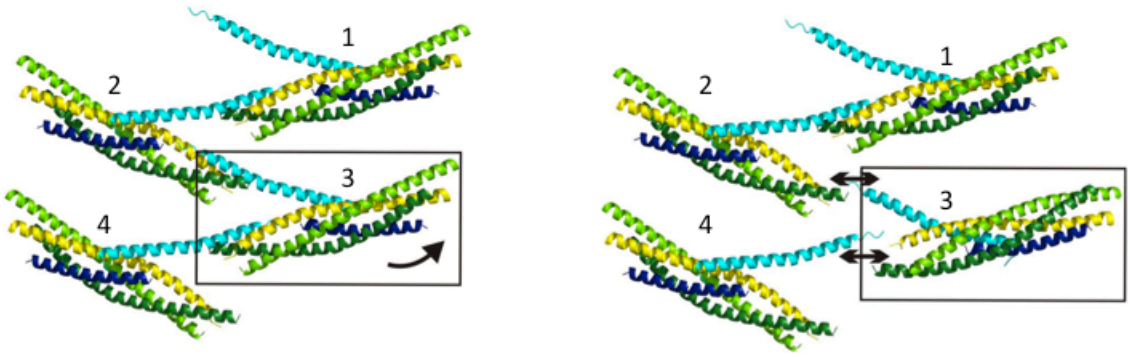

Figure 40: Perturbation of a single SNARE complex in the zig-zag array should be sufficient to rapidly disassemble the clamp in response to neuronal stimulus. A small perturbation of one CPX-SNARE complex in the clamped zig-zag array would eliminate interactions with both of its neighbors in the array. For example, a disruption of complex 3 would eliminate interaction with complexes 2 and 4. So, if one set of the CPXacc-SNAREpin interactions were to be perturbed by Syaptotagmin/Ca^{2+}, then VAMP2 could zipper up, and the entire zig-zag array would disassemble very rapidly, releasing the clamp and triggering fusion.

Of course, it is not known how much of Ca^{2+}-Synaptotagmin's energy resource is usefully funneled into disrupting the array, but these considerations make it tenable to suggest that activation of a single Synaptotagmin molecule (by its bound complement of calcium ions) could be sufficient to dislodge its single bound SNAREpin, and that this in turn is sufficient to trigger synchronous release of a quantum of neurotransmitter. Twisting, pulling, or pushing on a SNAREpin with sufficient (~20 k_BT) energy will remove it from the array, as is illustrated by SNAREpin 3 in **Figure 40**. Though the structural details are still missing, it is easy to imagine how a conformational change in Synaptotagmin (perhaps driven by stabilization of its compact conformation when it binds calcium[28,30,31] could perturb an attached SNAREpin in this manner. In addition, Synaptotagmin is expected to rapidly adhere to the acidic phospholipids (mainly PS and PIP2) in the nearby synaptic vesicle and/or plasma membrane cytoplasmic leaflets,[7,8,32-34] which would also be expected to perturb an attached SNAREpin out of planarity in the array. But, it is important to point out that lipid binding alone (~12 k_BT)[29] does not appear to be sufficient to activate fusion (~20 k_BT) though it may well make an important contribution. The N-terminal domain of CPX (residues 1-25, which precede the CPXacc) also contributes to the activation process *in vivo*[35], but is not needed in our minimal cell-cell fusion system[15]. Also, recent data suggests that Ca^{2+} alone could perturb the CPX-SNARE complexes even in the absence of Synaptotagmin, in certain cases[36].

Neurotransmitters can be released within as little as 200 μsec after calcium ions enter the nerve terminal[37]. Can activation in our single Synaptotagmin-SNAREpin hypothesis keep pace with this? The results from SFA show that the open and closed

states in the zig-zag array of SNAREpins and CPX (in the absence of Synaptotagmin) are separated by an activation energy barrier of $\geq 30\ k_BT$[20]. The rate of spontaneous fusion from the CPX-clamped state in the flipped SNARE fusion assay, $t_{off} \sim 1$ hour[14] indicates an energy barrier also close to 30 k_BT (based on the well-established Kramers-Evans relationship between activation energy and dissociation rate[38], which predicts t_{off} for a 30 k_BT barrier will be between 0.3 to 3 hours). Starting with the ~ 30 k_BT value for the spontaneous activation energy barrier from the array, removing a single SNAREpin (by Ca^{2+}-Synaptotagmin or any other means) is predicted to reduce the activation energy barrier by ~20 k_BT. The remaining barrier of ~10 k_BT will be transited[38] in 2-20 μsec, in no way limiting for the overall time required to release the first quanta of transmitter.

Put differently, the activation energy of ~10 k_BT for unbinding CPXacc in the clamped array implies that single CPXacc dissociation events will occur spontaneously every 2-20 μsec, but these will fruitlessly snap back into the array and not result in spontaneous fusion. The activation barrier for spontaneous fusion from the clamped state of ~30 k_BT suggests that it is only when three such contacts are broken (presumably in neighboring SNAREpins) that the fusion pore can successfully opens with high probability. In our model, perturbation by Ca^{2+}-Synaptotagmin serves to remove two of these three accessory helices, and when the third spontaneously dissociates (2-20 μsec) the fusion pore can now open. The lifetime of the Ca^{2+}-Synaptotagmin complex, whose lower limit is set by the duration of the rise in local calcium concentration, is far longer than this, and so the third and final CPXacc will have many chances to dissociate while calcium is still bound.

ACKNOWLEDGEMENTS

We wish to thank Jeff Coleman for technical assistance and Dr. Tom Melia for critical reading of the manuscript. This work was supported by NIH grants to JER and KMR, ANR PCV grant to FP, and a grant from the DFG to DK.

AUTHOR CONTRIBUTIONS

SSK, DTR and DK performed the mutagenesis and protein purification, SSK and DTR carried out the fluorescence measurements, FL did the ITC measurements and LK, SB and CGG contributed the cell-cell fusion assay. Results were analyzed and discussed by all authors. The manuscript was prepared by SSK, DTR, KR, FP & JER

METHODS

PLASMID CONSTRUCTS

The constructs used in this study are are pET28a oligohistidine-Thrombin-syntaxin1A (containing rSyntaxin1a residues 191-253), pET28a oligohistidine-MBP-Thrombin-SNAP25N (containing hSNAP25A residues 7-82 and a C-terminal tryptophan), pET28a oligohistidine-Thrombin-SNAP25C (containing hSNAP25A residues 141-203) and pET15b oligohistidine-Complexin (containing hcomplexin1 residues 1-134 with the following “super clamp” mutations: D27L, E34F, R37A).The VAMP2 c-terminal truncations were pET28a-oligohistidine-SUMO-VAMP2-60 (hVAMP2 residues 25-60) -VAMP2-65 (hVAMP2 residues 25-65); -VAMP-69 (hVAMP2 residues 25-69); -VAMP-73 (hVAMP2 residues 25-73); -VAMP-77 (hVAMP2 residues 25-77). VAMP-4X and VAMP-3xDA were generated by introducing L70D/A74R/A81D/L84D and D64A/D65A/D68A mutation, respectively into

pET15b-oligohistidine-Thrombin-VAMP2 (human VAMP2 residues 1-96) using QuickChange mutagenesis Kit (Stratagene). VAMP-D64A; -D65A and -D68A were also generated in the same fashion. In these constructs, 'Thrombin' and 'SUMO' refer to the protease cleavage site.

PROTEIN EXPRESSION AND PURIFICATION

All constructs were expressed and purified as described previously[21]. Briefly, recombinant fusion proteins were expressed in E.coli BL21 (DE3) cells by induction with 1 mM IPTG for 3 h at 37°C. Cells were harvested and re-suspended in Breaking Buffer (50mM Tris, 150 mM NaCl, 1 mM TCEP, pH 7.4) supplemented with protease inhibitors (SIGMAFAST cocktail, EDTA-free, SIGMA), then lysed using a cell disruptor (Avestin). A cleared lysate obtained by centrifugation was incubated for 3-4 hours with Ni-NTA-agarose (Qiagen) resin. The suspension was transferred into a polypropylene column and washed with 25 column volumes of Wash buffer (50mM Tris, 150 mM NaCl, 1 mM TCEP, pH 7.4), followed by 10 column volume of Wash buffer supplemented with 50mM Imidazole. For all v- and t-SNARE proteins, the beads were re-suspended in wash buffer and incubated with Thrombin or SUMO protease, as appropriate for the cleavage site, overnight at 4°C to remove the tags. For complexin, the protein was eluted from the beads using 400mM Imidazole in Wash buffer and excess Imidazole was removed by dialysis against wash buffer or by NAP25 desalting column (GE Healthcare) equilibrated with the wash buffer. In most cases, the proteins were pure and required no further clean-up. In few cases that required further clean up, the proteins

were subjected to size exclusion chromatography on a Hi-Load Superdex 75 (16/60, GE Healthcare) column equilibrated with Wash buffer.

FRET ANALYSIS

Positions D193 on SNAP25C and Q38 on CPX were mutated into cysteines using the Stratagene QuikChange Kit. SNAP25 D193C was labeled with the donor probe, Stilbene (4-acetamido-4'-((iodoacetyl)amino)-stilbene-2,2'-disulfonic acid, disodium salt, Invitrogen) and CPX Q38C was labeled with the acceptor Bimane (Monochlorobimane, Invitrogen) as described previously[21]. The double-labeled CPX-SNARE complexes were assembled overnight at 4°C and purified by gel-filtration on a Superdex 75 gel filtration column. All fluorescence data were obtained on a Perkin-Elmer LS55 luminescence spectrometer operating at 25°C and the conditions are similar to those used previously[21]. FRET distances were calculated as described previously using a R_0 for the Stilbene-Bimane FRET pair to be 27.5 Å[21]

TOXIN ACCESSIBILITY ASSAY

VAMP2 is the natural substrate for neurotoxins, Botulinum-B and Tetanus[39], but is protected from cleavage by the neurotoxins, if zippered into t-SNARE. To test the accessibility of VAMP-3xDA to the neurotoxins, 5μM of either free VAMP-3xDA or CPX-SNARE-3xDA complex were incubated with the neurotoxins at 1:20 toxin:protein ratio in a Tris Buffer pH 7.4 150 mM NaCl containing 100 μM Zn^{2+} at 37°C for 2 hours and was analyzed by SDS PAGE/Coomassie Stain. Botulinum-B and Tetanus light chains were purified as described previously[14]

LIPOSOME FUSION ASSAY

VAMP2 and t-SNARE proteins were incorporated in liposome at 1:400 protein:lipid ratio and liposome fusion assay was carried out as described previously[4,40,41]. Briefly, 45 μl unlabeled t-SNARE liposomes was mixed with 5 μl labeled v-SNARE liposomes in a 96-well plate and fusion was followed by measuring the increase in NBD fluorescence at 538 nm (excitation 460 nm) every 2 min at 37°C. At the end of the 2 hr reaction, 10 ml of 2.5% dodecyl-maltoside was added to the liposomes and the fusion is plotted as the percentage of the maximal NBD fluorescence[40].

CELL-CELL FUSION ASSAY

The flipped SNARE cell-cell fusion assay was performed essentially as described before[3,14,15,42]. In brief, HeLa cell lines were transiently transfected with flipped VAMP2 (WT or 3xDA), DsRed2-NES and either with or without CPX mutants and Synaptotagmin as indicated (v-cells). After one day, transfected v-cells were seeded onto glass coverslips containing cells stably co-expressing flipped syntaxin1, flipped SNAP-25 and CFP-NLS (t-cells). The following day, cells were fixed with 4% paraformaldehyde directly or after treatment with recovery solution (1 U/ml Phosphatidylinositol Specific Phospholipase-C, 20 μg/ml laminin, with or without 1.8 mM EGTA), washed and mounted with Prolong Antifade Gold mounting medium (Molecular Probes). Confocal images were acquired on a Zeiss 510-Meta confocal microscope and processed using Adobe Photoshop software. Kinetics of the reversal of the CPX clamp by Syanptotagmin/Ca^{2+} was essentially carried out as described, wherein 5 minutes after the addition of PI-PLC/EGTA, the free Ca^{2+} concentration raised to 1mM the samples were

fixed at 5 minute interval between 5 and 30 min after the addition the addition of Ca^{2+}. For the calcium sensitivity experiment, free Ca^{2+} was raised to the indicated concentration (ranging from 5 μM to 5000 μM) and the cells were incubated at 37°C for 30 min before fixing the cells for quantitation.

ISOTHERMAL TITRATION CALORIMETRY (ITC) ANALYSIS

SNARE complex and blocked-SNARE complex for ITC measurements were assembled and purified as described previously[21] using PBS (phosphate buffered saline, pH 7.4, 10 mM sodium phosphate dibasic, 2 mM potassium phosphate monobasic,137 mM NaCl, 3 mM KCl) with 0.25mM TCEP. ITC experiments were performed on a Microcal ITC200 instrument. Typically, about 200 μL of SNARE complex solution (~10 μM) was loaded into the sample cell and about 40 μL of CPX solution (~200 μM) was loaded into the syringe. An initial 0.2 μL injection was followed by several injections of constant volume. 180-second equilibration time was used after each injection to ensure complete binding. The heat change from each injection was integrated, and then normalized by the moles of CPX in the injection. "One-set-of-sites" binding mode was used to analyze the titration calorimetric data and obtain the stoichiometric number (*N*), the molar binding enthalpy (*ΔH*), and the association constant (K_a) using Microcal Origin ITC200 software package. The affinity constant (K_d), the binding free energy (*ΔG*), and the binding entropy (*ΔS)* were calculated using the thermodynamic equations:

$$K_d = 1/K_a \quad (17)$$

$$\Delta G = -RT \ln K_a \text{ and} \quad (18)$$

$$\Delta G = \Delta H - T\Delta S. \quad (19)$$

REFERENCES

1. Sollner, T. et al. SNAP receptors implicated in vesicle targeting and fusion. *Nature* **362**, 318-24 (1993).
2. McNew, J.A. et al. Compartmental specificity of cellular membrane fusion encoded in SNARE proteins. *Nature* **407**, 153-9 (2000).
3. Hu, C. et al. Fusion of cells by flipped SNAREs. *Science* **300**, 1745-9 (2003).
4. Weber, T. et al. SNAREpins: minimal machinery for membrane fusion. *Cell* **92**, 759-72 (1998).
5. Sutton, R.B., Fasshauer, D., Jahn, R. & Brunger, A.T. Crystal structure of a SNARE complex involved in synaptic exocytosis at 2.4 A resolution. *Nature* **395**, 347-53 (1998).
6. Karatekin, E. et al. A fast, single-vesicle fusion assay mimics physiological SNARE requirements. *Proc Natl Acad Sci U S A* **107**, 3517-21 (2010).
7. Perin, M.S., Fried, V.A., Mignery, G.A., Jahn, R. & Sudhof, T.C. Phospholipid binding by a synaptic vesicle protein homologous to the regulatory region of protein kinase C. *Nature* **345**, 260-3 (1990).
8. Brose, N., Petrenko, A.G., Sudhof, T.C. & Jahn, R. Synaptotagmin: a calcium sensor on the synaptic vesicle surface. *Science* **256**, 1021-5 (1992).
9. Fernandez-Chacon, R. et al. Synaptotagmin I functions as a calcium regulator of release probability. *Nature* **410**, 41-9 (2001).
10. Geppert, M. et al. Synaptotagmin I: a major Ca2+ sensor for transmitter release at a central synapse. *Cell* **79**, 717-27 (1994).

11. Pang, Z.P., Shin, O.H., Meyer, A.C., Rosenmund, C. & Sudhof, T.C. A gain-of-function mutation in synaptotagmin-1 reveals a critical role of Ca2+-dependent soluble N-ethylmaleimide-sensitive factor attachment protein receptor complex binding in synaptic exocytosis. *J Neurosci* **26**, 12556-65 (2006).

12. Ishizuka, T., Saisu, H., Odani, S. & Abe, T. Synaphin: a protein associated with the docking/fusion complex in presynaptic terminals. *Biochem Biophys Res Commun* **213**, 1107-14 (1995).

13. McMahon, H.T., Missler, M., Li, C. & Sudhof, T.C. Complexins: cytosolic proteins that regulate SNAP receptor function. *Cell* **83**, 111-9 (1995).

14. Giraudo, C.G., Eng, W.S., Melia, T.J. & Rothman, J.E. A clamping mechanism involved in SNARE-dependent exocytosis. *Science* **313**, 676-80 (2006).

15. Giraudo, C.G. et al. Alternative zippering as an on-off switch for SNARE-mediated fusion. *Science* **323**, 512-6 (2009).

16. Maximov, A., Tang, J., Yang, X., Pang, Z.P. & Sudhof, T.C. Complexin controls the force transfer from SNARE complexes to membranes in fusion. *Science* **323**, 516-21 (2009).

17. Xue, M. et al. Distinct domains of complexin I differentially regulate neurotransmitter release. *Nat Struct Mol Biol* **14**, 949-58 (2007).

18. Xue, M. et al. Tilting the balance between facilitatory and inhibitory functions of mammalian and Drosophila Complexins orchestrates synaptic vesicle exocytosis. *Neuron* **64**, 367-80 (2009).

19. Sudhof, T.C. & Rothman, J.E. Membrane fusion: grappling with SNARE and SM proteins. *Science* **323**, 474-7 (2009).

20. Li, F. et al. Complexin: How Can the Same Protein Both Activate and Clamp Membrane Fusion. *Manuscript Submitted* (2011).

21. Kümmel, D. et al. Complexin Crosslinks Pre-fusion SNAREs into Zig-Zag Array: A Structure Based Model for Complexin Clamping. *Manuscript Submitted* (2011).

22. Hua, S.Y. & Charlton, M.P. Activity-dependent changes in partial VAMP complexes during neurotransmitter release. *Nat Neurosci* **2**, 1078-83 (1999).

23. Reim, K. et al. Complexins regulate a late step in Ca2+-dependent neurotransmitter release. *Cell* **104**, 71-81 (2001).

24. Tang, J. et al. A complexin/synaptotagmin 1 switch controls fast synaptic vesicle exocytosis. *Cell* **126**, 1175-87 (2006).

25. Chen, X. et al. Three-dimensional structure of the complexin/SNARE complex. *Neuron* **33**, 397-409 (2002).

26. Bracher, A., Kadlec, J., Betz, H. & Weissenhorn, W. X-ray structure of a neuronal complexin-SNARE complex from squid. *J Biol Chem* **277**, 26517-23 (2002).

27. Yang, X., Kaeser-Woo, Y.J., Pang, Z.P., Xu, W. & Sudhof, T.C. Complexin clamps asynchronous release by blocking a secondary Ca(2+) sensor via its accessory alpha helix. *Neuron* **68**, 907-20 (2010).

28. Shao, X., Fernandez, I., Sudhof, T.C. & Rizo, J. Solution structures of the Ca2+-free and Ca2+-bound C2A domain of synaptotagmin I: does Ca2+ induce a conformational change? *Biochemistry* **37**, 16106-15 (1998).

29. Radhakrishnan, A., Stein, A., Jahn, R. & Fasshauer, D. The Ca2+ affinity of synaptotagmin 1 is markedly increased by a specific interaction of its C2B domain with phosphatidylinositol 4,5-bisphosphate. *J Biol Chem* **284**, 25749-60 (2009).

30. Vrljic, M. et al. Molecular mechanism of the synaptotagmin-SNARE interaction in Ca2+-triggered vesicle fusion. *Nat Struct Mol Biol* **17**, 325-31 (2010).

31. Ubach, J., Zhang, X., Shao, X., Sudhof, T.C. & Rizo, J. Ca2+ binding to synaptotagmin: how many Ca2+ ions bind to the tip of a C2-domain? *EMBO J* **17**, 3921-30 (1998).

32. Bai, J., Tucker, W.C. & Chapman, E.R. PIP2 increases the speed of response of synaptotagmin and steers its membrane-penetration activity toward the plasma membrane. *Nat Struct Mol Biol* **11**, 36-44 (2004).

33. Chapman, E.R. & Davis, A.F. Direct interaction of a Ca2+-binding loop of synaptotagmin with lipid bilayers. *J Biol Chem* **273**, 13995-4001 (1998).

34. McMahon, H.T., Kozlov, M.M. & Martens, S. Membrane curvature in synaptic vesicle fusion and beyond. *Cell* **140**, 601-5 (2010).

35. Xue, M. et al. Binding of the complexin N terminus to the SNARE complex potentiates synaptic-vesicle fusogenicity. *Nat Struct Mol Biol* **17**, 568-75 (2010).

36. Yoon, T.Y. et al. Complexin and Ca2+ stimulate SNARE-mediated membrane fusion. *Nat Struct Mol Biol* **15**, 707-13 (2008).

37. Sabatini, B.L. & Regehr, W.G. Timing of neurotransmission at fast synapses in the mammalian brain. *Nature* **384**, 170-2 (1996).

38. Evans, E. Probing the relation between force--lifetime--and chemistry in single molecular bonds. *Annu Rev Biophys Biomol Struct* **30**, 105-28 (2001).

39. Sikorra, S., Henke, T., Galli, T. & Binz, T. Substrate recognition mechanism of VAMP/synaptobrevin-cleaving clostridial neurotoxins. *J Biol Chem* **283**, 21145-52 (2008).

40. Scott, B.L. et al. Liposome fusion assay to monitor intracellular membrane fusion machines. *Methods Enzymol* **372**, 274-300 (2003).

41. Ji, H. et al. Protein determinants of SNARE-mediated lipid mixing. *Biophys J* **99**, 553-60 (2010).

42. Giraudo, C.G. et al. Distinct domains of complexins bind SNARE complexes and clamp fusion in vitro. *J Biol Chem* **283**, 21211-9 (2008).

CHAPTER FIVE

CONCLUSIONS

In the previous three chapters, I demonstrated that I succeeded in developing a new FRET pair (Chapter 2) and using it to validate the novel crystal structure put forth in Kümmel, *et al* (Chapter 3). Further, I explored the nature of the *trans*-SNARE complex in depth and developed a model for clamping (Chapter 3). I also looked at the mechanism of release of the Complexin clamp and identified three VAMP2 residues required for the unclamping of Complexin by Synaptotagmin (Chapter 4).

To review, the crystal structure of a *trans*-SNARE/Complexin mimetic was obtained by truncating the v-SNARE to residue 60, the +1 layer, and making use of the superclamping Complexin mutant used in Giraudo *et al.*[1]. The recently solved crystal structure is similar to that of the post-fusion crystal structure [2, 3]in many ways. Namely, in both of the structures, both the t- and present v-SNARE residues align nearly perfectly. Further, the Complexin molecule still binds via its Central Helix in an antiparallel fashion. This internal consistency serves as a control to validate that the novel part of the structure is at least in the realm of possibility.

The most significant difference between the two crystal structures is a large displacement of the Accessory Helix from a position nearly alongside the SNAREpin to one at a 45° angle, pointing away from the SNAREs. In the crystal, the Accessory Helix is stabilized by an interaction with the C-terminal region of the t-SNAREs of a neighboring complex. While this is precisely why the crystal was stable and ordered enough to form, the veracity of this structure is called into question, both because the

VAMP2 truncation mutant and the superclamping Complexin were used and neither is what occurs in biology. The main concern is that this positioning of Complexin is due to an artifact of crystallization both because the VAMP2 C-terminus is absent and the Complexin has a higher propensity to bind in the clamped state than wild-type. I used FRET to address these concerns; if the positioning of the Complexin is solely a function of crystal interactions, the Accessory Helix would not maintain its 45° angle in solution, where the low concentration and high entropy would not "force" the stabilizing Accessory Helix/t-SNARE interaction found in the crystal structure.

In my FRET studies, I developed a novel FRET pair based on the previously used Pyrene and Bimane [4]and calculated the pair's spectroscopic parameters. Then, I used this FRET pair to determine whether the Accessory Helix was indeed sticking out into space in solution. I placed the donor dye Stilbene on SNAP25 at position 193 and the acceptor dye Bimane at two positions on Complexin, 38 and 31. By using labeled versions of the same constructs as were used in the crystal structure (including the truncated VAMP2), I was able to validate that the Accessory Helix does, in fact, extend away from the four helix bundle in solution. I also established that the 45° angle was not due to the truncation of VAMP2's C-terminus as one might predict. Rather, a full length mutant in which critical C-terminal hydrophobic layer residues are mutated to charged residues (VAMP-4X) demonstrated that the Complexin sticks away from the four helix bundle despite the presence of the VAMP2 C-terminus; rather, it is because the VAMP2 C-terminus is not zippered into the four helix bundle. The mere presence of the C-

terminal residues of VAMP2 is not sufficient to result in a Complexin angled in, rather than angled out configuration.

Because I performed bulk FRET, it was possible that instead of seeing the Accessory Helix positioned at 45°, I could have been observing a time or population average of various populations of Accessory Helix positions both closer to and further away from the four helix bundle. I was able to discern that the 45° angle configuration is a biologically relevant state for the Accessory Helix, and not simply a time average of the entire space sampled by an unstructured patch of Complexin, by introducing a helix-breaking motif between the Central and the Accessory Helices. This helix-breaking motif caused the Accessory Helix to lose its structure as demonstrated by CD. Without the helix-breaking motif, the Accessory Helix was rigidly positioned, and not freely moving into space. On the other hand, in Complexin containing the helix-breaking motif, the acceptor is further away than that of Complexin lacking the helix breaker. This means that the positioning of the Accessory Helix is, in fact, real and not an average of two disparate states in solution. Thus, the crystal structure solved represents reality and is not an artifact of crystallization.

Because the Accessory Helix sticks away from the SNARE complex at such a large angle, the intramolecular clamping model posited in by Giraudo *et al.*[1] cannot occur. Instead, it is the Accessory Helix must clamp via another model. A hint at this new model is gleaned by examining the formula unit of the recent crystal structure. In this formula unit, a zig-zag array is formed, wherein the Accessory Helix of one SNARE/Complexin complex forms an “alternate four helix bundle” with the C-terminal

region of a *second* SNARE/Complexin complex. This suggests that the clamp might be formed intermolecularly, with any given SNAREpin unable to fully zipper because its v-SNARE is prevented from zippering by its neighbor's Complexin Accessory Helix. This model then further suggests several lines of evidence of how clamping could occur. First, fusion is prevented because the Accessory Helix physically blocks the area where the v-SNARE would normally zipper. Fusion is also blocked because bringing the SNAREpins closer at their zippering ends would cause steric clash in the zig-zag model. Further, fusion is blocked because the linker regions of Syntaxin1 and VAMP2 are on different sides of the zig-zag midline, which interferes with complete zippering. And lastly, fusion is blocked because of the zig-zag array due to the fact the SNAREpins are locked in place and unable to move into a circular configuration.

Subsequently I set out to discover the region of VAMP2 responsible for allowing the Accessory Helix to be released from the 45° angle position down to the parallel to the SNAREpin position. I did so by progressively increasing the length of the VAMP2 construct from its initial length (residues 26-60) to the full length cytoplasmic domain, (residues 26-96). I discovered that the presence of the VAMP2 region between residues 69 and 73 is required for this transition. An examination of the crystal structure [2] reveals three patches of binding interactions between VAMP2 and Complexin. The first patch is a hydrophobic contact between VAMP2's V50 and L54 and CPX's M62 and I66. The second is a salt bridge between VAMP2's D67 and CPX's R63 and R59. The third is a grouping of salt bridge and hydrogen bonding interactions between residues Y52 and R48 on Complexin and aspartates 64, 65, and 68 on VAMP2.

I hypothesized that these three residues were responsible for the positioning of the Accessory Helix with respect to the four helix bundle. To test this, I mutated the aspartates to alanines. This triple mutation, VAMP-3xDA prevents the Accessory Helix from coming down to the SNAREpin, while the individual single mutations yield intermediate profiles. I demonstrated that these three residues are important for the release of the clamp by Synaptotagmin in cell-cell fusion assays. In fact, this mutant shares a phenotype with that of the superclamping Complexin in these cell-cell fusion assays[1], suggesting two separate processes are involved in clamp removal: first, the Accessory Helix must be able to be removed from the t-SNARE C-terminal region so VAMP2 can zipper in, and second, the VAMP2 must be capable of receiving the Accessory Helix upon its release from the neighboring SNAREpin, preventing the Accessory Helix from re-interacting with its neighbor.

This provides an insight into the mechanism of release of the Complexin clamp by Synaptotagmin. Once Synaptotagmin removes one SNAREpin/Complexin complex from the zig-zag structure, its t-SNAREs' C-terminal region is no longer blocked by a neighboring Accessory Helix, which means the VAMP2 can zipper into the C-terminal region of the Four Helix Bundle. Further, the associated Complexin's Accessory Helix is then able to move from its clamped 45° position to the unclamped position, running alongside the four helix bundle. This prevents the Accessory Helix from blocking its neighbor on its other side, enabling the neighbor's VAMP2 to zipper up as well. Because the Accessory Helix is tethered to its own SNAREpin, it is prevented from reassociating with a neighboring complex. This rapid cascade of clamp release enables the fast and

synchronous fusion associated with calcium-dependent synaptic fusion which occurs *in vivo*.

FUTURE DIRECTIONS

While this model addresses several experimental observations that have arisen with Complexin, it fails to directly address others. It has been proposed that CPX facilitates fusion by keeping the SNAREs in a primed, fusogenic state[5-7]. The model we propose posits that the SNAREs are primed for fusion, in keeping with this prediction. Our model also addresses the biochemical predictions made in the Giraudo *et al* paper[1]; namely, the residues found to be in the interacting face between CPX's Accessory Helix and the t-SNARE groove include the residues Giraudo *et al* [1]mutated to make the superclamping mutation.

Not addressed in our model, however, is the functionality of either the N-terminal or C-terminal domains of Complexin. It is easy to imagine, however, that the N-terminal domain is capable of stabilizing the SNAREs in the context of a zig-zag array as suggested by[8, 9], perhaps acting as a glue to hold the N-terminal domain of VAMP into the acceptor t-SNARE complex. Also our model leaves room for the C-terminal domain to interact with the membrane as predicted by[8, 10]. This C-terminal membrane interaction may help recruit Complexin to the site of SNARE action helping to increase its local concentration. But for now, neither of these domains is described in the model.

To learn more about these domains, one might choose to use FRET. For example, by retaining the donor dye on position 193 in the C-terminal helix of SNAP25, and moving the acceptor positions around in the N- and C-terminal regions of Complexin, a

distance profile could be obtained for each domain, suggesting the positioning of these regions with respect to the SNARE four helix bundle. Cross-linking or NMR experiments could further confirm the proximity of the N- or C-terminal domains to various parts of the SNAREs or membranes.

The issue of greatest importance which is not explicitly proven in the previous chapters is the veracity of the zig-zag array *in vivo*. While it is very clear that the Complexin Accessory Helix sticks away from the four helix bundle, and while no other mechanism of clamping seems feasible, it is irresponsible to claim with 100% certainty that the zig-zag array is definitely what happens in a cell. To assay this, membranes will be required, not only to order the molecules in solution, but also to increase their local concentration. In the lab, we are currently trying to achieve this using nanodiscs[11]. Also, it is likely that single-molecule assays will also be required. One other option to monitor the association of two SNAREpins through a bridging Complexin molecule is to label one population of SNARE/Complexin complexes with VAMP60 or VAMP-4X with donor dye and another population of SNARE-only complexes with VAMP60 or VAMP-4X with acceptor dye and look for FRET. If FRET occurs, one SNARE complex must interact with a second SNARE complex, and the molecule bringing them together must be Complexin.

Our proposed model also does not directly address why Complexin appears to have different functions in different animals. Perhaps this is because of different Accessory Helix binding interfaces in different species(ref), but it could also be a combination of differences in N- and C-terminal region sequences. For example, the

Drosophila melanogaster Accessory Helix contains more hydrophobic residues than the mouse version(ref); because of this, it likely acts as a better clamp. Another difference in Complexin Accessory Helices between species occurs with *C. elegans*, wherein the Accessory Helix is disrupted by a helix-breaking proline residue[12]. And yet, somehow this domain remains inhibitory towards fusion in the nematode, potentially via some other method than what occurs in mammals. The Accessory Helix question can best be addressed by crystallography, to examine how these different species' Complexins interact with the SNAREpins.

Another aspect our model does not explain is precisely how the zig-zag array is disrupted beyond hypothesizing that Synaptotagmin can provide enough energy to disrupt the array. Many further experiments must be performed to assay how and with which residues Synaptotagmin binds the *trans*-SNARE complex. For example, FRET experiments can be performed to examine the interaction interface. Because Synaptotagmin requires membranes for function(ref), these experiments should be performed both with and without membranes to determine whether Synaptotagmin's ability to bind the *trans*-SNARE is dependent on its membrane-binding capability. Bulk FRET studies could likely determine the interaction interface, but single molecule studies would be required to visualize Synaptotagmin disrupt the zipper. Furthermore, as Synaptotagmin is the calcium sensor, experiments should be carried out in both the presence and absence of Ca^{2+} to determine the effect of calcium-binding on the positioning of Synaptotagmin's C2A and C2B domains. Another question is: does Synaptotagmin bind the *trans*-SNARE complex better when Complexin is present,

suggesting it binds after Complexin does, as Yang *et al*. suggest[13], does Synaptotagmin bind the *trans*-SNARE complex without Complexin, suggesting Synaptotagmin binds first, as Sorensen *et al.* [14] propose or that they compete, as Tang *et al*.[15] suggest?

While the structural predictions made in the Giraudo *et al.* paper[1] are addressed by the papers contained in this thesis *in vitro*, real *in vivo* data are lacking besides the cell-cell fusion assay. To address this, experiments both in stable nerve cell or other secretory cell lines as well as in live animals must be performed using these mutations. Currently, the only *in vivo* experiments addressing the superclamping mutations were recently published by the Südhof lab (Yang et al 2010), and they validate that the superclamping mutations effectively inhibit fusion events in cortical mammalian neurons. Further studies must be done on the superclamping mutations in organisms to obtain actual phenotypes. And now that the 3xDA mutations have been discovered, they must be examined in both cultured cells and live animals for a phenotype, as well. It is very clear that much more work remains to be done to understand the intricacies of clamping and release within synaptic release, and to answer all of the questions regarding the interplay among Complexin, Synaptotagmin, calcium, membranes, and SNAREs. The work presented in this thesis helps to explain both the clamping and release from a mechanistic perspective.

REFERENCES

1. Giraudo, C.G., et al., *Alternative zippering as an on-off switch for SNARE-mediated fusion.* Science, 2009. **323**(5913): p. 512-6.
2. Chen, X., et al., *Three-dimensional structure of the complexin/SNARE complex.* Neuron, 2002. **33**(3): p. 397-409.
3. Bracher, A., et al., *X-ray structure of a neuronal complexin-SNARE complex from squid.* J Biol Chem, 2002. **277**(29): p. 26517-23.
4. Borochov-Neori, H. and M. Montal, *Rhodopsin-G-protein interactions monitored by resonance energy transfer.* Biochemistry, 1989. **28**(4): p. 1711-8.
5. Hobson, R.J., et al., *Complexin maintains vesicles in the primed state in C. elegans.* Curr Biol, 2011. **21**(2): p. 106-13.
6. Pabst, S., et al., *Rapid and selective binding to the synaptic SNARE complex suggests a modulatory role of complexins in neuroexocytosis.* J Biol Chem, 2002. **277**(10): p. 7838-48.
7. Yoon, T.Y., et al., *Complexin and Ca2+ stimulate SNARE-mediated membrane fusion.* Nat Struct Mol Biol, 2008. **15**(7): p. 707-13.
8. Xue, M., et al., *Distinct domains of complexin I differentially regulate neurotransmitter release.* Nat Struct Mol Biol, 2007. **14**(10): p. 949-58.
9. Xue, M., et al., *Binding of the complexin N terminus to the SNARE complex potentiates synaptic-vesicle fusogenicity.* Nat Struct Mol Biol, 2010. **17**(5): p. 568-75.

10. Maximov, A., et al., *Complexin controls the force transfer from SNARE complexes to membranes in fusion.* Science, 2009. **323**(5913): p. 516-21.

11. Borch, J. and T. Hamann, *The nanodisc: a novel tool for membrane protein studies.* Biol Chem, 2009. **390**(8): p. 805-14.

12. Martin, J.A., et al., *Complexin has opposite effects on two modes of synaptic vesicle fusion.* Curr Biol, 2011. **21**(2): p. 97-105.

13. Yang, X., et al., *Complexin clamps asynchronous release by blocking a secondary Ca(2+) sensor via its accessory alpha helix.* Neuron, 2010. **68**(5): p. 907-20.

14. Sorensen, J.B., *Conflicting views on the membrane fusion machinery and the fusion pore.* Annu Rev Cell Dev Biol, 2009. **25**: p. 513-37.

15. Tang, J., et al., *A complexin/synaptotagmin 1 switch controls fast synaptic vesicle exocytosis.* Cell, 2006. **126**(6): p. 1175-87.